

**Synthesis, Structural Studies and Reactivity of
Monomeric Organo Aluminum and Gallium Amides,
Hydrogensulfides and Hydroxides Using N-
Heterocyclic Carbene: Precursor for
Heterobimetallic Systems**

Dissertation
zur Erlangung des Doktorgrades
der Mathematisch-Naturwissenschaftlichen Fakultäten
der Georg-August-Universität zu Göttingen

vorgelegt von

Vojtěch Jančík
aus Prostějov
(Tschechische Republik)

Göttingen 2004

D 7

Referent: Prof. Dr. Dr. h.c. mult. H. W. Roesky

Koreferent: Prof. G. M. Sheldrick, Ph.D.

Tag der mündlichen Prüfung: 3.11.2004

*Dedicated to my wife Mónica
for her love and affection*

Acknowledgement

The work described in this doctoral thesis has been carried out under the guidance and supervision of Professor Dr. Dr. h.c. mult. H. W. Roesky at the Institute of Inorganic Chemistry of the Georg-August-Universität Göttingen between August 2001 and July 2004.

My sincere thanks and gratitude are due to

Prof. Dr. Dr. h.c. mult. H. W. Roesky

for his constant guidance, motivation, suggestions, and discussions throughout this work.

I would like to express my special thanks to Professor Dr. Jiri Pinkas for numerous fruitful discussions and his help during this work. I thank Dr. Dante Neculai, Dr. Ana Mirela Neculai, Dr. Mathias Noltemeyer, and Mr. Hans-Georg Schmidt for their help in the X-ray crystal structural investigations and their friendship. My special thanks in this field go to Dr. Regine Herbst-Irmer for her time and valuable lessons on refinement of disordered molecules and twinned crystals. I thank Dr. A. Claudia Stückl and Dr. J. Li (DFT calculations), Mr. Wolfgang Zolke, Mr. Ralf Schöne and Dr. Gernot Elter (NMR spectra), Dr. Dieter Böhler, Mr. Thomas Schuchardt and Mr. Jörg Schöne (mass spectra), Mr. Mathias Hesse and Mr. H.-J. Feine (IR spectra), Mr. Jürgen Schimkowiak, Mr. Martin Schlote and the staff of the Analytical Laboratories and Werkstatt for their timely support during this research work.

I would like to thank the Stiftung Stipendien-Fonds des Verbandes der Chemischen Industrie e.V. for their financial support of a Chemiefonds-Stipendium für Doktoranden, which I was receiving for the first two years of my studies.

I thank all colleagues in our research group for the good and motivating working atmosphere. I would like to express my special thanks to Leslie W. Pineda Cedeño, Dr. Haijun Hao, Dr. Andreas Stasch, Dr. Carsten Ackerhans, Dr. Michael Gorol, Mircea Braban, Ying Peng, Gurubasavaraj P. M., Dr. Yuqiang Ding, Torsten Blunck, Dr. Holger Hohmeister, Dr. Peter Lobinger, Dr. Jörg Janssen, Dr. Jörg Prust, S. Shravan Kumar, Hans-Jürgen Ahn, Sanjay Sing, Umesh Nehete, Jiangfan Chai, Dr. Kerstin Most, Dr. Marcus Schiefer, Hongping Zhu, Dr. Guangcai Bai for their friendliness. The help offered by Dr. Michael Witt for final proof-reading is gratefully acknowledged.

The full support and encouragement from my wife Mónica Mercedes Moya Cabrera, my mother, brothers, sister, and friends made this work possible.

1. Introduction	1
1.1. β -Diketiminato Ligands	1
1.2. Aluminum Chalcogenides	3
1.3. Aluminum Amides	4
1.4. Gallium Amides	5
1.5. Aluminum Hydroxides	5
1.6. Gallium Hydroxides	7
1.7. Scope and Aim of the Present Work	8
2. Results and Discussion	9
2.1. Compounds Containing Aluminum–Chalcogen Bonds	9
2.1.1. Phosphine Catalysed Reactions of LAlH_2 with Elemental Chalcogenides ...	9
2.1.2. X-Ray Structural Characterization of $\text{LAl}(\text{SH})_2$ (1)	12
2.1.3. Molecular Structures of $\text{LAl}(\mu\text{-E})_2\text{AlL}$ ($\text{E} = \text{Se}(\textbf{2}), \text{Te}(\textbf{3}), \text{S}(\textbf{4})$)	14
2.2. Reactions of $\text{LAl}(\text{SH})_2$	16
2.2.1. Lithiation of the SH Groups	16
2.2.2. Structures of $\{\text{LAl}[(\text{SLi})_2(\text{thf})_3]\}_2 \cdot 2\text{THF}$ (5) and $\{\text{LAl}(\text{SH})[\text{SLi}(\text{thf})_2]\}_2$ (6)..	17
2.2.3. Reactions of 5' and 6 with Cp_2MCl_2 ($\text{M} = \text{Ti}, \text{Zr}$) and Structural Characterization of $\text{LAl}(\mu\text{-S})_2\text{TiCp}_2$ (7)	20
2.2.4. Deprotonation of $\text{LAl}(\text{SH})_2$ with N-Heterocyclic Carbenes and Crystal Structures of $\text{C}_t\text{H}^+[\text{LAl}(\text{SH})(\text{S})]^-$ (9) and $\text{C}_m\text{H}^+[\text{LAl}(\text{SH})(\text{S})]^-$ (11)	22
2.2.5. Preparation of Al–S–Si Systems	27
2.3. Ammonolysis and Hydrolysis of LAlCl_2 , $\text{LAl}(\text{Cl})\text{Me}$ and LGaCl_2 in the Presence of N-Heterocyclic Carbenes as HCl Scavengers	28
2.3.1. Synthesis of $\text{LAl}(\text{OH})_2$ (15) and $\text{LAl}(\text{NH}_2)_2$ (16)	28
2.3.2. Crystal Structure Description of $\text{LAl}(\text{NH}_2)_2$ (16)	30
2.3.3. Preparation of $\text{LAl}(\text{NH}_2)\text{Cl}$ (17) and $\text{LAl}(\text{NH}_2)\text{Me}$ (18)	32

2.3.4. Molecular Structures of $LAl(NH_2)Cl$ (17) and $LAl(NH_2)Me$ (18)	32
2.3.5. Preparation of $LGa(NH_2)_2$ (19) and $LGa(OH)_2$ (20)	35
2.3.6. X-Ray Study of Compounds 19 and 20 and DFT Calculations of 16 and 19	37
2.4. Controlled Degradation of Amides and Sulfides	42
2.4.1. Controlled Hydrolysis of Amides $LAl(NH_2)_2$ (16), $LAl(NH_2)Cl$ (17), $LAl(NH_2)Me$ (18) and $LGa(NH_2)_2$ (19)	42
2.4.2. Reaction of $LAl(NH_2)Me$ (18) with H_2S	43
2.4.3. Solid State Structure of $LAl(SH)Me$ (21)	44
2.4.4. Controlled Hydrolysis of $LAl(SH)_2$ (1) and $LAl(\mu-S)_2MCp_2$ (7 , $M = Ti$; 8 , $M = Zr$)	45
2.4.5. Crystal Structure Determinations of $LAl(OH)(\mu-O)M(SH)Cp_2$ (22 , $M = Ti$; 23 , $M = Zr$)	47
3. Summary and Outlook	50
3.1. Summary	50
3.2. Outlook	56
4. Experimental Section	57
4.1. General Procedures	57
4.2. Physical Measurements	57
4.3. Starting Materials	58
4.4. Syntheses of Compounds 1–23	59
4.4.1. Synthesis of $LAl(SH)_2$ (1)	59
4.4.2. Synthesis of $LAl(\mu-Se)_2AlL$ (2)	59
4.4.3. Synthesis of $LAl(\mu-Te)_2AlL$ (3)	60
4.4.4. Synthesis of $LAl(\mu-S)_2AlL$ (4)	60
4.4.5. Synthesis of $\{LAl[(SLi)_2(thf)_2]\}_2$ (5').....	61

4.4.6. Synthesis of $\{LAl(SH)[SLi(thf)_2]\}_2$ (6)	61
4.4.7. Synthesis of $LAl(\mu-S)_2TiCp_2$ (7)	62
4.4.8. Synthesis of $LAl(\mu-S)_2ZrCp_2$ (8)	62
4.4.9. Synthesis of $C_tH^+[LAl(SH)(S)]^-$ (9)	63
4.4.10. Synthesis of $C_mH^+_2[LAl(S)_2]^{2-}$ (10)	63
4.4.11. Synthesis of $C_mH^+[LAl(SH)(S)]^-$ (11)	64
4.4.12. Synthesis of $LAl(SSiMe_3)_2$ (12)	64
4.4.13. Synthesis of $LAl(\mu-S)_2SiMe_2$ (13)	65
4.4.14. Synthesis of $LAl(SSiMe_2)_2O$ (14)	65
4.4.15. Synthesis of $LAl(OH)_2$ (15)	66
4.4.16. Synthesis of $LAl(NH_2)_2$ (16)	66
4.4.17. Synthesis of $LAl(NH_2)Cl$ (17)	67
4.4.18. Synthesis of $LAl(NH_2)Me$ (18)	68
4.4.19. Synthesis of $LGa(NH_2)_2$ (19)	68
4.4.20. Synthesis of $LGa(OH)_2$ (20)	69
4.4.21. Synthesis of $LAl(SH)Me$ (21)	69
4.4.22. Synthesis of $LAl(OH)(\mu-O)Ti(SH)Cp_2$ (22)	70
4.4.23. Synthesis of $LAl(OH)(\mu-O)Zr(SH)Cp_2$ (23)	71
4.4.24. Alternative Preparation of $[LAl(OH)]_2O$	71
5. Handling and Disposal of Solvents and Residual Waste	72
6. Crystal Data and Refinement Details	73
7. Supporting Materials	90
8. References	94

List of publications

Lebenslauf

Abbreviations

δ	chemical shift
λ	wavelength
μ	bridging
ν	wave number
Ar	aryl
av	average
br	broad
<i>t</i> Bu	<i>tert</i> -butyl
C	Celsius
calcd.	calculated
C _m	N,N'- <i>bis</i> -mesitylimidazolyl carbene
C _m H ⁺	N,N'- <i>bis</i> -mesitylimidazolium ⁺
Cp	cyclopentadienyl
C _t	N,N'- <i>bis</i> - <i>t</i> butylimidazolyl carbene
C _t H ⁺	N,N'- <i>bis</i> - <i>t</i> butylimidazolium ⁺
CVD	Chemical Vapour Deposition
d	doublet
decomp.	decomposition
DFT	density functional theory
DMSO	dimethylsulfoxide
EI	electron impact ionization
Et	ethyl
eqivs.	equivalents
eV	electron volt
g	grams, gaseous
HOMO	highest occupied molecular orbital
Hz	Hertz
<i>i</i> Pr	<i>iso</i> -propyl
IR	infrared
<i>J</i>	coupling constant
K	Kelvin

L	ligand
LUMO	lowest unoccupied molecular orbital
M	metal
m	multiplet
m/z	mass/charge
M.p.	melting point
M^+	molecular ion
Me	methyl
mes	mesityl
min.	minutes
MS	mass spectrometry, mass spectra
NMR	nuclear magnetic resonance
Ph	phenyl
ppm	parts per million
q	quartet
R, R', R''	organic substituent
s	singlet
sept	septet
sh	shoulder
st	strong
t	triplet
THF	tetrahydrofuran
TMS	tetramethylsilane
UV	ultraviolet
V	volume
vst	very strong
w	weak
Z	number of molecules in the unit cell

1. Introduction

1.1. β -Diketiminato Ligands

The first complexes of β -diketiminato ligands have been reported in the mid to late 1960's for Co, Ni, Cu and Zn.^[1–14] These species have been mostly characterized by spectral and elemental analyses. They contain two different bonding modes of the ligands. The first exhibit RN–C(R')–C(R'')–C(R')–NR acyclic arrangement with R = H, alkyl, aryl, R' = H, alkyl and R'' = H or Me,^[2,3,5–7,9,12–14] whereas the second is formed by two pyrrol rings bridged in position 2 by a CH moiety.^[8,10,11] In 1969 E. Elder and B. R. Penfold reported the X-ray structure of {Cu[((2-NC₄Me₂-3,5)CO₂Et-4))₂CH]₂}^[11] and one year later F. A. Cotton, *et al.* published structural data for a similar complex of nickel {Ni[(2-NC₄HMe₂-3,5)₂CH]₂}^[10] containing substituted pyrrole type ligands and unequivocally confirmed the N, N' coordination mode for this species. The main impuls in this field began in the mid 1990's, when β -diketiminato ligands started to be used as spectator ligands offering strong metal-ligand bonds like cyclopentadienyls. Compared to the latter, β -diketiminato ligands offer much a wider possibility of tuning their electronic and steric properties by simple variation of the substituents on nitrogen and adjacent carbon atoms. When R is small like H, Me or the SiMe₃ group the substances form easily dimers and allow higher coordination of the metal centers, whereas substitution at the nitrogens by bulky aryl groups leads to isolation of unique species with low coordination numbers. Up to date there are numerous reports on a wide variety of these ligands and their complexes with most of the elements from the periodic system, which found application in catalysis (e.g. Cr,^[15–18] Mg,^[19] Ni,^[20] Pd,^[20] Ti,^[21] V,^[22] Zn,^[19] and Zr^[23]), as models in bioinorganic chemistry (Cu)^[24,25] or are interesting from a scientific point of view (e.g. Al,^[26,27] Fe,^[28,29] Ga,^[30] Ge,^[31,32] and Zn^[33]).

The N-aryl substituted ligands [HN(Ar)C(Me)CHC(Me)N(Ar)]^[34,35] (**L**) and [HN(Ar)C(*t*Bu)CHC(*t*Bu)N(Ar)]^[28] (**L'**) (Ar = 2,6-*i*Pr₂C₆H₃) (Figure 1) showed to be the best for stabilization of low coordination numbers of 3 on such electropositive elements as Mg²⁺ in L'MgMe^[36] and Fe²⁺ in L'FeCl.^[28] Their other advantage is the possibility to stabilize such unique species as the first monomeric LAl containing aluminum in the rare oxidation state +I,^[27] the first stable Ge²⁺ hydride LGeH,^[37] and the first structurally characterized metal hydroselenides of LAl(SeH)₂ and a Se bridged species [LAl(SeH)]₂Se.^[26] Recently, H. W. Roesky *et al.* reported on the preparation of the first stable aluminum congener of boronic

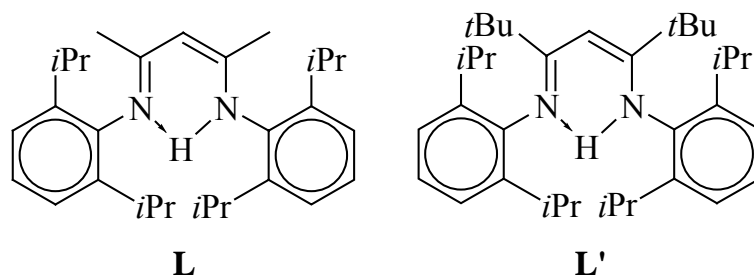
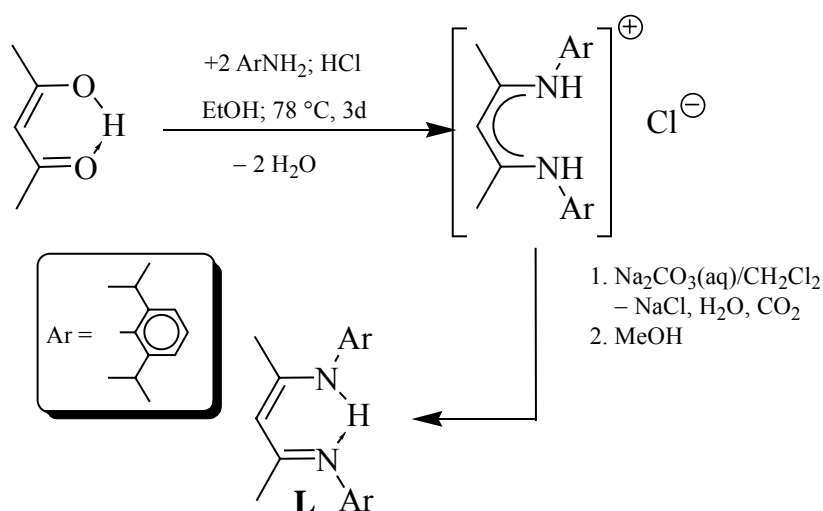


Figure 1: Bulky β -diketiminato ligands $[\text{HN}(\text{Ar})\text{C}(\text{Me})\text{CHC}(\text{Me})\text{N}(\text{Ar})]$ (**L**) and $[\text{HN}(\text{Ar})\text{C}(\text{tBu})\text{CHC}(\text{tBu})\text{N}(\text{Ar})]$ (**L'**) ($\text{Ar} = 2,6\text{-iPr}_2\text{C}_6\text{H}_3$).

acid $\text{LAl}(\text{OH})_2$.^[38] Furthermore, the ligand **L** exhibits also different coordination modes. The backbone $(\text{Ar})\text{N}=\text{C}(\text{Me})-\text{CH}=\text{C}(\text{Me})-\text{N}(\text{Ar})^-$ skeleton, usually delocalized to $[(\text{Ar})\text{N}\cdots\text{C}(\text{Me})\cdots\text{CH}\cdots\text{C}(\text{Me})\cdots\text{N}(\text{Ar})]^-$, can reveal $(\text{Ar})\text{N}=\text{C}(\text{Me})-\text{CH}=\text{C}(\text{Me})-\text{N}(\text{Ar})^- \rightleftharpoons (\text{Ar})\text{N}=\text{C}(\text{Me})-\text{CH}^--\text{C}(\text{Me})=\text{N}(\text{Ar})$ isomerism and thus allows coordination of the metal to the γ -carbon atom of the backbone. In this manner, species as $\text{Ge}[\text{C}((\text{C})(\text{Me})\text{N}(2,6\text{-iPr}_2\text{C}_6\text{H}_3))_2]\text{Cl}_3$ ^[31] or $[(\text{Et}_2\text{O})\text{Li}][\text{N}(2,6\text{-iPr}_2\text{C}_6\text{H}_3)\text{C}(\text{Me})]_2\text{CHCu}(\mu\text{-I})_2\text{CuCH}[\text{C}(\text{Me})\text{N}(2,6\text{-iPr}_2\text{C}_6\text{H}_3)]_2[\text{Li}(\text{Et}_2\text{O})]$ ^[39] have been isolated and structurally characterized.

Currently, there are various routes to obtain β -diketiminato ligands. Most use β -diketones and corresponding amines as educts,^[34,35] but some specific pathways, starting from metal alkyls and 2 equivs. of a nitrile or acylamide leading directly to metal complexes have been reported (Al, Li).^[14,40,41] Whereas the ligand **L** can be synthesized by direct condensation of 2,4-pentanedion, 2,6-diisopropylaniline, and HCl in boiling ethanol and subsequent neutralization of the generated ligand hydrochloride with Na_2CO_3 to obtain free **L** (Scheme 1).^[34,35]



Scheme 1: Synthesis of the β -diketiminato ligand $[\text{HN}(\text{Ar})\text{C}(\text{Me})\text{CHC}(\text{Me})\text{N}(\text{Ar})]$ (**L**).

Because the work in this thesis consists of several research areas, in the following part, some of the work related to these topics will be presented.

1.2. Aluminum Chalcogenides

Aluminum compounds containing heavier Group 16 elements are less well studied than those containing Al–O bonds, due to the low thermodynamical stability of the latter species. Thus, there are only a few examples of known compounds containing Al–E moieties, in which the chalcogen atoms are not directly bonded to alkyl, aryl or trialkylsilyl groups.^[42–63] Three different aggregation modes have been observed for species containing Al and chalcogen atoms in an equimolar ratio depending on the hapticity of the chalcogen atom. In these systems chalcogenes can act either as μ or μ_3 bridging ligand, as a consequence of the steric hindrance of the substituents present on the aluminum atoms. Thus, the (AlE)_n core can be either square planar ($n = 2$),^[42–51,55] cubic ($n = 4$)^[51–55] or adopt a hexagonal drum structure ($n = 6$) (Figure 2).^[52] Other examples containing Al and E in a ratio deviating from the 1:1

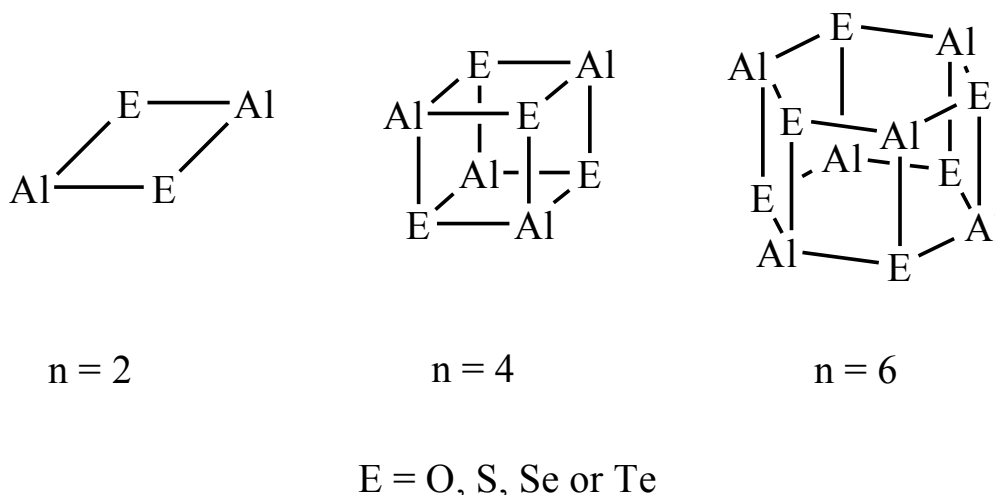


Figure 2: Major geometries of (Al–E)_n oligomers: square planar ($n = 2$), cubic ($n = 4$) and hexagonal drum-shaped ($n = 6$).

ratio have been reported exhibiting bent Al–E–Al, adamantane-like Al₄E₆ or more complex structures, respectively.^[26,58–61] We have recently shown that LAlH₂ (**2**), prepared from LH and AlH₃·NMe₃, reacts with elemental selenium^[26] to yield LAl(SeH)₂. This derivative is thermodynamically unstable and decomposes to yield [LAl(SeH)]₂Se under elimination of H₂Se.^[26] These species represent first examples of stable and structurally characterized

M–SeH moieties (M = metal). So far, there are no reports on derivatives of aluminum containing SH or TeH moieties.

1.3. Aluminum Amides

Aluminum amides supported by organic ligands are an important part of aluminum chemistry due to their significant application as molecular precursor for aluminum nitrides, AlN based semiconductors, and AlN ceramics.^[64–72] Amides with the general formula $R_2Al(NH_2)$, where R corresponds to organic substituents are rare, though desired, because of the presence of reactive NH_2 group, which can be involved in further substitution reactions leading to mixed-metal amides containing aluminum. These amides show a strong tendency to oligomerize into unstable trimers $[R_2Al(\mu-NH_2)]_3$ (R = Me, *t*Bu)^[73,74] or dimers $[R_2Al(\mu-NH_2)]_2$ (R = SiMe₃)^[75,76] due to the Lewis acidity of the aluminum center and to the presence of the electron lone pair of the amido group. The steric bulk of the substituents is the major factor that determines the degree of association. The latest example of such an aluminum amide $[(Me_3Si)_2Al(\mu-NH_2)_2]_3Al$ was published in 1988 by J. F. Janik *et. al.*, where the central aluminum atom is octahedrally coordinated by three $[(Me_3Si)_2Al(\mu-NH_2)_2]^-$ anions (Figure 3).^[75] The only known aluminum amide containing terminal NH_2 moiety

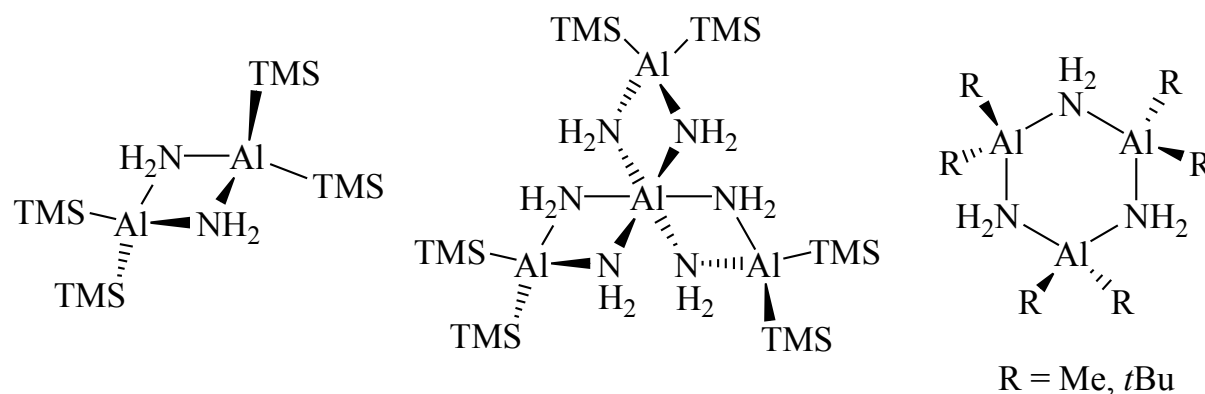


Figure 3: Examples of known aluminum amides.

$AlCl_3(NH_2iPr)_2\{Al(NH_3)(NH_2)[Al(NH_2iPr)(NiPr)Cl]_2\}_2$ has been prepared in low yield in 1997 by C.-C. Chang *et al.* in the reaction of $AlCl_3$ with $iPrNHLi$ and an excess of $iPrNH_2$, but the mechanism of its formation remains unclear.^[77] The only known well characterized pathway leading to these derivatives is manifested in the reactions between ammonia and trialkyl- or tris(trimethylsilyl)-aluminum reagents, which results in the case of R = alkyl in the

formation of $R_3Al \cdot NH_3$ type of adducts. These adducts are thermodynamically unstable and thus decompose at elevated temperature into the corresponding amides and alkanes,^[73,78] whereas no such adducts have been observed in the case of $R = SiMe_3$.^[74] There has been no report yet on the preparation of such species containing NH_2 group(s) by reactions of e.g. KNH_2 or $NaNH_2$ with appropriate aluminum halides. From our experience such reactions result mostly in decomposition of the starting materials to insoluble white powders and the free ligands. This is probably due to the formation of insoluble complexes such as $KAl(NH_2)_4$ with NH_2^- anions.^[79,80]

1.4. Gallium Amides

Until now only four gallium amides containing a NH_2 moiety – trimeric $[R_2Ga(\mu-NH_2)]_3$ ($R = H$,^[81,82] Me ,^[83,84] Et ^[85] and tBu ^[86]) are known, but only the Me and tBu derivatives have been structurally characterized. The Ga_3N_3 ring in the methyl derivative possesses a twisted boat conformation, whereas it is essentially planar in the case of the tBu derivative.^[83,84,86] All of them have been used as precursor for the CVD deposition of GaN, an important material for the manufacture of UV blue-light laser diodes, high-temperature electronics, and ultrahigh-density optical storage systems,^[87–98] respectively. Obviously, this method suffers from lack of suitable precursor.^[99,100] Current processes use mostly N_2 or NH_3 as additional sources of nitrogen, with the disadvantage of their high volatility at the reaction temperatures (500–1000 °C). This leads to GaN with higher number of nitrogen vacancies and thus lower quality of the final product.^[99,100]

1.5. Aluminum Hydroxides

The chemistry of molecular metal- and organometallic oxides and hydroxides is one of the most challenging fields of chemistry since significant application of these species as catalysts, cocatalysts and models for fixation of the catalysts on oxide surfaces.^[101–106] Recently, H. W. Roesky *et al.* have successfully synthesized several unique molecular hydroxides based e.g. on silicon $((2,6-iPrC_6H_3)(SiMe_3)NSi(OH)_3$, and $[(Me_3Si)_2CHSi(\mu-O)(OH)]_3$,^[107,108] aluminum $(LaAl(OH)_2$, and $[LaAl(OH)]_2O$)^[38,109] or tin $[(Me_3Si)_3CSn(\mu-O)(OH)]_3$ ^[110] (Figure 4). Aluminum hydroxides and aluminoxanes play an important role in this field due to the application as cocatalysts, and numerous examples of these species have

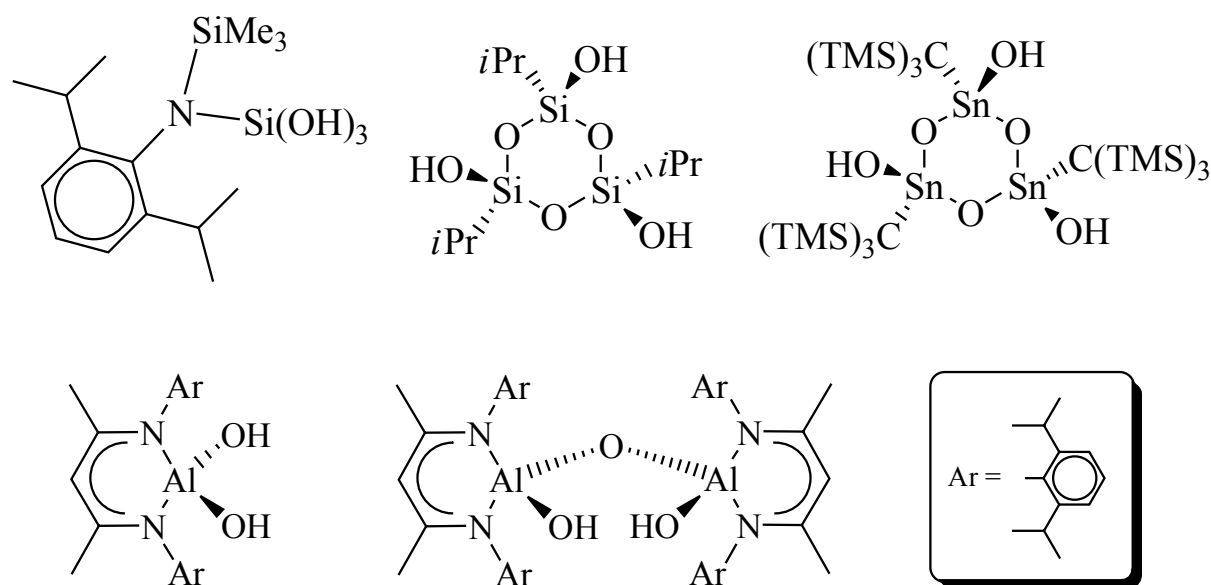
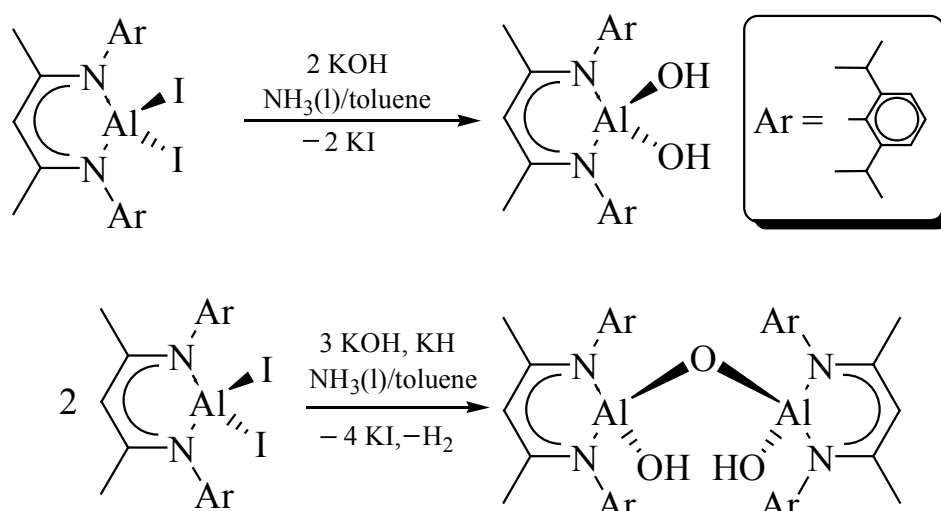


Figure 4: Examples of molecular hydroxides prepared previously in our group.

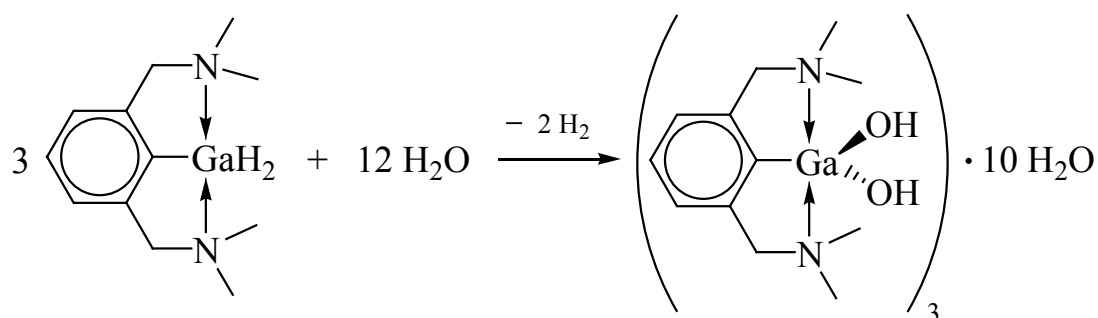
already been published. Similar to the amides discussed above, the hydroxides tend to oligomerize to higher aggregates due to the electropositive aluminum atom and the donor possibilities of the OH ligand. Tetrameric $\{[(\text{Ph}_2\text{Si})_2\text{O}_3]\text{Al}(\mu\text{-OH})\}_4$,^[111] dimeric $[\text{Mes}_2\text{Al}(\mu\text{-OH})]_2 \cdot 3.5\text{THF}$ ^[112] and $\{[(\text{Me}_3\text{Si})_3\text{CAI}(\text{Me})](\mu\text{-OH})\}_2$,^[113] adamantane-like $[(\text{Me}_3\text{Si})_3\text{CAI}]_4(\mu_3\text{-OH})_6 \cdot 0.5\text{THF}$,^[113] and the complex $[\text{Al}_5(t\text{Bu})_5(\mu_3\text{-O})_2(\mu_3\text{-OH})_2(\mu\text{-OH})_2(\mu\text{-O}_2\text{CPh})_2]$ ^[114] can serve as examples of such molecular aluminum hydroxides. The above mentioned $\text{LAl}(\text{OH})_2$,^[38] $[\text{LAl}(\text{OH})]_2\text{O}$,^[109] prepared recently in our group in the two phase system $\text{NH}_3(\text{l})/\text{toluene}$ (Scheme 2), represent the first examples of molecular aluminum hydroxides containing terminal OH moieties.



Scheme 2: Synthesis of $\text{LAl}(\text{OH})_2$ and $[\text{LAl}(\text{OH})]_2\text{O}$ in the two phase system liquid ammonia/toluene.

1.6. Gallium Hydroxides

Compared to the amides the chemistry of gallium hydroxides is more widespread; numerous examples of species containing bridging OH groups are known and also several examples with terminal ones have been described.^[112,113,115–125] The compounds $[\text{R}_2\text{Ga}(\mu\text{-OH})]_2$ ($\text{R} = \text{Mes},^{[28]} i\text{Pr},^{[115]} (\text{Me}_3\text{Si})_2\text{CH},^{[116]}$ and $[\text{RR}'\text{Ga}(\mu\text{-OH})]_3$ ($\text{R} = \text{R}' = t\text{Bu},^{[117,118]} \text{R} = \text{R}' = \text{Ph},^{[119]} \text{R} = (\text{Me}_3\text{Si})_3\text{C} \text{ R}' = \text{Me})^{[113]}$ are representatives of bridged hydroxides, whereas $[(t\text{Bu}_3\text{Si})\text{Ga}(\text{OH})(\mu\text{-OH})]_4$ ^[120] contains both, bridging and terminal OH groups, respectively. In 1994 D. A. Atwood *et al.* reported the preparation of the first gallium dihydroxide stabilized by a bulky pincer type ligand, $\{[2,6\text{-(Me}_2\text{NCH}_2\text{)C}_6\text{H}_3]\text{Ga}(\text{OH})_2\}_3 \cdot 10\text{H}_2\text{O}$ (Scheme 3), from the corresponding dihydride and water.^[121] Its surprising stability is demonstrated by the presence of ten equivalents of water per three molecules of the dihydroxide in the crystal lattice. Recently, J. C. Goodwin *et al.* reported on hydroxo clusters based on gallium $[\text{Ga}_8(\text{heidi})_4(\mu_3\text{-OH})_2(\mu\text{-OH})_8(\text{H}_2\text{O})_4(\text{py})_2]^{3+}$ and $[\text{Ga}_{13}(\text{heidi})_6(\mu_3\text{-OH})_6(\mu\text{-OH})_{12}(\text{H}_2\text{O})_6]^{3+}$ (heidi = $[\text{HOCH}_2\text{CH}_2\text{N}(\text{CH}_2\text{COOH})_2]$, py = pyridine).^[122]



Scheme 3: Synthesis of $\{[2,6\text{-(Me}_2\text{NCH}_2\text{)C}_6\text{H}_3]\text{Ga}(\text{OH})_2\}_3 \cdot 10\text{H}_2\text{O}$

1.7. Scope and Aim of the Present Work

The Sections 1.2.–1.6. describe the importance of aluminum and gallium chalcogenides, amides and hydroxides as precursor for material science and industry. Furthermore, the chemistry of aluminum and gallium compounds containing simple functionalities as SH, OH, NH₂ is not well explored. New synthetic strategies starting from easily accessible precursor as halides or hydrides leading to these species are thus desired. Based on these premises, the objectives of the present work are:

1. to develop new synthetic strategies for the preparation of molecular hydrogensulfides, hydroxides and amides based on aluminum and gallium β -diketiminato complexes.
2. to use these species to synthesize heterobimetallic systems.
3. to use spectral methods such as NMR spectroscopy, IR spectrometry and X-Ray structural analysis to characterize the obtained products.
4. to elucidate the reaction mechanisms for these systems.

2. Results and Discussion

2.1. Compounds Containing Aluminum–Chalcogen Bonds

2.1.1. Phosphine Catalyzed Reactions of LAIH_2 with Elemental Chalcogenides

Recently we have developed an easy access for the the preparation of $\text{LAl}(\text{SeH})_2$ from LAIH_2 and gray selenium.^[26] The reaction between LAIH_2 and elemental tellurium was examined, but no pure product was obtained. Green needles obtained from the reaction mixture after 15 h reflux in toluene were interpreted based on their MS spectra as $\text{LAl}(\mu\text{-Te})_2\text{Al}$.^[126] As the next step the reaction of LAIH_2 and S_8 in toluene was examined, but did not lead to any isolable product even at elevated temperature. Nevertheless, the EI-MS spectra revealed the presence of traces of the desired product $\text{LAl}(\text{SH})_2$. Because phosphines are known to activate elemental chalcogenides,^[127–129] a catalytical amount of trimethylphosphine was added to a toluene solution of LAIH_2 and S_8 in a molar ratio of 4:1 at ambient temperature. Immediately after the addition the pale yellow solution turned to deep yellow. The solution was stirred for additional 5 hours and then all the volatiles were removed *in vacuo*. After recrystallization from toluene pale yellow crystals of $\text{LAl}(\text{SH})_2$ (**1**) were isolated. Further experiments determined $\text{P}(\text{NMe}_2)_3$ to be the best catalyst for this reaction leading to quantitative conversion of LAIH_2 into **1**. In order to investigate the role of phosphine in the reaction, the ^1H and ^{31}P NMR spectra were periodically monitored. From ^1H NMR studies it was evident that the reaction proceeds *via* the unstable reactive intermediate $\text{LAlH}(\text{SH})$ (Figure 5). The ^{31}P NMR spectrum showed, that the phosphine is oxidized to $\text{SP}(\text{NMe}_2)_3$ (^{31}P NMR δ 82.4 ppm; literature 81.5 ppm),^[130] indicating its role as the catalyst in the reaction. This hypothesis was confirmed by carrying out another experiment directly with $\text{SP}(\text{NMe}_2)_3$ as catalyst instead of $\text{P}(\text{NMe}_2)_3$. Indeed, the conversion of LAIH_2 to **1** was observed. However, no reaction between LAIH_2 and $\text{SP}(\text{NMe}_2)_3$ occurred when the components were mixed in a 1:2 molar ratio without additional sulfur. Therefore we believe that $\text{SP}(\text{NMe}_2)_3$ reacts in the first step by a [2+1]-cycloaddition with sulfur to form the reactive intermediate $(\text{S}_2)\text{P}(\text{NMe}_2)_3$. The formation of such a species was shown to be favored by theoretical calculations of the model compound SPH_3 using the RHF/3-21 G* method,^[131] where ΔE has been estimated to -183.0 kJ/mol for the reaction of SPH_3 and S to $(\text{S}_2)\text{PH}_3$. Most likely $(\text{S}_2)\text{P}(\text{NMe}_2)_3$ forms a complex with LAIH_2 by opening the S–S bond and subsequently

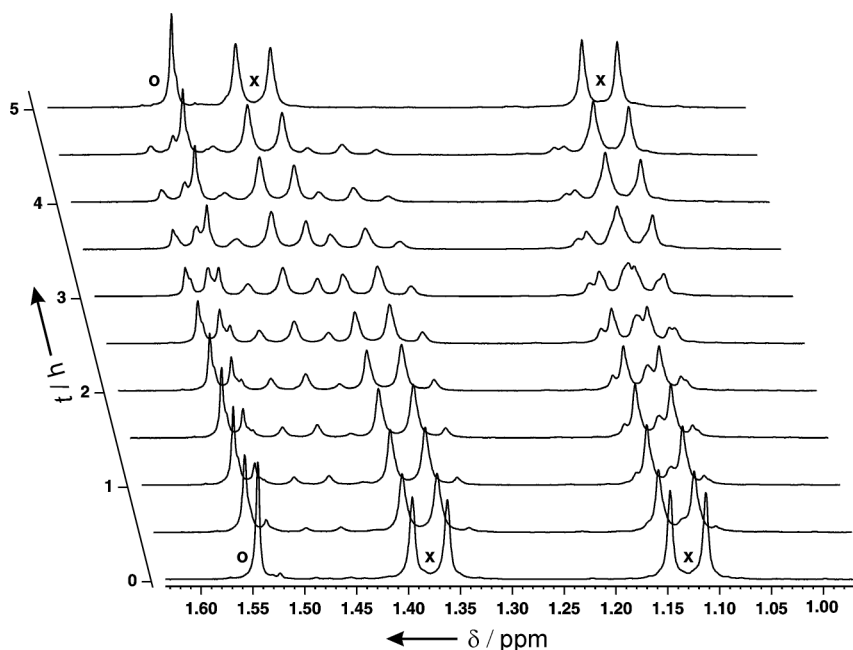
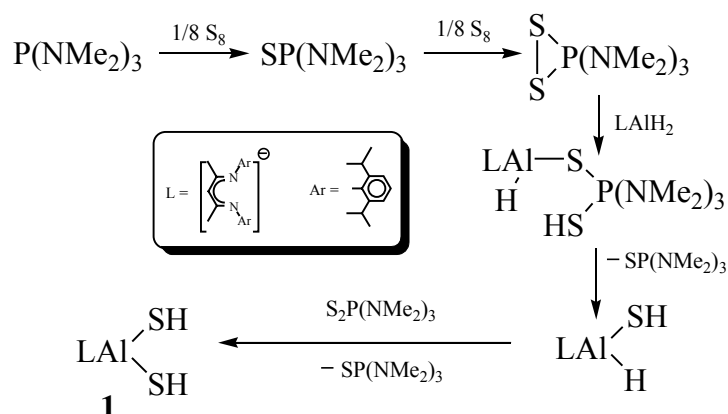


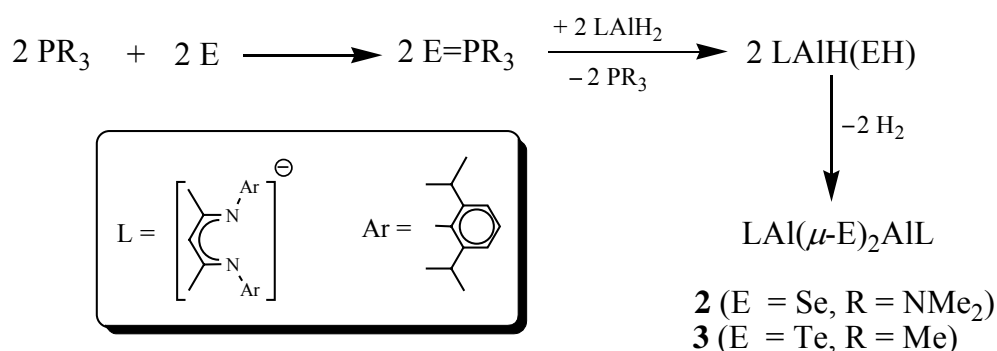
Figure 5: ^1H NMR kinetic study of the conversion of LAIH_2 to $\text{LAI}(\text{SH})_2$. Resonances between δ 1.5 and 1.55 ppm are assigned to the backbone methyl protons (o) and the doublets belong to the diastereotopic methyl protons of the *i*Pr moieties (x).

inserts into one of the Al–H bonds to yield $[\text{LAI}(\text{H})\text{--S--P}(\text{SH})(\text{NMe}_2)_3]$ as an intermediate. In the following step, hydrogen transfer and, ‘umpolung’ of the hydridic to the protonic form of the hydrogen atom takes place. Finally, a proton transfer occurs from one sulfur atom to the other and thus the catalyst is regenerated (Scheme 4). Compound **1** is thermally reasonable stable and does not decompose even after heating to 80 °C for 5 h, but as discussed later, undergoes easily hydrolysis after contact with water. Taking into account this influence of the phosphine on the reaction, the same phosphine catalyst was applied within the $\text{LAIH}_2/\text{Se}(\text{Te})$ systems. Addition of catalytic amounts of $\text{P}(\text{NMe}_2)_3$ or PMe_3 to suspensions of LAIH_2 with red Se and Te, respectively, resulted in the formation of $\text{LAI}(\mu\text{-E})_2\text{AlI}$ (**2** E = Se; **3** E = Te) in



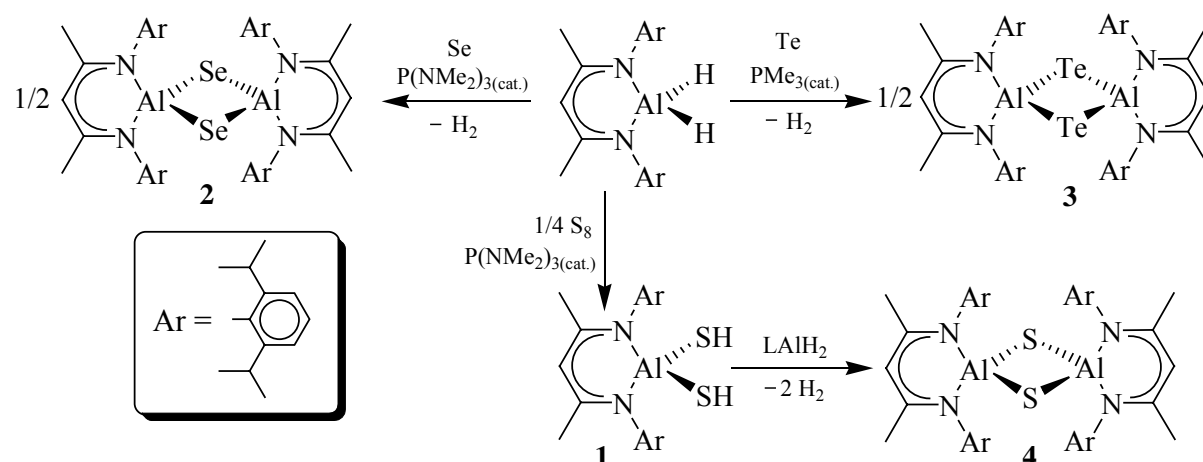
Scheme 4: Proposed mechanism for insertion of sulfur into Al–H bonds

high yields at ambient temperature. Compounds **2** (white) and **3** (pale yellow) are sparingly soluble in common organic solvents such as toluene, dichloromethane, tetrahydrofuran, and thus the green needles obtained from the uncatalyzed reaction by C. Cui *et al.* could not be **3**.^[126] In order to gain further insight regarding the role of the phosphine in these systems, we investigated the reaction mechanism and possible byproducts involved in these reactions. All attempts to monitor the kinetics of these reactions by means of ¹H NMR spectroscopy failed due to the poor solubility of the elemental chalcogens and resulting products. However, earlier experimental data revealed that the formation of **1** proceeds *via* the reactive intermediate, LAIH(SH). In order to obtain further insight into the reaction mechanism, we carried out several experiments by varying the stoichiometry of the starting materials. The most striking result was, that in the presence of the phosphine, LAl(μ -E)₂AlL, analogous to LGa(μ -E)₂GaL (E = O, S) derivatives prepared recently by P. P. Power *et al.*,^[132] were the only products formed, regardless of the stoichiometry of the reagents employed, whereas the direct reaction of LAIH₂ with elemental Se in absence of the phosphine led entirely to the formation of LAl(SeH)₂.^[26] In the latter case, another type of reaction mechanism involving a higher coordinated aluminum center by complexation of Se₂ toward the aluminum has been suggested.^[26,133–135] Due to the fact that TePR₃ compounds are known to be good sources of soluble and reactive Te,^[127–129] we carried out the direct reaction of LAIH₂ with TePET₃ in an equimolar ratio. The reaction led to pure **3** and free PET₃ in almost quantitative yield, indicating that the gas evolved during the reaction is H₂ instead of H₂Te. All the experimental results outlined here are supportive for the proposed reaction mechanism. Therefore, we assume that Se and Te initially react with the corresponding phosphines to yield SeP(NMe₂)₃ and TePMe₃, respectively. These compounds are unstable^[127–129] and react in successive steps with LAIH₂ to yield LAIH(EH) (E = Se, Te) under elimination of phosphine. The last step corresponds to the formation of the LAl(μ -E)₂AlL (E = Se, Te) through an elimination of two molecules of H₂. The cleavage of these species into monomeric units LAIE in the gas phase



Scheme 5: Proposed mechanism of the phosphine catalysis in the synthesis of **2** and **3**.

can indicate an intramolecular elimination followed by dimerization, but we were not able to isolate such intermediates. Scheme 5 shows the steps involved in this reaction. As mentioned above, the reaction between LiAlH_2 and elemental sulfur catalyzed by phosphine leads to $\text{LiAl}(\text{SH})_2$ (**1**) and not to the desired $\text{LiAl}(\mu\text{-S})_2\text{AlLi}$ (**4**). Therefore we used the latent protic character of the hydrogen atoms from the SH groups of **1** and reacted the latter species in refluxing toluene with LiAlH_2 . After 15 h **4** was obtained as an insoluble white microcrystalline solid in 92% yield. Scheme 6 summarizes the preparation of the three compounds. All three compounds decompose without melting at temperatures above 200 °C, indicating their high thermal stability. The high stability of compounds **2–4** is further supported by the EI-mass spectra exhibiting the M^+ ions for the three molecules: m/z 952 (100%) E = S, 1048 (48%) E = Se and 1144 (25%) E = Te. Unfortunately, due to the low solubility of **2–4** we were not able to record NMR spectra.



Scheme 6: Preparation of compounds **2–4**.

2.1.2. X-Ray Structural Characterization of $\text{LiAl}(\text{SH})_2$ (**1**)

The unambiguous molecular geometry of **1** was determined by X-ray crystallography. Pale yellow crystals of **1** were obtained by slow cooling of its saturated toluene solution. The structure of **1** is shown in Figure 6. Compound **1** is isostructural to the Se-analogue. Taking the difference in covalent radii (0.14 Å)^[136] into account, the Al–S bonds (2.223 and 2.217 Å) are comparable to the Al–Se bonds (2.331 and 2.340 Å). Furthermore, the angle S–Al–S (105.4°) is very similar to the Se–Al–Se angle (103.7°).^[26] The Al–S bond distances are also comparable with those of other bridging aluminum-($\mu\text{-S}$)-sulfide bonds, as well as the S–Al–S angle is in the range of those reported in the literature.^[47–49,57,58] The S–H bonds (1.2

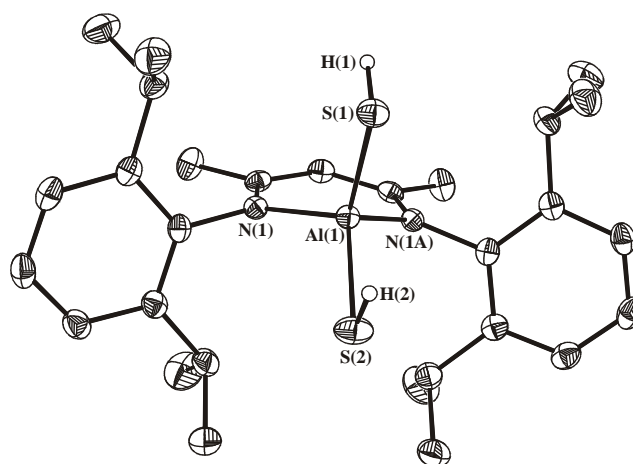


Figure 6: Molecular structure of **1** (50% probability ellipsoids). Hydrogen atoms with the exception of the protons of the SH units, are omitted for clarity. Selected bond lengths [Å] and angles [°]: Al(1)–N(1) 1.891(1), Al(1)–S(1) 2.223(1), Al(1)–S(2) 2.217(1), S(1)–H(1) 1.20 (2), S(2)–H(2) 1.21(3); N(1)–Al(1)–N(1A) 97.3(1), N(1)–Al(1)–S(1) 114.3(1), N(1)–Al(1)–S(2) 112.9(1), S(1)–Al(1)–S(2) 105.4(1), Al(1)–S(1)–H(1) 97(1), Al(1)–S(2)–H(2) 91(2).

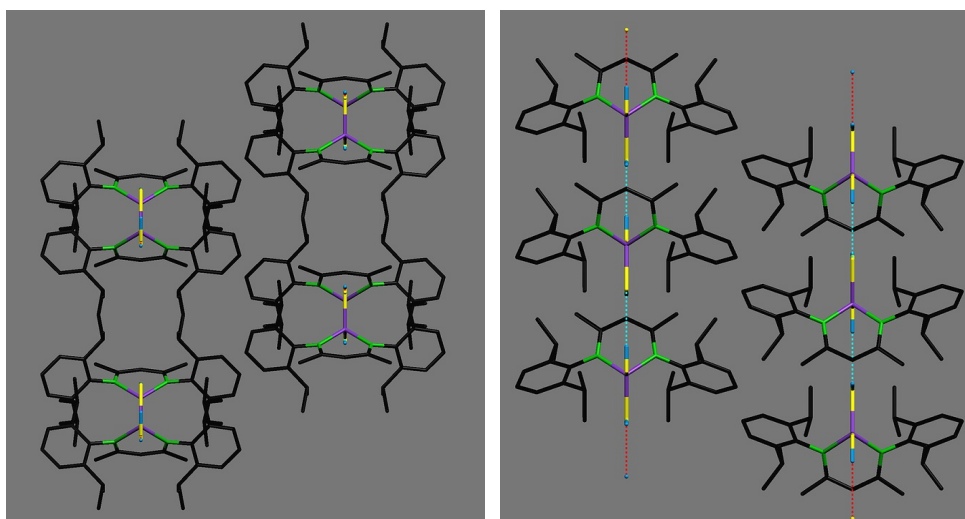


Figure 7: Channels and chains in the crystal of **1** formed by S···H hydrogen bonding. Hydrogen atoms with the exception of the protons of the SH units are omitted for clarity. S·····S 3.531 Å, S–H···S 2.834 Å, 137.3°.

Å) lie in the range (0.99–1.40 Å) of those of terminal S–H groups in other metal complexes.^[137–140] SCF/3-21G* calculations for monomeric H–S–Al=S gave values for Al–S(H) (2.160 Å), S–H (1.33 Å) and Al–S–H (96.0°), respectively.^[141,142] The latter angle is close to those in **1** (97° and 91°). The packing diagram of **1** shows the presence of S–H···S hydrogen bonds forming channels along the crystal c axis and linear chains (along the a axis (Figure 7)).

2.1.3. Molecular Structures of $\text{LAl}(\mu\text{-E})_2\text{AlL}$ ($\text{E} = \text{Se}(\mathbf{2})$, $\text{Te}(\mathbf{3})$, $\text{S}(\mathbf{4})$)

Compounds **2–4** are only sparingly soluble in common organic solvents, and the powders obtained after the syntheses yielded nicely shaped monocrystals from a mixture of toluene/trichloromethane (10:1). The crystallization was achieved by solvation of $\text{LAl}(\mu\text{-E})_2\text{AlL}$ with 2.32 equivalents of trichloromethane and 0.68 equivalents of toluene, sharing the same spatial positions (**4**; $\text{E} = \text{S}$), two molecules of trichloromethane and one molecule of toluene (**2**; $\text{E} = \text{Se}$), and 2.73 molecules of trichloromethane and 0.27 molecules of toluene alternating at the same spatial position (**3**; $\text{E} = \text{Te}$) in the crystal lattice as shown by single crystal X-ray structural analyses (Figures 8–10). The three isostructural compounds

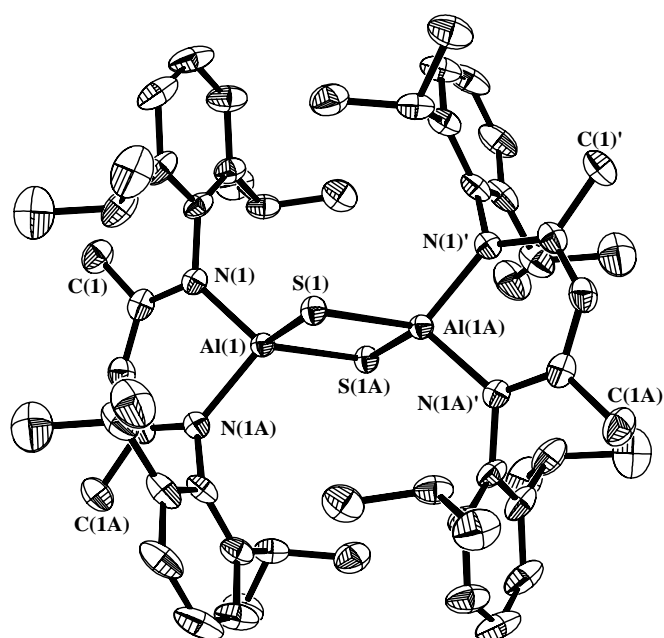


Figure 8: Molecular structure of $\text{LAl}(\mu\text{-S})_2\text{AlL}$ (**4**) $\cdot 0.68\text{C}_7\text{H}_8 \cdot 2.32\text{CHCl}_3$ showing the numbering scheme (50% probability ellipsoids). Hydrogen atoms and solvent molecules are omitted for clarity.

crystallize in the monoclinic space group $C2/m$ and possess almost identical cell parameters (see Tables CD2–CD4 in the Section 6.). Taking into account the covalent radii (1.02 S, 1.17 Se and 1.35 Å Te),^[136] the Al–S (2.237 and 2.245 Å), Al–Se (2.359 and 2.370 Å) and Al–Te bonds (2.575 and 2.581 Å) are comparable to one another. Furthermore, the $\text{E}(1)\text{–Al–E}(1\text{A})$ angles vary from 96.5° in **4** to 97.9° in **3** due to the larger radius of the chalcogen atom. All Al_2E_2 rings are due to the symmetry essentially planar, and the Al–E bond distances are analogous to those of similar Al_2E_2 species (2.208–2.248 Å, $\text{E} = \text{S}$; 2.221–2.381 Å, $\text{E} = \text{Se}$;

2.562–2.588 Å, E = Te), but the E(1)–Al–E(1A) (E = Se, Te) angles are significantly less obtuse than those reported in the literature (99.9–103.6° for Se and 102.8–103.8° for Te) [42–50] due to the steric bulk of the β -diketiminato ligand. The latter values are comparable to those of Al_4E_4 clusters, (94.2–99.2° for Se and 94.1–96.3° for Te), [52,53] where the chalcogen atoms are always coordinated to three aluminum atoms. The S(1)–Al–S(1A) angle fits within the range of similar compounds (95.9–101.9°). [47–49] Selected bond lengths and angles for **2–4** are listed in Table 1.

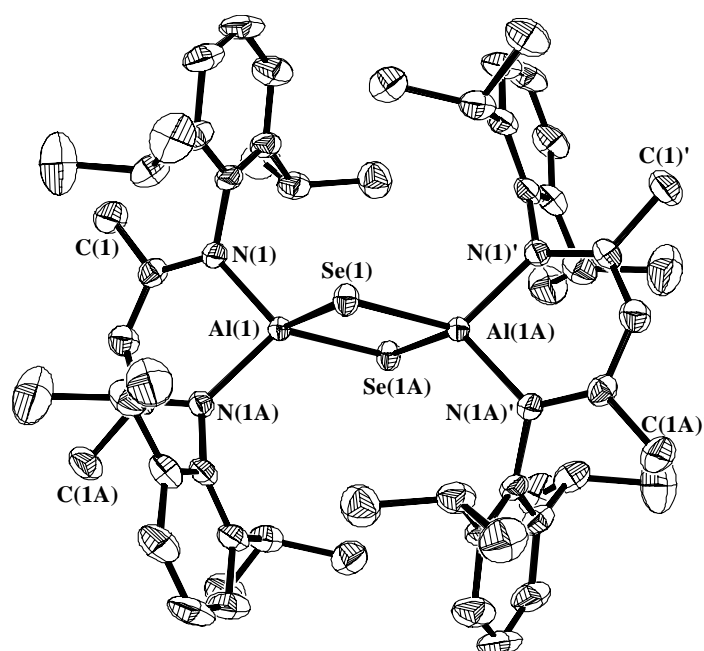


Figure 9: Molecular structure of $\text{LAl}(\mu\text{-Se})_2\text{AlL}$ (**2**) · C_7H_8 · 2CHCl_3 showing the numbering scheme (50% probability ellipsoids). Hydrogen atoms and solvent molecules are omitted for clarity.

Table 1: Comparison of selected bond lengths [Å] and angles [°] for **2–4** (esd's in brackets)

	2 · C_7H_8 · 2CHCl_3 [E = Se]	3 · $0.27\text{C}_7\text{H}_8$ · 2.73 CHCl_3 [E = Te]	4 · $0.68\text{C}_7\text{H}_8$ · 2.32 CHCl_3 [E = S]
Al–N	1.924(3)	1.908(5)	1.928(2)
Al–E(1)	2.359(2)	2.575(3)	2.237(1)
Al–E(1A)	2.370(2)	2.581(2)	2.245(1)
E(1)–Al–E(1A)	97.5(1)	97.9(1)	96.5(1)
Al(1)–E–Al(1A)	82.5(1)	82.1(1)	83.5(1)

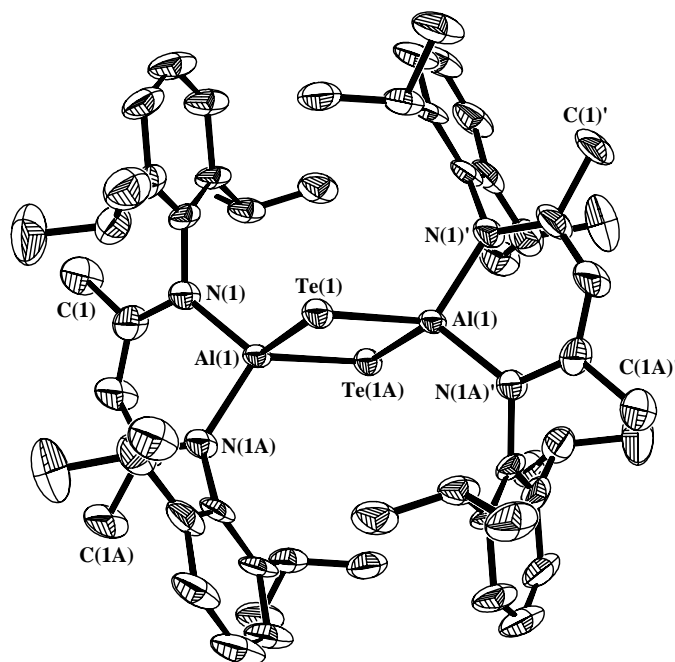


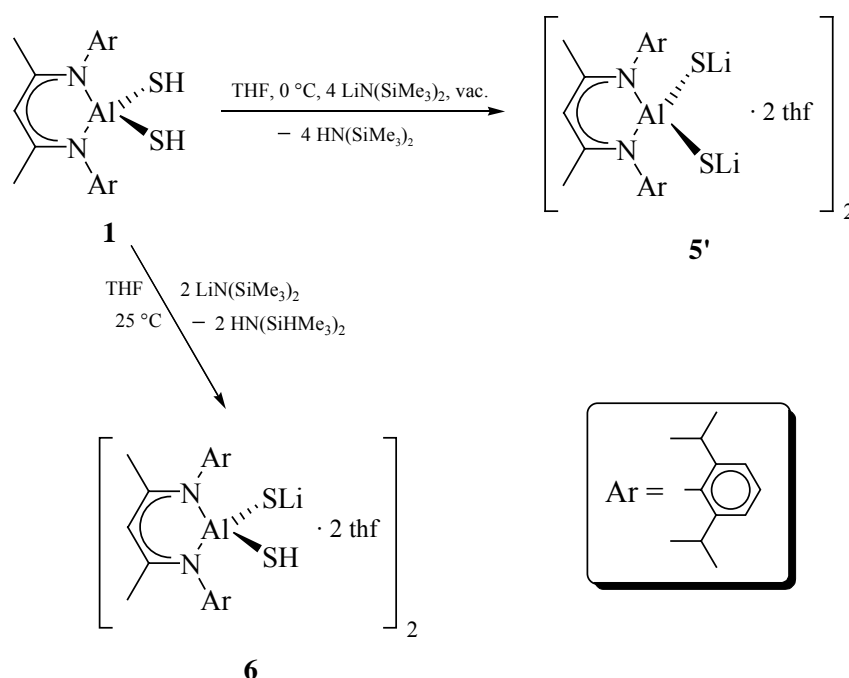
Figure 10: Molecular structure of $\text{LAl}(\mu\text{-Te})_2\text{AIL}$ (**3**) $\cdot 0.27\text{C}_7\text{H}_8 \cdot 2.73\text{CHCl}_3$ showing the numbering scheme (50% probability ellipsoids). Hydrogen atoms and solvent molecules are omitted for clarity.

2.2. Reactions of $\text{LAl}(\text{SH})_2$

2.2.1. Lithiation of the SH Groups

Following the protocol of H. Nöth *et al.* on the preparation of aluminum-lithium salts from LiAlH_4 and thiols,^[143] we chose the lithiation of **1** with MeLi and *n*BuLi in diethyl ether or THF as an alternative route to the desired compounds. Unfortunately, under the given conditions the decomposition of **1** was observed. However, the difficulties encountered in the preparation of the dilithium salt $\{\text{LAl}[(\text{SLi})_2(\text{thf})_3]\}_2 \cdot 2\text{THF}$ (**5**) were overcome by direct reaction of **1** with two equivalents of $\text{LiN}(\text{SiMe}_3)_2$ in THF at 0 °C. The extremely sensitive pale yellow product **5** is a dimer solvated by eight molecules of THF as proved by X-ray structural analysis. It has low solubility in THF and forms a microcrystalline precipitate within a few seconds of starting materials being mixed. The recovery of the crystals was performed within 15 min. of the addition of the solvent to avoid decomposition caused by free $\text{HN}(\text{SiMe}_3)_2$. However, compound **5** loses THF upon drying *in vacuo*, leading to a dimeric product $\{\text{LAl}[(\text{SLi})_2(\text{thf})_2]\}_2$ (**5'**) containing only four molecules of THF as determined by ^1H NMR spectroscopy. This final product proved to be stable upon storage for several months

under an inert atmosphere. After the successful isolation of **5'**, we became interested in the preparation of the monolithium salt $\{LAl(SH)[SLi(thf)_2]\}_2$ (**6**). To our knowledge such systems are not known for any kind of metal and, could be precursors for substitution reactions. For the preparation of **6** a similar method was used as for **5'**. After removal of all volatiles *in vacuo* compound **6** was isolated in an 85% yield. Moreover, no decomposition was detected in the presence of $HN(SiMe_3)_2$ or during the removal of the solvent, thus demonstrating a higher stability of **6** compared to that of **5**. As expected, **6** has a dimeric arrangement in the solid state, with each lithium atom coordinated to two molecules of THF and two sulfur atoms. The amount of THF in **6** remains unchanged even after keeping **6** for several hours *in vacuo* (Scheme 7).



Scheme 7: Synthesis of the lithium salts **5'** and **6**.

2.2.2. Structures of $\{LAl[(SLi)_2(thf)_3]\}_2 \cdot 2THF$ (**5**) and $\{LAl(SH)[SLi(thf)_2]\}_2$ (**6**)

X-ray quality crystals of **5** and **6** were obtained by slow cooling their THF solutions. Both derivatives crystallize in the monoclinic space group $P2(1)/n$ as pale yellow crystals. Compound **6** shows a simple coordination environment for the Li atoms $[LAl(SH)(\mu_3-S)(\mu-Li \cdot 2THF)_2(\mu_3-S)Al(SH)L]$, while the structure of **5** is more complex and none of the four lithium atoms are equivalent. As depicted in Figure 11, the lithium atoms Li(1), Li(2) and Li(4) are coordinated by two, one, and three THF molecules, respectively, whereas the Li(3)

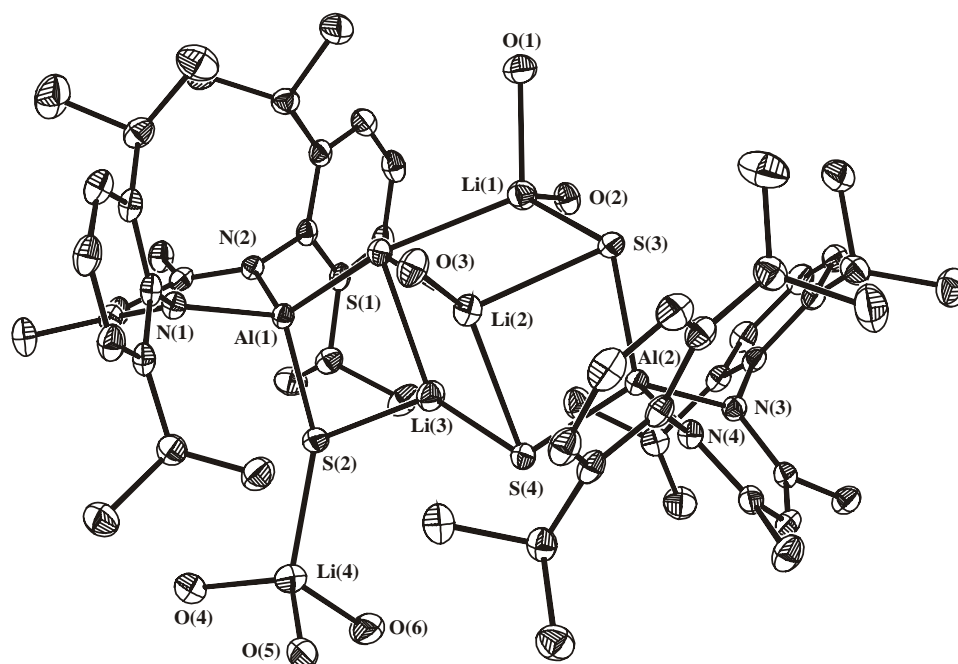


Figure 11: Molecular structure of $\{LAl[(SLi)_2(thf)_3]\}_2 \cdot 2THF$ (**5**) with 50% probability ellipsoids. All hydrogen atoms, uncoordinated THF molecules and carbon atoms of the coordinated THF molecules are omitted for clarity. Selected bond lengths [Å] and angles [°]: Al(1)–S(1) 2.186(1), Al(1)–S(2) 2.182(1), Al(2)–S(3) 2.173(1), Al(2)–S(4) 2.181(1), Li(1)–S(1) 2.482(2), Li(1)–S(3) 2.414(2), Li(2)–S(1) 2.544(2), Li(2)–S(3) 2.449(2), Li(2)–S(4) 2.565(2), Li(3)–S(1) 2.502(2), Li(3)–S(2) 2.345(2), Li(3)–S(4) 2.323(2), Li(4)–S(2) 2.343(3); S(1)–Al(1)–S(2) 111.6(1), S(3)–Al(2)–S(4) 113.0(1), Al(1)–S(1)–Li(1) 149.6(1), Al(1)–S(1)–Li(2) 126.3(1), Al(1)–S(1)–Li(3) 74.3(1), Al(1)–S(2)–Li(3) 77.7(1), Al(1)–S(2)–Li(4) 152.1(1), Al(2)–S(3)–Li(1) 114.8(1), Al(2)–S(3)–Li(2) 76.3(1), Al(2)–S(4)–Li(2) 73.7(1), Al(2)–S(4)–Li(3) 118.0(1), Li(1)–S(1)–Li(2) 68.2(1), Li(1)–S(1)–Li(3) 92.5(1), Li(1)–S(3)–Li(2) 70.8(1), Li(2)–S(1)–Li(3) 66.0(1), Li(2)–S(4)–Li(3) 68.2(1), Li(3)–S(2)–Li(4) 116.8(1), S(1)–Li(1)–S(3) 112.1(1), S(1)–Li(2)–S(3) 108.9(1), S(1)–Li(2)–S(4) 107.8(1), S(1)–Li(3)–S(2) 96.4(1), S(1)–Li(3)–S(4) 117.6(1), S(2)–Li(3)–S(4) 134.6(1), S(3)–Li(2)–S(4) 92.8(1).

atom is not coordinated to THF. This structural diversity may be due to the steric bulk of the ligands L. The two THF molecules coordinated to Li(1) require there to be more space between the 2,6-*i*Pr₂C₆H₃ moieties of L and thus force the substituents on the opposite side closer together. This steric pressure results in Li(4) being pushed out of the central area of the dimer. Subsequently the coordination of three THF molecules covers the unsaturated sites on Li(4). For the two remaining Li atoms the situation is similar. Li(2) can still be coordinated by one THF molecule whereas Li(3) is coordinated only to three sulfur atoms. These different

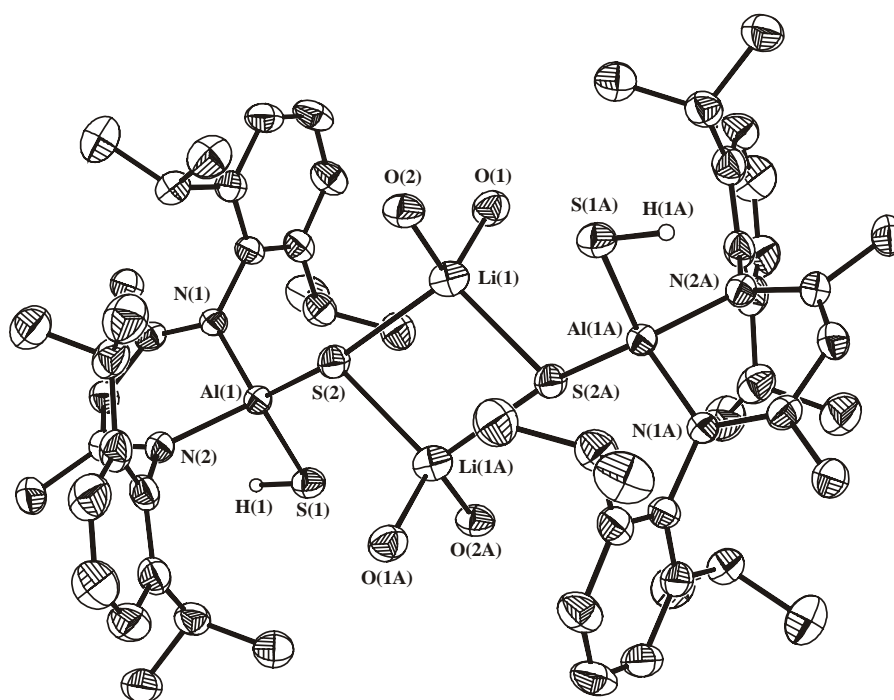
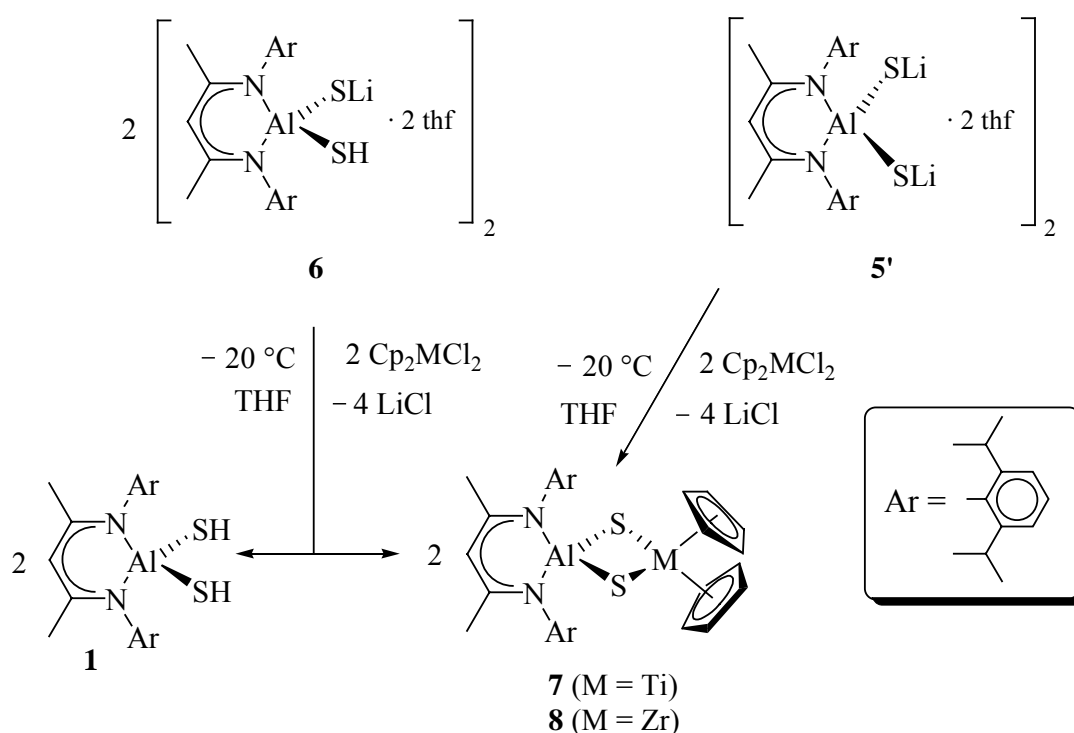


Figure 12: Molecular structure of $\{LAl(SH)[SLi(thf)_2]\}_2$ (**6**) with 50% thermal ellipsoids. All hydrogen atoms except the ones from S–H groups and carbon atoms of the THF molecules are omitted for clarity. Selected bond lengths [\AA] and angles [$^\circ$]: Al(1)–N(1) 1.928(2), Al(1)–N(2) 1.935(2), Al(1)–S(1) 2.268(1), Al(1)–S(2) 2.123(1), H(1)–S(1) 1.28(5), Li(1)–S(2) 2.478(5), Li(1)–S(2A) 2.424(5), S(1)–Al(1)–S(2) 115.7(1), Al(1)–S(2)–Li(1) 151.6(1), Al(1)–S(2)–Li(1A) 111.7(1), Li(1)–S(2)–Li(1A) 78.0(2), S(2)–Li(1)–S(2A) 102.0(2).

coordination sites of lithium atoms are compensated by the variation of the Li–S bond lengths (2.323–2.565 \AA). The $Al_2S_4Li_4$ core can also be described as being a six-membered AlS_3Li_2 ring with alternating sulphur and metal atoms, which is capped by another lithium atom and a bent Al–S–Li unit is joined to one of the S–Li edges of this hexagonal pyramid to form a condensed four-membered AlS_2Li ring. The shortness of the S(4)–Li(3) bond (2.323 \AA) is caused by the unsaturated coordination sphere of Li(3) which contains only three sulfur atoms and is one of the shortest S–Li bonds observed to date.^[144–146] All other S–Li bonds of **5** (2.343–2.565 \AA) and **6** (2.424 and 2.478 \AA) are in the range observed for similar species (2.327–2.964 \AA).^[143–154] Figure 12 shows the molecular structure of **6** in which the S_2Li_2 core is essentially planar owing to the crystal symmetry. This S_2Li_2 motif can be found in many substances containing these two elements including **5**.^[143–154] The free SH groups are not involved in any kind of hydrogen bonding and are orientated *trans* to each other.

2.2.3. Reactions of **5** and **6** with Cp_2MCl_2 ($M = \text{Ti}, \text{Zr}$) and Structural Characterization of $\text{LAl}(\mu\text{-S})_2\text{TiCp}_2$ (**7**)

To date very few examples of heterobimetallic sulfides with aluminum bridging sulfide are known. Such species include $[(t\text{BuAl})(t\text{BuAlMe})_2(\mu_3\text{-S})_3\text{ZrCp}_2]$ ($\text{Cp} = \text{C}_5\text{H}_5$), prepared by degradation of the $[\text{tBuAl}(\mu_3\text{-S})]_4$ cage with two equivalents of Cp_2ZrMe_2 .^[155] Moreover, there are known aluminum sulfides with $[\text{AlS}]_n$ core, which can be either planar ($n = 2$), cubic ($n = 4$), drum ($n = 6$), or possess more complex structures with an Al:S molar ratio different from 1:1.^[42–63] Attempts to prepare heterobimetallic sulfides with **1** and ZnMe_2 or CdMe_2 through alkane elimination failed, in spite of the high affinity of these elements toward chalcogens.^[157] We observed even at low temperature only the formation of inseparable mixtures of products and the free ligand. This situation is in contrast to the successful preparation of $\text{LAl}(\mu\text{-S})_2\text{AlL}$ (**4**) from **1** and LAlH_2 . Having the two salts **5** and **6** available, we focussed on reactivity studies of **5'** and **6** toward the transition metal halides, namely Cp_2TiCl_2 and Cp_2ZrCl_2 . When a solution of Cp_2MCl_2 ($M = \text{Ti}, \text{Zr}$) in THF was added dropwise to the solution of **5'** in THF at -20°C , the color of the resulting mixtures became brownish-green, $M = \text{Ti}$, and deep yellow for $M = \text{Zr}$. After removal of the THF, extraction of the crude product with toluene, and several purification steps, compounds $\text{LAl}(\mu\text{-S})_2\text{MCp}_2$ (M



Scheme 7: Preparation of bimetallic sulfides **7** and **8**.

= Ti (**7**), M = Zr (**8**)) were isolated in 89% and 85% yield, respectively. Surprisingly the reaction of **6** with Cp_2TiCl_2 or Cp_2ZrCl_2 in a molar ratio of 2:1 did not yield the expected $[\text{LAl}(\text{SH})\text{S}]_2\text{MCp}_2$ but rather mixture of **1** and **7** (or **8**) is formed. This result suggests that the formation of the four-membered ring $\text{LAl}(\mu\text{-S})_2\text{MCp}_2$ is preferred over a $\text{LAl}(\text{SH})\text{-S-M}(\text{Cp}_2)\text{-S-Al}(\text{SH})\text{L}$ chain arrangement containing free SH groups. One pathway for the formation of **1** and **7** (or **8**) in the above reaction may involve the intermediate $\text{LAl}(\text{SH})(\mu\text{-S})\text{M}(\text{Cl})\text{Cp}_2$, followed by translithiation with a second molecule of **6** yielding **1** and $\text{LAl}(\text{SLi})(\mu\text{-S})\text{M}(\text{Cl})\text{Cp}_2$. Subsequently, $\text{LAl}(\text{SLi})(\mu\text{-S})\text{M}(\text{Cl})\text{Cp}_2$ undergoes an intramolecular elimination of LiCl to yield $\text{LAl}(\mu\text{-S})_2\text{MCp}_2$. A second possible mechanism is an *in situ* formation of $[\text{LAl}(\text{SH})(\mu\text{-S})]_2\text{MCp}_2$ followed by its rapid rearrangement to yield **1** and **7** (or **8**) (Scheme 7).

Crystals of **7** were obtained by slow cooling of a toluene/hexane solution. Compound **7** crystallizes in the monoclinic space group $P2_1$ and its molecular structure is shown in Figure 13. The AlS_2Ti ring is essentially planar with the sum of the inner angles of 360° . The widest angle (102.5°) corresponds to that at the aluminum center, while the one at the

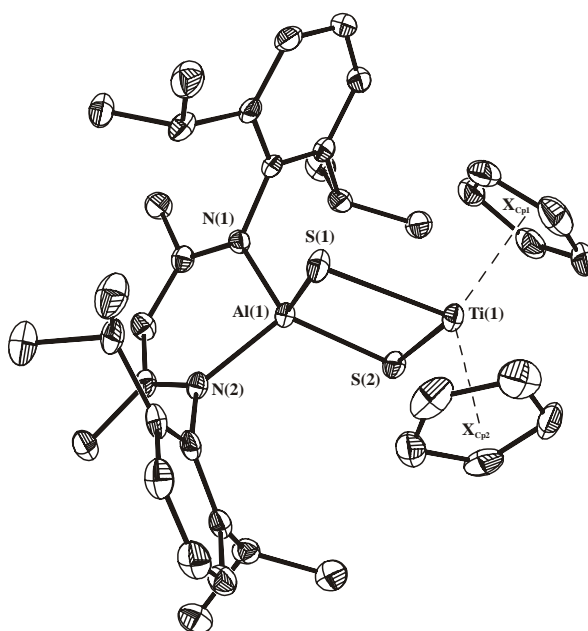
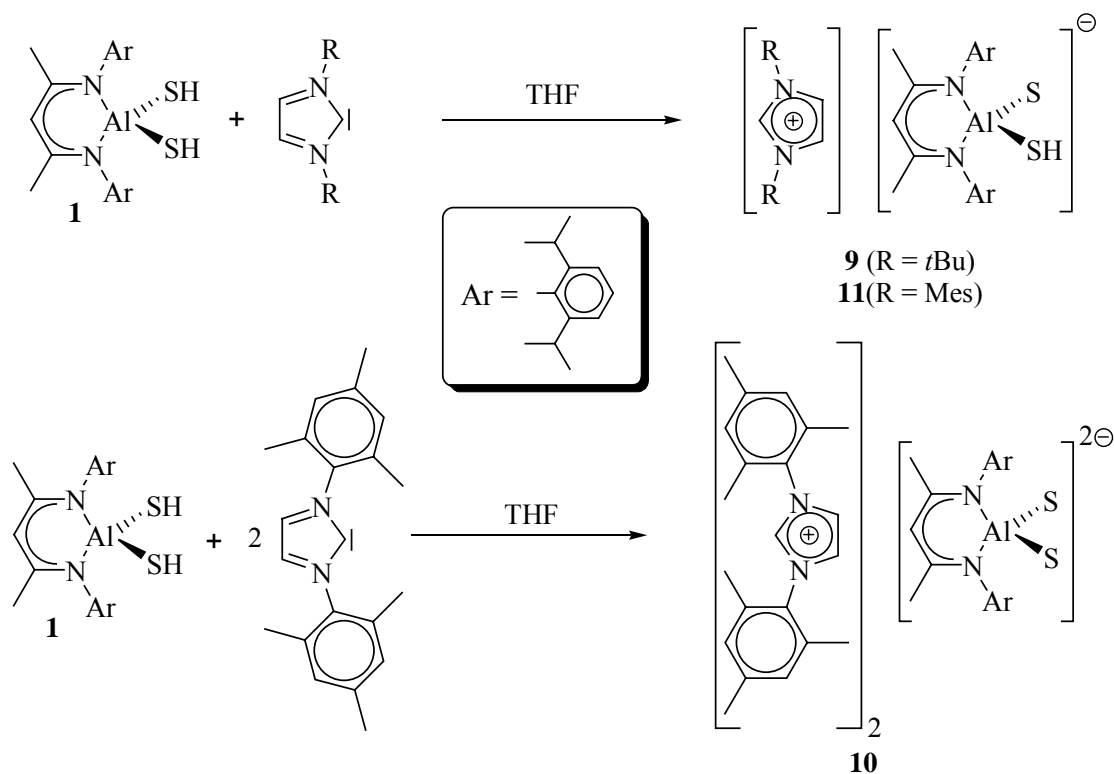


Figure 13: Molecular structure of $\text{LAl}(\mu\text{-S})_2\text{TiCp}_2$ (**7**) with 50% thermal ellipsoids. All hydrogen atoms are omitted for clarity. Selected bond lengths [\AA] and angles [$^\circ$]: $\text{Al}(1)\text{-N}(1)$ 1.918(2), $\text{Al}(1)\text{-N}(2)$ 1.921(2), $\text{Al}(1)\text{-S}(1)$ 2.208(1), $\text{Al}(1)\text{-S}(2)$ 2.197(1), $\text{Ti}(1)\text{-S}(1)$ 2.416(1), $\text{Ti}(1)\text{-S}(2)$ 2.473(1), $\text{Ti}(1)\text{-X}_{\text{Cp1}}$ 2.091(3), $\text{Ti}(1)\text{-X}_{\text{Cp2}}$ 2.090(3); $\text{S}(1)\text{-Al}(1)\text{-S}(2)$ $102.5(1)$, $\text{Al}(1)\text{-S}(1)\text{-Ti}(1)$ $84.7(1)$, $\text{Al}(1)\text{-S}(2)\text{-Ti}(1)$ $83.6(1)$, $\text{S}(1)\text{-Ti}(1)\text{-S}(2)$ $89.3(1)$, $\text{X}_{\text{Cp1}}\text{-Ti}(1)\text{-X}_{\text{Cp2}}$ $130.0(2)$.

titanium center is almost a right angle (89.3°). The Ti–X_{Cp} distances (X_{Cp} is the centroid of the Cp group) are 2.091 and 2.090 Å and the X_{Cp1}–Ti–X_{Cp2} angle is 130°. All these data are in good agreement with those reported for Cp₂Ti(μ-S)₂ML'L'' (M = Si, Ti, Ru, L' = Cp, L'' = Cl) species (2.425–2.458 Å for Ti–S, 2.059–2.093 Å for X_{Cp}–Ti, 129.6–131.6° for X_{Cp1}–Ti–X_{Cp2} and 86.5–95.9° for the S–Ti–S angle).^[157–160] The substitution of the SH protons by Li or Ti has a significant influence on the Al–S bond length. The Al–S bond lengths decrease in the series from **1** (2.223 and 2.217 Å) to **7** (2.208 and 2.197 Å), to **5** (2.173–2.186 Å), and finally to **6** (2.123 Å). The partial negative charge on the substituted sulfur atoms in **6** causes a shortening of the Al–S bond and thus, increases the electron density on the aluminum centers resulting in an elongation of the Al–S(H) bonds (2.268 Å).

2.2.4. Deprotonation of LAl(SH)₂ with N-Heterocyclic Carbenes and Crystal Structures of C_tH⁺[LAl(SH)(S)][–] (**9**) and C_mH⁺[LAl(SH)(S)][–] (**11**)

Next we focused on the preparation of compounds containing “free” Al–S[–] groups, which have not yet been reported. These species were of interest as a precursors for further reactions, due to their high nucleophilicity. The N-heterocyclic carbenes were chosen for deprotonation of the SH moieties, because they have proved to be strong bases;^[161] the formation of the σ C–H bond between the carbene and the proton is almost irreversible in absence of a stronger base (*t*BuOK, KH).^[162] Furthermore, many imidazolium salts stabilized by weakly coordinating anions (e.g. BPh₄[–], PF₆[–], Cd(SCN)₃[–])^[163–166] have been synthesized so far. The reaction between **1** and N,N'-bis-*t*butylimidazolyl carbene^[162] in an equimolar ratio in THF resulted in a formation of expected monoimidazolium salt C_tH⁺[LAl(SH)(S)][–] (C_tH⁺ = N,N'-bis-*t*butylimidazolium) (**9**) as proved by structural analysis. Surprisingly, the reaction between **1** and N,N'-bis-*t*butylimidazolyl carbene in the molar ratio 1:2 did not give the expected C_tH⁺₂[LAl(S)₂]^{2–}, but led to a mixture of **9** and unreacted free carbene. Double deprotonation was successfully achieved by using two equivalents of N,N'-bis-mesitylimidazolyl carbene^[167] giving quantitatively C_mH⁺₂[LAl(S)₂]^{2–} (C_mH⁺ = N,N'-bis-mesitylimidazolium) (**10**). This species is not stable and decomposes in both in solution and in solid state even at low temperature to C_mH⁺[LAl(SH)(S)][–] (**11**), which can also be prepared by direct reaction of **1** with one equivalent of N,N'-bis-mesitylimidazolyl carbene (Scheme 8). The ¹H NMR spectra of **10** and **11** are very similar and indicate for both species symmetric



Scheme 8: Synthesis of imidazolium salts **9–11**.

substitution on the Al center with absence of SH protons, although this condition is not fulfilled for **11** (one Al–S[−] and one Al–SH moiety). This can be explained by fast proton migration. Further measurements revealed, that this process is fast even at low temperature and starts immediately after mixing **1** with small amounts of the carbene. In the presence of traces of air, the pale yellow solutions of these three salts turned to green-blue indicating their easy decomposition to unidentified products with most probably radical character. This color remained for three days when the flasks were stored at −30 °C, but disappeared within one hour at ambient temperature. Small amounts of insoluble material were formed during this period, but longer storage of these solutions did not lead to further decomposition. Pale yellow crystals of compounds **9** and **11** were obtained by slow crystallization of their saturated THF solutions at −32 °C. Compound **9** crystallizes in the orthorhombic space group *P*2₁2₁2₁, and **11** in the monoclinic space group *P*2₁/*c*. Both **9** and **11** contain one ion pair and one solvating THF molecule in the asymmetric unit (Figures 14–17). The deprotonation of the SH moiety resulted in formation of a “naked” Al–S[−] center and had big influence on the geometry of the N₂AlS₂ core. The Al–S[−] bond lengths are 2.114 Å for **9** and 2.115 Å for **11**. These two are the shortest Al–S bonds described so far (compare with 2.159–2.483 Å for known covalent Al–S bonds),^[49,57,58,61,168–173] while the remaining Al–S(H) bonds are with

2.288 (**9**) and 2.279 Å (**11**) significantly longer than those in **1** (2.217 and 2.223 Å). The negative charge on the sulfur is in both cases compensated by two close contacts to hydrogen atoms of the two independent imidazolium cations. In the case of **11** the first cation coordinates to the sulfur by the hydrogen on the C(2) (MesN–CH–NMe₃; S \cdots H 2.455 Å), while the second cation involves the hydrogen atom on the C(4) (MesN–CH–CH–NMe₃; 2.631 Å) in this interaction. In compound **9** the bonding mode is the same as for **11**, the first cation (*t*BuN–CH–N*t*Bu; S \cdots H 2.538 Å) and the second (*t*BuN–CH–CH–N*t*Bu; 2.761 Å). These weak interactions are depicted in Figures 16 and 17. The originally deformed tetrahedral core N₂AlS₂ in LAl(SH)₂ is in **9** and **11** further deformed so the N–Al–N angles are less obtuse (97.3 in **1**, 95.1 in **9**, 95.7° in **11**) and the S–Al–S angles become wider (105.4 in **1**, 115.0 in **9**, 117.8° in **11**). Selected bond lengths and angles for lithium and imidazolium salts of LAl(SH)₂ are tabulated for comparison in Table 2.

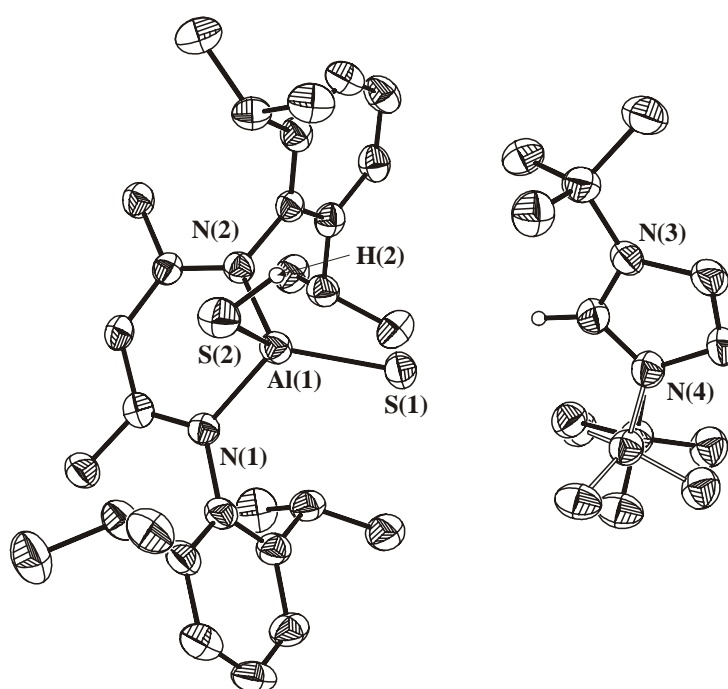


Figure 14: Molecular structure of **9** · THF (50% probability ellipsoids). Hydrogen atoms (except the S–H and N–CH–N protons), and solvent molecule are omitted for clarity. Selected bond lengths [Å] and angles [°]: Al(1)–N(1) 1.945(2), Al(1)–N(2) 1.920(2), Al(1)–S(1) 2.114(1), Al(1)–S(2) 2.288(1), S(2)–H(2) 1.18(3), S(1) \cdots H 2.538; N(1)–Al(1)–N(2) 95.1(1), S(1)–Al(1)–S(2) 115.0(1), Al(1)–S(2)–H(2) 97(2).

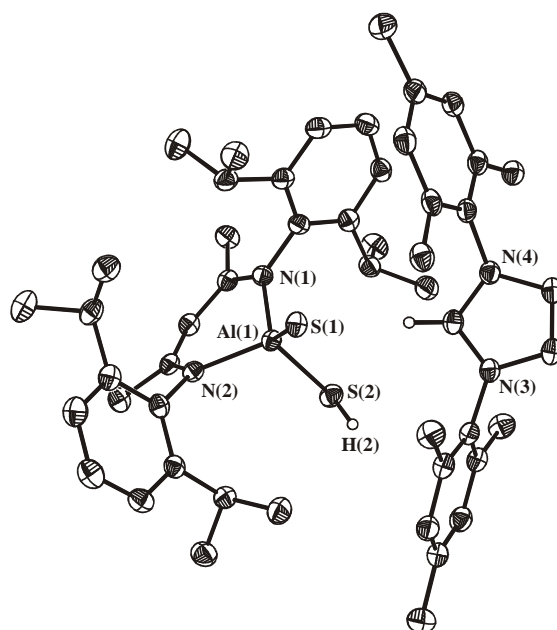


Figure 15: Molecular structure of **11** · THF (50% probability ellipsoids). Hydrogen atoms (except the S–H and N–CH–N protons), and solvent molecule are omitted for clarity. Selected bond lengths [Å] and angles [°]: Al(1)–N(1) 1.938(2), Al(1)–N(2) 1.930(2), Al(1)–S(1) 2.115(1), Al(1)–S(2) 2.278(1), S(2)–H(2) 1.25(3), S(1)⋯H 2.455; N(1)–Al(1)–N(2) 95.7(1), S(1)–Al(1)–S(2) 117.8(1), Al(1)–S(2)–H(2) 93(1).

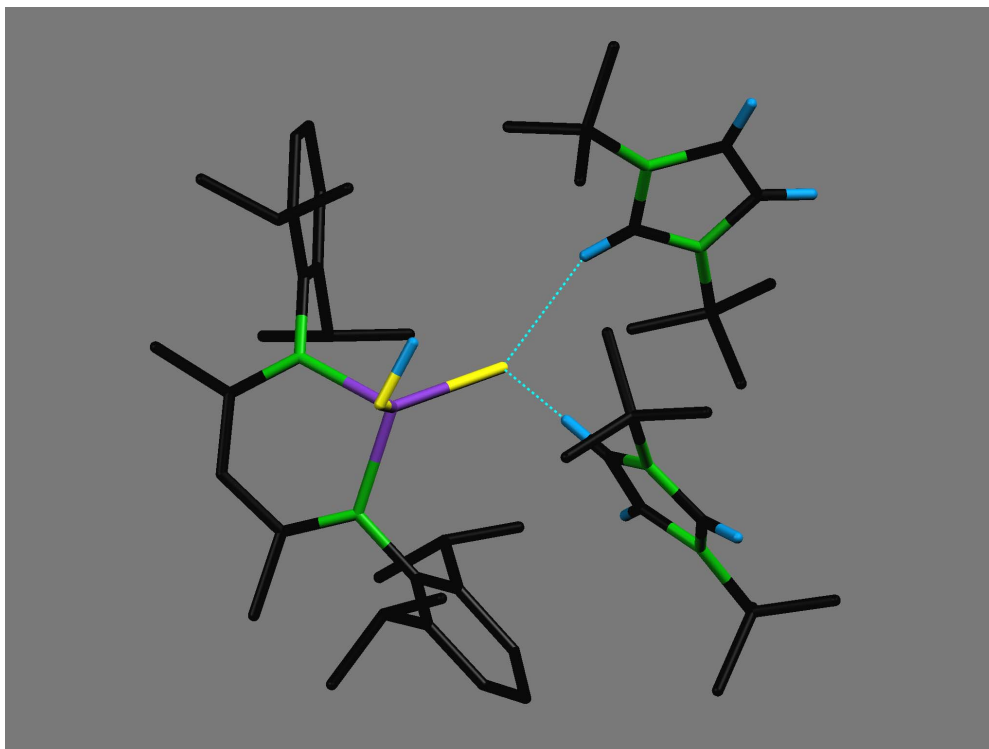


Figure 16: Close H⋯S interactions in the crystal of **9**.

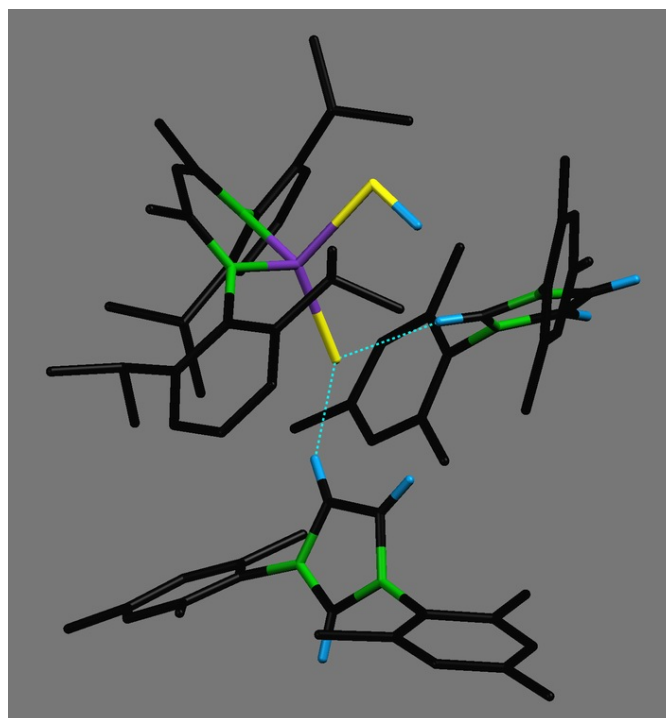


Figure 17: Close H \cdots S interactions in the crystal of **11**.

Table 2. Selected bond lengths [\AA] and angles [$^\circ$] for **1**, **5–7**, **9**, **11** (esd's in brackets).

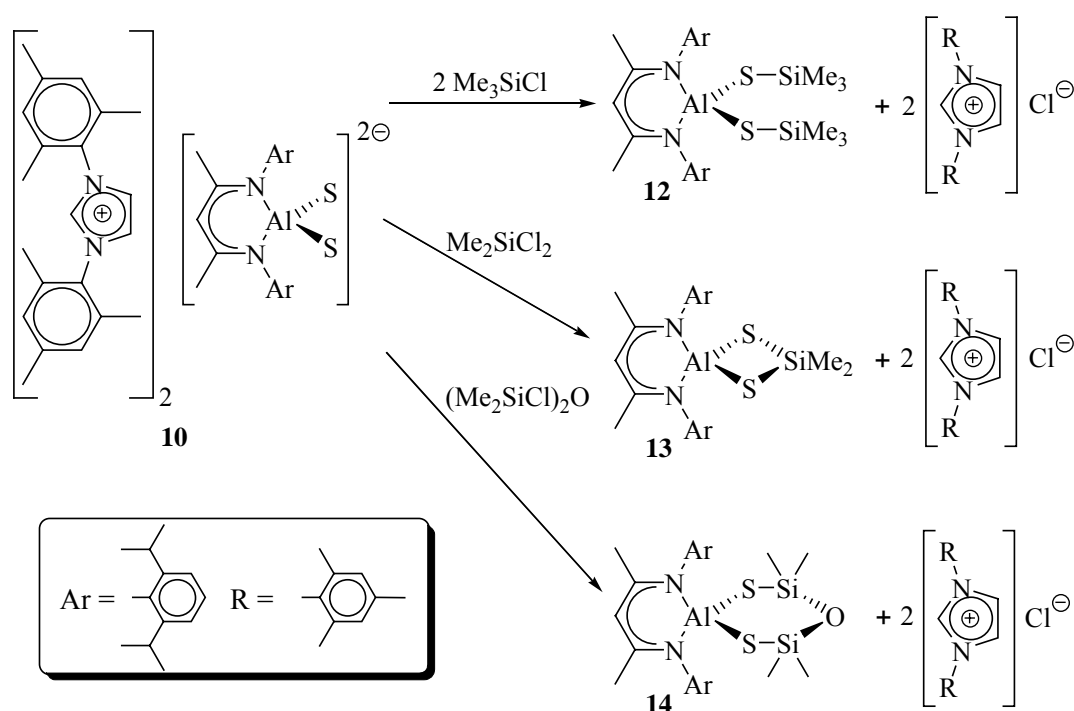
	$\text{LAl}(\text{SH})_2$	$\{\text{LAl}(\text{SLi})_2(\text{thf})_3\}_2 \cdot 2\text{THF}$	$\{\text{LAl}(\text{SH})[\text{SLi}(\text{thf})_2]\}_2$	$\text{C}_6\text{H}^+[\text{LAl}(\text{SH})(\text{S})]^- \cdot \text{THF}$	$\text{C}_m\text{H}^+[\text{LAl}(\text{SH})(\text{S})]^- \cdot \text{THF}$	$\text{LAl}(\mu\text{-S})_2\text{TiCp}_2$
Al–N	1.891(1)	1.928(2) 1.935(2)	1.932(1)– 1.973(1) ¹	1.920(2) 1.945(2)	1.938(2) 1.930(2)	1.918(2) 1.921(2)
Al–S	2.223(1) 2.217(1)	2.268(1) ² 2.123(1) ²	2.173(1)– 2.186(1) ¹	2.288(1) ² 2.114(1) ²	2.279(1) ² 2.115(1) ²	2.208(1) 2.197(1)
S–H	1.20(2) 1.21(3)	1.28(5)	–	1.18(3)	1.25(2)	–
S–Al–S	105.4(1)	115.7(1)	111.6(1) 113.0(1)	115.0(1)	117.8(1)	102.5(1)
N–Al–N	97.3(1)	95.5(1)	94.1(1) 93.3(1)	95.1(1)	95.7(1)	95.6(1)
Al–S–H	97(1) 91(2)	–	–	97(1)	93(1)	–

¹ The shortest and longest bond lengths in the molecule

² The first number belongs to the Al–S(H) unit, the second to the substituted one

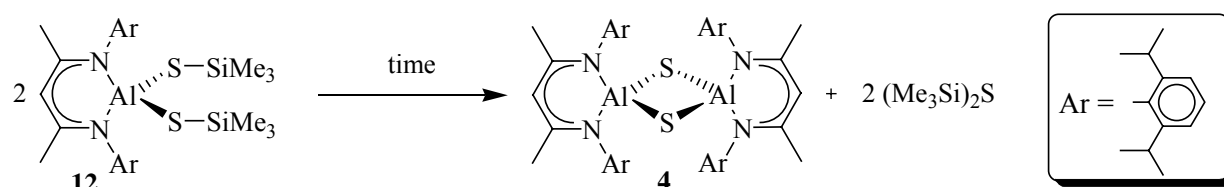
2.2.5. Preparation of Al–S–Si Systems

After isolation of AlS_2M , we became interested in the synthesis of Al–S–Si systems. To the best of our knowledge, only one example of such a species has been reported so far. In 1995 M. Taghiof *et al.* published the synthesis and the structure of $\text{Me}_2\text{Al}(\mu\text{-SSiPh}_3)_2\text{AlMe}_2$ from the reaction of AlMe_3 and HS-SiPh_3 .^[174] No reports on the preparation of such a moiety from Al–S fragments are known. Earlier attempts to use the lithium salts **5** and **6** as the Al–S source failed and only mixtures of products were isolated from the reactions with Me_3SiCl , Me_2SiCl_2 and $(\text{Me}_2\text{SiCl})_2\text{O}$. When the freshly prepared imidazolium salt **10** was treated in THF with the above silicon precursors in the appropriate molar ratios, conversion into the Al–S–Si moiety containing $\text{LAl}(\text{SSiMe}_3)_2$ (**12**), $\text{LAl}(\mu\text{-S})_2\text{SiMe}_2$ (**13**) and $\text{LAl}(\text{SSiMe}_2)_2\text{O}$ (**14**) was observed (Scheme 9). Furthermore, the *N,N'*-bis-mesitylimidazolium chloride can be easily separated due to its low solubility in THF from the products by filtration. Compounds **12–14** have been obtained as white microcrystalline solids sensitive toward moisture, and their composition and structure has been determined by multinuclear NMR spectroscopy and mass spectrometry, but so far no crystals suitable for X-ray structural analysis have been obtained. Scheme 9 shows the preparation of these substances. The EI-MS



Scheme 9: Synthesis of compounds **12–14**.

spectra show in all three cases the molecular ion peaks at m/z 654 (1%) (**12**), 566 (30%) (**13**) and 640 (90%) (**14**). This indicates a low thermal stability of **12**. Malodorous compound **12** decomposes slowly in both solution and the solid state even in the dry box with formation of a white insoluble powder identified by EI-MS and IR as $\text{LAl}(\mu\text{-S})_2\text{AlL}$ (**4**). This indicates that $(\text{Me}_3\text{Si})_2\text{S}$ is the second decomposition product causing the malodorous character of **12** (Scheme 10).

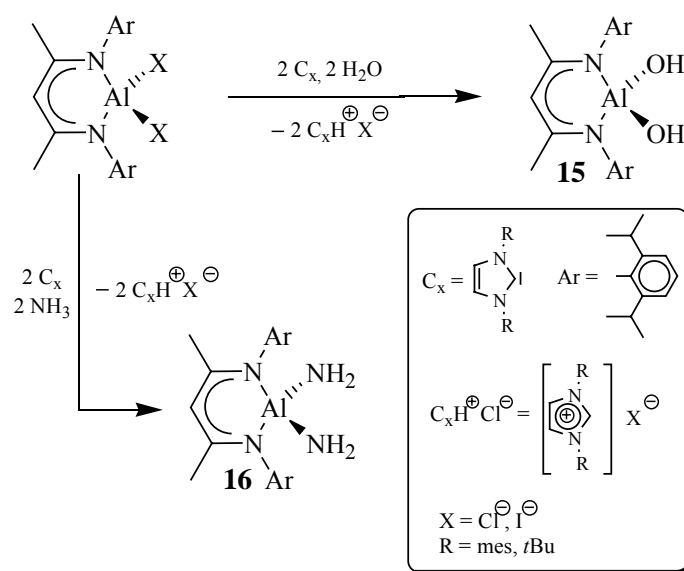


Scheme 10: Decomposition of **12**.

2.3. Ammonolysis and Hydrolysis of LAlCl_2 , $\text{LAl}(\text{Cl})\text{Me}$ and LGaCl_2 in the Presence of N-Heterocyclic Carbenes as HCl Scavengers

2.3.1. Synthesis of $\text{LAl}(\text{OH})_2$ (**15**) and $\text{LAl}(\text{NH}_2)_2$ (**16**)

Recently we have obtained the molecular aluminum dihydroxides $\text{LAl}(\text{OH})_2$ (**15**) and $[\text{LAl}(\text{OH})]_2\text{O}$ from LAlI_2 and a $\text{KOH}/\text{H}_2\text{O}/\text{KH}$ mixture in the two phase system liquid ammonia/toluene at -78°C . It is noteworthy that previous attempts to prepare compounds with terminal Al-OH and Al-NH_2 groups in the presence of NMe_3 , NEt_3 or pyridine as HCl



Scheme 10: Synthesis of **15** and **16**.

acceptor were not successful.^[175] Successful employment of the imidazolium salts **9–11** in the reactions with different chlorosilanes prompted us to use the N-heterocyclic carbenes directly as HCl scavengers. Thus, we decided to prove this pathway as an alternative route for the preparation of **15**. A quick addition of two equivalents of H₂O to a benzene solution of LAlI₂^[27] and two equivalents of N,N'-bis-mesitylimidazolyl carbene at 5 °C resulted after 10 min. in the formation of the expected LAl(OH)₂ and a slurry of insoluble N,N'-bis-mesitylimidazolium iodide. Filtration followed by extraction of the remaining solid with 10 mL of toluene gave an oily residue after removal of the volatiles *in vacuo*. Treatment of the residue with cold pentane afforded **15** as a white powder in 65% yield (compare with 48% yield obtained from the two phase system NH₃(l)/toluene after 7 h). Furthermore, when ammonia was used instead of water with toluene as solvent, a white microcrystalline powder of LAl(NH₂)₂ (**16**) has been obtained in 70% yield. Due to the higher reactivity of NH₃ compared to that of H₂O in these reactions, the ammonia has to be added to the LAlI₂ slowly at -25 °C (Scheme 10). This new method clearly demonstrates the advantages for the preparation of aluminum amides and hydroxides. So far we have not given an answer to the question: Why does the addition of the N-heterocyclic carbene lead to the desired product? Obviously due to the high reactivity of **15** and **16** toward protonic reagents it appears that the amine is not suitable as a HCl acceptor. On the one hand, there is an equilibrium between the protonated amine and the free base, thus causing side reactions by the protons. On the other hand, in the presence of the N-heterocyclic carbenes no such equilibrium of free protons has been formed due to the favored covalent C–H bond formation.^[176] Moreover, the resulting imidazolium chloride is only sparingly soluble in hydrocarbon solvents such as hexane, toluene or THF, which allows an easy separation from the reaction mixture by filtration. In addition the imidazolium chloride can be easily recycled to the free carbene using strong base such as KO^tBu or NaH.^[167]

Surprisingly, compound **16** is monomeric in the solid state, and what is even more striking, the NH₂ groups are not involved in any kind of hydrogen bonding as shown by the X-ray structural analysis and IR spectroscopy. Compound **16** is thermally stable and can be maintained at 70 °C for 2 h without significant decomposition, also reflected by its high melting point (166 °C). When **16** is exposed to air the rate of decomposition is significantly slower than that of **15** (see below). Furthermore additional investigations on **15** gave more information about its stability. Compound **15** is unstable and decomposes upon heating to temperatures exceeding 70 °C or after contact with air rapidly as shown by temperature

dependent ^1H NMR studies (Figure 18). The ^1H NMR spectrum of **15** shows the typical pattern for the ligand (L) and a broad singlet at -0.55 ppm assigned to the NH_2 moieties with ^{15}N satellites ($^1J_{\text{NH}} = 64$ Hz). The NH_2 groups resonate in the ^{15}N NMR at -378 ppm, whereas the remaining two nitrogen atoms have a resonance at -205 ppm. The IR spectrum shows two weak sharp absorptions for $\tilde{\nu}_{\text{as}}$ at 3468 and $\tilde{\nu}_{\text{s}}$ at 3396 cm^{-1} , which also confirm the absence of hydrogen bonds in the crystal lattice. Because of the high thermal stability of **16**, the EI-MS spectrum shows the molecular ion at m/z 476 (16%) while the most intense peak at m/z 444 (100%) was assigned to the $[\text{M} - 2 \text{NH}_2]^+$ fragment.

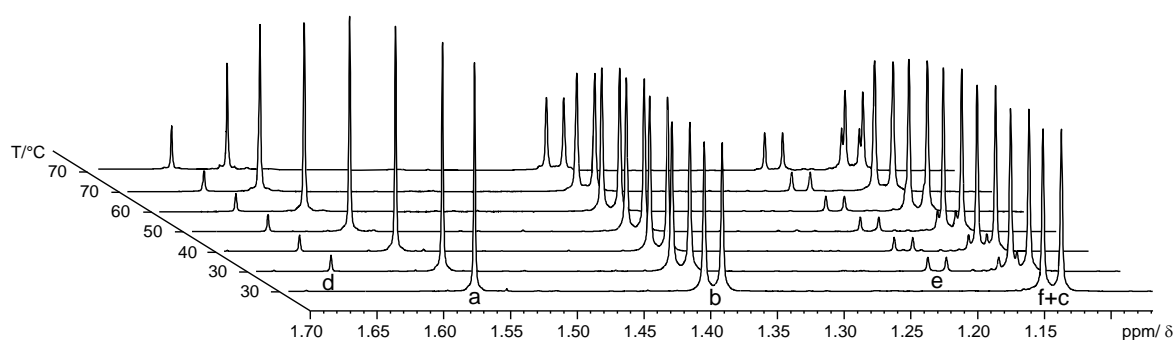


Figure 18: ^1H NMR kinetic study of the thermal decomposition of **15** to the free ligand LH. Resonances between δ 1.5 and 1.7 ppm are assigned to the α -methyl groups (a - **15**, d - LH), and the doublets belong to the diastereotopic methyl groups of the *i*Pr moieties (b, c - **15**; e, f - LH). The only soluble organic product of this decomposition is the free ligand, which was identified by comparison with an original sample. The spectrum measured in a sealed tube at 30 $^\circ\text{C}$ represents pure **15**, whereas the following one was measured after three days. Further spectra show thermally initiated decomposition of **15**, which is slow below 60 $^\circ\text{C}$, but accelerates significantly at 70 $^\circ\text{C}$. The last spectrum was recorded after 15 min maintained at 70 $^\circ\text{C}$ and confirms the thermal lability of **15**. A similar degradation of **15** was observed after its exposure to air in both the solid and solution states.

2.3.2. Crystal Structure Description of $\text{LAl}(\text{NH}_2)_2$ (**16**)

Single crystals of **16** suitable for X-ray structural analysis were obtained by crystallization of a saturated pentane solution at -32 $^\circ\text{C}$. Compound **16** crystallizes in the monoclinic space group $P2_1/c$. Figure 19 shows the molecular structure and numbering scheme of **16**. The AlN_4 core has a distorted tetrahedral geometry with the smallest and biggest $\text{N}-\text{Al}-\text{N}$ angle of 95.7

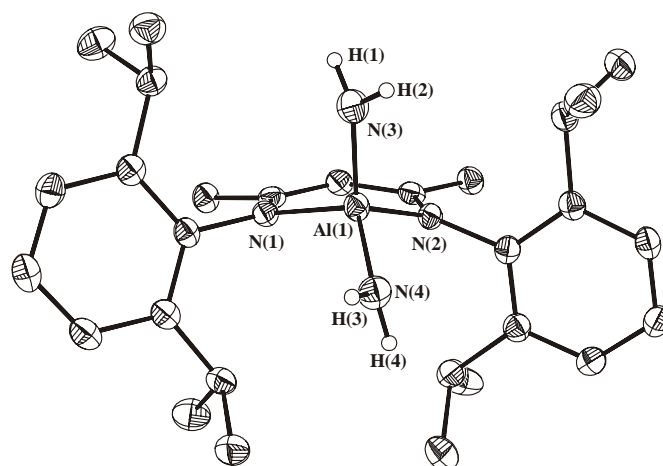


Figure 19: Thermal ellipsoids plot of **16** showing the 50% probability level. H atoms, except N–H, are omitted for clarity. Selected bond lengths [Å] and angles [°]: Al(1)–N(1), N(2), N(3), N(4) 1.921(2), 1.903(2), 1.790(2), 1.788(2), N(3)–H(1), H(2) 0.879, 0.846, N(4)–H(3), H(4) 0.869, 0.864, N(1)–Al(1)–N(2), N(3), N(4) 95.7(1), 107.2(1), 117.2(1), N(3)–Al(1)–N(4) 112.2(1), H(1)–N(3)–H(2) 106.0, H(3)–N(4)–H(4) 108.5, H(1)–N(3)–Al(1) 122.7(1), H(2)–N(3)–Al(1) 127.3(1), H(3)–N(4)–Al(1) 122.9(1), H(4)–N(4)–Al(1) 125.1(1).

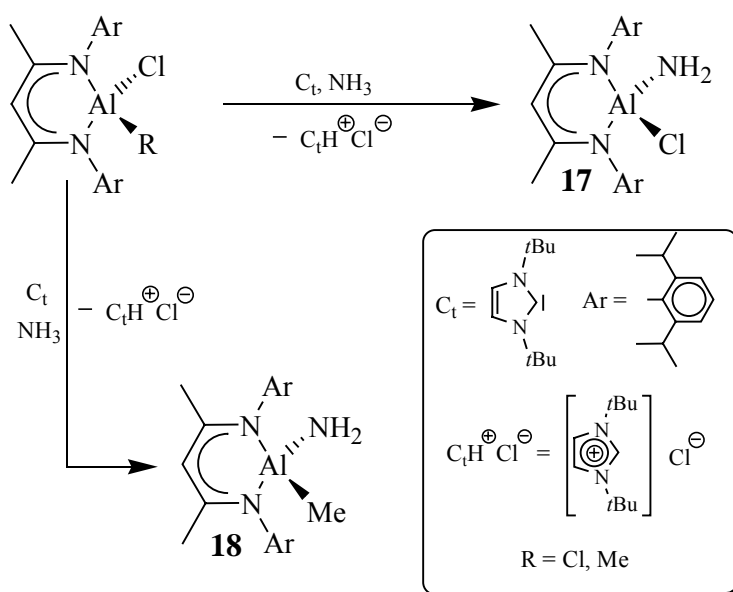
and 117.2°, respectively. The N(1)–Al–N(2) angle (95.7°) within the six-membered ring is in the normal range, whereas the large N(3)–Al–N(4) angle of 112.2° compared to 86.9–106.1° in dimeric and trimeric cyclic species^[73–77] might be due to the monomeric nature of **16** and the absence of ring strain characteristics of the cyclic congeners. There are significant differences of the Al–N bond lengths within the molecule. The Al–N(1) and Al–N(2) bond lengths (1.921, 1.903 Å) are in the normal range, while the Al–N(3) and Al–N(4) bond lengths (1.790, 1.788 Å) represent the shortest for Al–NH₂ bonds known so far compared to those in the known organoaluminum amides (1.873–2.034 Å).^[73–77] A similar shortening of the Al–(NH₂)_{terminal} bond length was observed in AlCl₃(NH₂*i*Pr)₂{Al(NH₃)(NH₂)[Al(NH*i*Pr)–(NH*i*Pr)Cl]₂}₂ and was assigned to the ionic resonance effects of the Al–N bond.^[77,177,178] The hydrogen atoms of the NH₂ groups were localized in the difference electron density map and the N–H bond lengths (0.85 to 0.88 Å) are in the range of known compounds (0.75–1.10 Å).^[73–77] The nitrogen atoms of the NH₂ groups have almost planar environments (the sum of the surrounding angles are 356° for N(3) and 357° for N(4)), which indicates a lowering of the inversion barrier at the nitrogen centers due to electropositive aluminum atom.^[179] A similar phenomenon was observed for Cp*₂TiNH₂ and {[DippN(SiMe₃)]Ge(NH₂)NH}₃ respectively.^[180,181]

2.3.3. Preparation of $\text{LAl}(\text{NH}_2)\text{Cl}$ (**17**) and $\text{LAl}(\text{NH}_2)\text{Me}$ (**18**)

After the preparation of compound **16** we focused on the optimization of the reaction conditions. Variation of the basicity of the carbenes by changing the substituents on nitrogen was tried with the easier obtainable LAlCl_2 ^[182] instead of LAlI_2 . Whereas the change of $\text{N,N}'$ -*bis*-mesitylimidazolyl carbene^[167] for $\text{N,N}'$ -*bis*-*t*-butylimidazolyl carbene^[162] did not have any influence on the reaction, the change of LAlI_2 for LAlCl_2 resulted in the isolation of $\text{LAl}(\text{NH}_2)\text{Cl}$ (**17**). When LAlI_2 was used for the reaction with NH_3 in the presence of only one equivalent of $\text{N,N}'$ -*bis*-*t*-butylimidazolyl carbene, a mixture of LAlI_2 and **16** was isolated. Clearly, the intermediate $\text{LAl}(\text{NH}_2)\text{I}$ is under these condition more reactive as LAlI_2 . $\text{LAl}(\text{NH}_2)\text{Cl}$ (**17**) is stable in comparison to $\text{LAl}(\text{NH}_2)\text{I}$ and can be isolated. It is noteworthy, that this reaction is not straightforward and the $\text{LAl}(\text{NH}_2)\text{Cl}$ is always contaminated up to 6% of LAlCl_2 and $\text{LAl}(\text{NH}_2)_2$ (**16**). Separation of these three species is very difficult due to their easy cocrystallization.^[183] The amount of **17** in the product can be reduced by recrystallization due to the higher solubility of **16** (solubility of **17** is almost like that of LAlCl_2), but repeated recrystallization can be found contraproductive owing to increasing concentration of LAlCl_2 in the final product. By using 1.2 equivalents of the carbene, we obtained a mixture of **16** (ca 14%) and **17** and after repeated crystallizations, almost pure **17** (6% of **16** as determined by ^1H NMR spectroscopy) was obtained. This sample was used for growing X-ray quality monocrystals. Furthermore, when $\text{LAl}(\text{Me})\text{Cl}$ ^[184] is used as the starting material, $\text{LAl}(\text{NH}_2)\text{Me}$ (**18**) has been isolated in 78% yield (Scheme 11). Both **17** and **18** are thermally stable and melt at 140 °C (**17**) and 150 °C (**18**), respectively. The EI-MS spectra show the molecular ion peaks at m/z 495 (15%) (**17**) and 475 (30%) (**18**). In the ^1H NMR spectra, the NH_2 protons resonate at δ -0.31 (**17**) and -0.20 (**18**) ppm.

2.3.4. Molecular Structures of $\text{LAl}(\text{NH}_2)\text{Cl}$ (**17**) and $\text{LAl}(\text{NH}_2)\text{Me}$ (**18**)

Both compounds **17** and **18** are monomeric in the solid state and the NH_2 groups are not involved in any kind of hydrogen bonding as observed also for **16**. Slow cooling of their saturated toluene solutions to -32 °C afforded within three days X-ray quality crystals. Compounds **17** and **18** crystallize both in the monoclinic space group $P2_1/c$ with one independent molecule in the asymmetric unit (Figures 20–22). The steric demand of both NH_2 and Cl is very similar^[183] resulting in a disorder of these two groups in **17**. The Al- NH_2 and



Scheme 11: Synthesis of monomeric aluminum amides **17** and **18**.

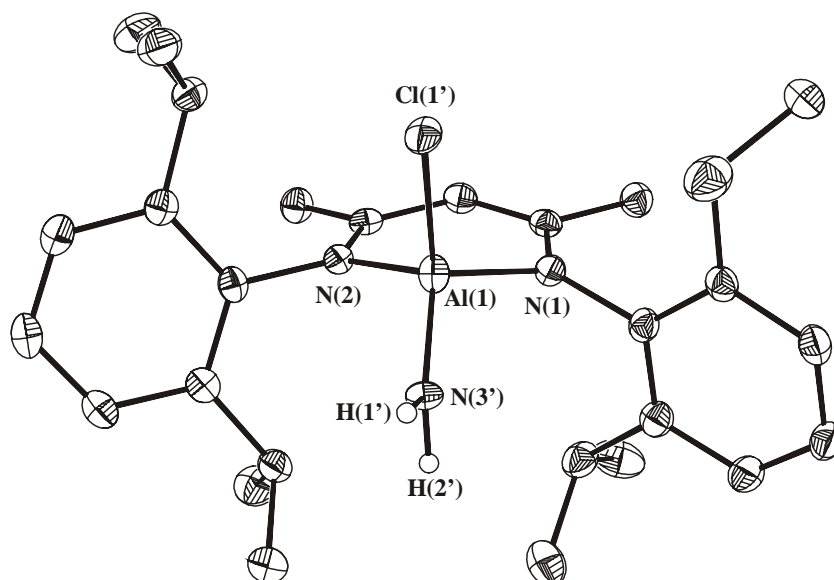


Figure 20: Preferred (64%) conformer of **17** with the NH_2 group in equatorial position.

Al–Cl bond lengths are affected by this disorder and thus are not very exact due to the applied geometry restraints. The $\text{C}_3\text{N}_2\text{Al}$ ring possesses a boat conformation and therefore the NH_2 group can occupy either the axial or equatorial position. Both conformations were refined separately with final occupancy factors NH_2/Cl 36/64% (axial) and 68/32% (equatorial) indicating the presence of ca. 4% of $\text{LAl}(\text{NH}_2)_2$ in the crystal. This is in good agreement with the NMR results. The preferred conformation of **17** has the NH_2 group in the equatorial position. The Al– N_{endo} (1.877 and 1.896 Å) and Al–Cl (2.084 and 2.118 Å) bond lengths are similar to those in LAlCl_2 (Al–N 1.884 and 1.866 Å; Al–Cl 2.134 and 2.119 Å),^[182] whereas

the Al–N bonds lengths in **16** (endo: 1.921 and 1.903, exo: 1.790 and 1.788 Å) are comparable to those in **17** (exo: Al–N 1.797 and 1.762 Å). The N(1)–Al–N(2) angle (98.0°) is smaller than in LaAlCl_2 (99.4°) and larger than in **16** (95.7°).

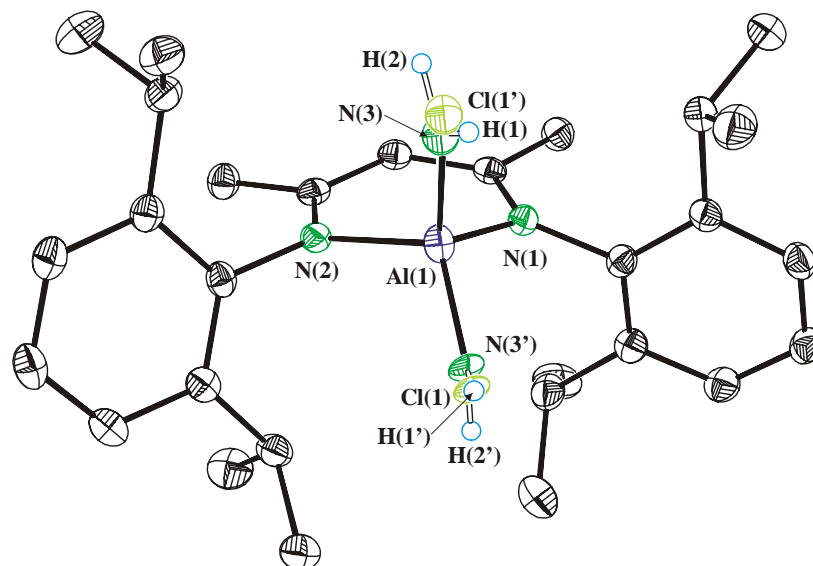


Figure 21: Molecular structure of **17** · THF (50% probability ellipsoids). Hydrogen atoms except the NH_2 protons are omitted for clarity. Selected bond lengths [Å] and angles [°]: Al(1)–N(1) 1.877(1), Al(1)–N(2) 1.896(1), Al(1)–N(3),N(3') 1.797(8), 1.762(6), Al(1)–Cl(1),Cl(1') 2.084(4), 2.118(1), N(3)–H(1),H(2) 0.91(4), 0.92(4), N(3')–H(1'),H(2') 0.91(4), 0.91(4); N(1)–Al(1)–N(2) 98.0(1), N(1)–Al(1)–N(3),N(3') 113.0(4), 111.8(3), N(2)–Al(1)–N(3), N(3') 108.0(4), 114.9(3), N(1)–Al(1)–Cl(1),Cl(1') 112.5(2), 112.2(1), N(2)–Al(1)–Cl(1), Cl(1') 115.6(2), 108.8(1), N(3)–Al(1)–Cl(1), 109.4(4), N(3')–Al(1)–Cl(1') 110.7(4), Al(1)–N(3)–H(1),H(2) 129(5), 132(4), H(1)–N(3)–H(2) 99(4), Al(1)–N(3')–H(1'),H(2') 131(3), 129(3), H(1')–N(3')–H(2') 99(4) .

The NH_2 group in **18** occupies the axial position on aluminum and with the sum of surrounding angles of 359° is almost planar as in the case of **16**. The Al– NH_2 bond length (1.795 Å) is similar to those in **16** (1.790 and 1.788 Å) but is shorter than those in other organoaluminum amides (1.873–2.034 Å)^[73–77] and the Al(1)–N(1) (1.909 Å) and Al(1)–N(3) (1.911 Å). The Al(1)–C(30) bond length (1.943 Å) is in good agreement with those of LaAlMe_2 (1.958 and 1.970 Å).^[185] The angles of the N_3AlC core have values of 95.8° (N(1)–Al–N(2)), 107.2° (N(1)–Al–N(3)), 110.2° (N(2)–Al–N(3)) 115.5° (N(1)–Al–C(30)), 112.0°

(N(2)–Al–C(30)), and 114.6° (N(1)–Al–C(30)), respectively, and indicate the distorted tetrahedral configuration.

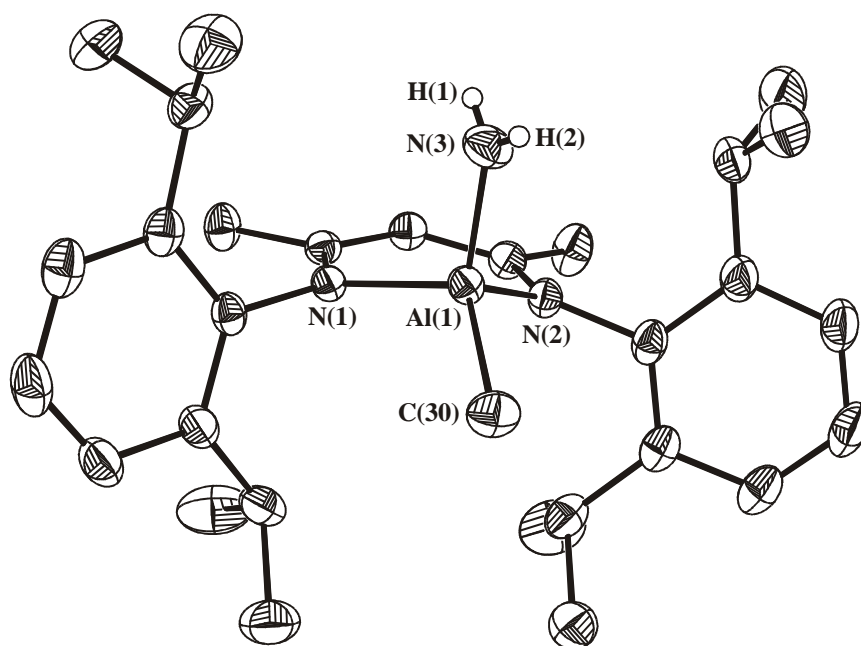
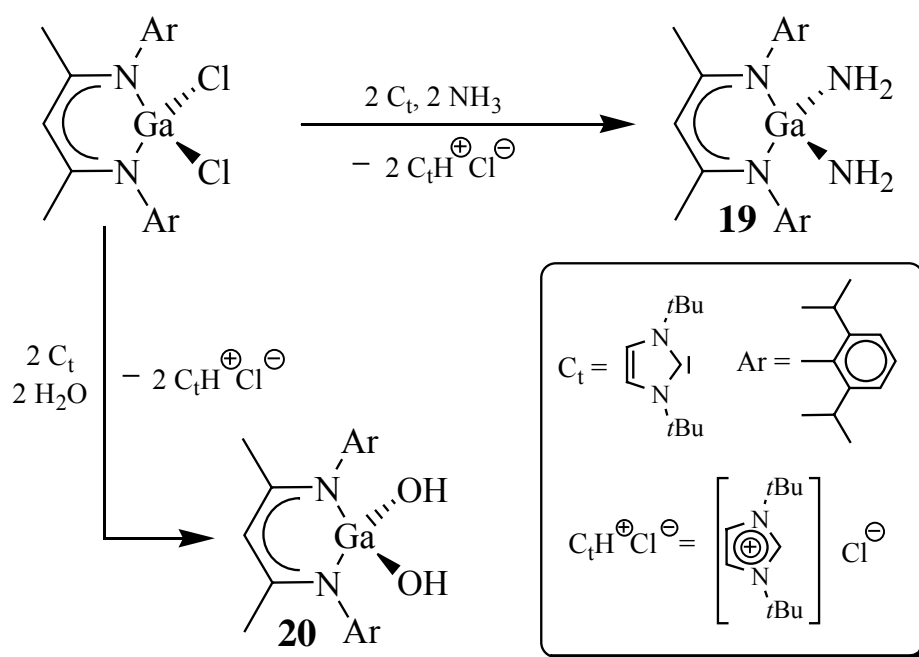


Figure 22: Molecular structure of **18** (50% probability ellipsoids). Hydrogen atoms (except the N–H protons), are omitted for clarity. Selected bond lengths [Å] and angles [°]: Al(1)–N(1) 1.911(1), Al(1)–N(2) 1.909(1), Al(1)–N(3) 1.795(1), Al(1)–C(30) 1.945(1), N(3)–H(1) 0.70(2), N(3)–H(2) 0.71(2); N(1)–Al(1)–N(2) $95.8(1)$, N(1)–Al(1)–N(3) $107.2(1)$, N(2)–Al(1)–N(3) $110.2(1)$, N(1)–Al(1)–C(30) $115.5(1)$, N(2)–Al(1)–C(30) $112.0(1)$, N(3)–Al(1)–C(30) $114.6(1)$.

2.3.5. Preparation of $\text{LGa}(\text{NH}_2)_2$ (**19**) and $\text{LGa}(\text{OH})_2$ (**20**)

After the preparation of $\text{LAl}(\text{OH})_2$ and $\text{LAl}(\text{NH}_2)_2$ from LAlCl_2 , H_2O and NH_3 , respectively, by means of different N-heterocyclic carbenes as HCl acceptors. We became interested in using this method also for gallium compounds to generate similar species. First, a cold toluene solution (-25°C) of 1,3-*bis*-*tert*-butylimidazolyl carbene saturated with gaseous NH_3 was slowly added to a toluene solution of LGaCl_2 ^[182] at -35°C . Warming the solution to ambient temperature resulted in the formation of a slurry of 1,3-*bis*-*tert*-butylimidazolium chloride. After filtration, removal of all the volatiles *in vacuo*, and recrystallization from pentane colorless microcrystalline $\text{LGa}(\text{NH}_2)_2$ (**19**) was isolated in 70% yield. Furthermore,

$\text{LGa}(\text{OH})_2$ (**20**) was the only product isolated in 80% yield from the reaction between LGaCl_2 and 1,3-*bis*-*t*butylimidazolyl carbene in a 1:2 molar ratio and two equivalents of H_2O in toluene at $-5\text{ }^\circ\text{C}$. These results confirmed our expectations that the carbene/ $\text{NH}_3(\text{H}_2\text{O})$ system offers synthetic potential also for gallium. As mentioned earlier, preparation of such species is problematic and very often leads to condensed products, if protic byproducts are not properly trapped (e.g. HCl , $\text{NR}_3\text{H}^+\text{X}^-$, etc.).^[175] Thus most of these products were prepared by elimination of small aprotic molecules such as H_2 , alkanes or strong bases (dialkylamines etc.). Recent measurements and theoretical calculations confirmed a high basicity of the N-heterocyclic carbenes in polar solvents such as DMSO or acetonitrile. The 1,3-*bis*-*t*butylimidazolyl carbene, used in our case as a HCl acceptor, reveals a pK_a of 24.0 (exp./theor. 24.5 ± 0.2 .) in DMSO and 33.7 ± 0.1 (theor.) in acetonitrile.^[161] This clearly explains the almost irreversible bonding of the free protons to the carbene and high yields of the unique species **19** and **20**. Scheme 12 summarises all the results.



Scheme 12: Preparation of **19** and **20**.

In analogy to the aluminum derivative, **20** forms a dimer, whereas **19** is strictly monomeric in both the solid state and solution as proved by X-ray structural analysis and IR spectroscopy. Both compounds are thermally stable and do not decompose even upon heating up to $70\text{ }^\circ\text{C}$ in a sealed tube as determined by temperature dependent ^1H NMR spectroscopy

and MS spectrometry. Compound **19** is very sensitive toward moisture and decomposes rapidly under formation of NH_3 and other unidentified products. The hydrolysis products of **19** have a similar solubility like the diamide, therefore it is necessary to work carefully under strictly moisture-free conditions to obtain pure **19** (more than 95% purity of **19**). Compound **19** contains often 3–5% of impurities as shown by ^1H NMR spectroscopy. Nevertheless, pure **19** can be obtained using a closed vacuum line equipped with Swagelock Teflon fittings for the condensation of the solvent and $\text{NH}_3(\text{l})$ to the reagents. The reaction flasks have been equipped with Young Teflon valves and treated prior to use with Me_3SiCl to eliminate free OH groups on the glass surface.

2.3.6. X-ray Study of Compounds **19** and **20** and DFT Calculations of **16** and **19**

Single crystals of **19** were obtained by storing a saturated pentane solution at $-32\text{ }^\circ\text{C}$. Compound **19** crystallizes in the monoclinic space group $P2_1/c$ with one molecule in the asymmetric unit and is isostructural to $\text{LaI}(\text{NH}_2)_2$ (**16**) (Figure 23, Tables CD10 and CD13 in Section 6). Compound **19** is monomeric in the solid state with no observable hydrogen bonding. The GaN_4 core has a distorted tetrahedral geometry with the smallest and largest N–Ga–N angles of 95.4 and 118.5° , respectively. The N(1)–Ga(1)–N(2) angle (95.4°) within the six-membered ring is in the normal range, whereas the N(3)–Ga(1)–N(4) angle (111.8°) is significantly larger than those of the trimeric cyclic species ($(\text{Me}_2\text{GaNH}_2)_3$ and $(t\text{Bu}_2\text{GaNH}_2)_3$ 93.8 – 105.6°).^[83,84,86] This difference is obviously due to the monomeric nature of **19** and thus missing the ring strain characteristics of the cyclic molecules. As expected, the endocyclic Ga(1)–N(1) and Ga(1)–N(2) bonds (1.955 and 1.976 \AA) are significantly longer than the exocyclic ones (Ga(1)–N(3) and Ga(1)–N(4) 1.852 and 1.847 \AA). The latter values represent the shortest bond lengths for Ga– NH_2 moieties known so far (compared to 1.928 – 2.053 \AA of $(\text{Me}_2\text{GaNH}_2)_3$ and $(t\text{Bu}_2\text{GaNH}_2)_3$).^[83,84,86] A similar phenomenon has been observed for the Al analogues. The hydrogen atoms of the NH_2 groups were localized in the difference electron density map and the N–H bonds (0.81 – 0.82 \AA) are shorter than those of $(\text{Me}_2\text{GaNH}_2)_3$ (0.95 \AA) and $(t\text{Bu}_2\text{GaNH}_2)_3$ (1.05 \AA), but are comparable to those of **16** (0.85 – 0.88 \AA).^[83,84,86] Although **19** is isostructural with the Al analogue **16**, it reveals one significant difference, the geometry of the NH_2 groups in **16** is almost planar with a sum of angles $357(2)$ and $356(2)^\circ$ compared to those in **19** (sum of angles $337(2)$ and $344(2)^\circ$).

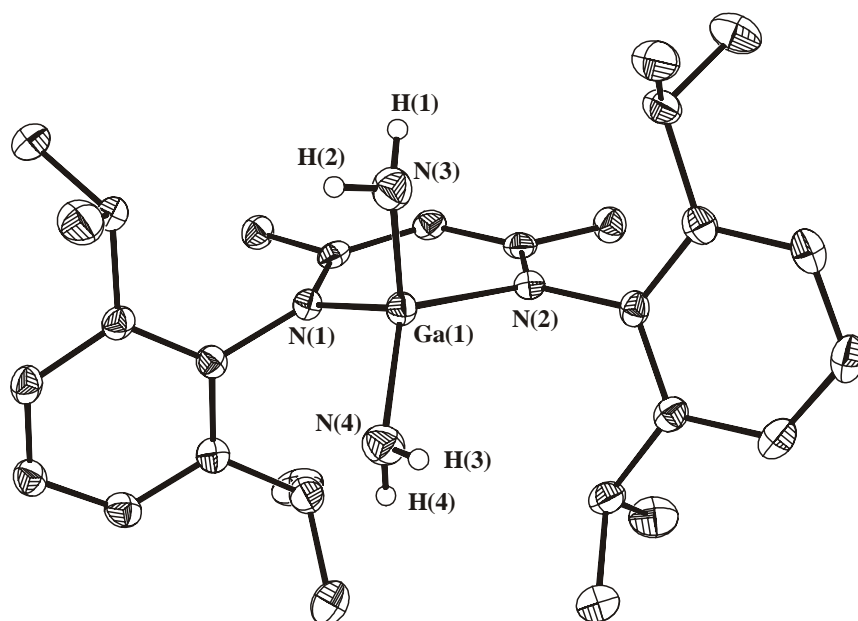


Figure 23: Thermal ellipsoids plot of **19** showing the 50% probability level. H atoms, except N–H, are omitted for clarity. Selected bond lengths [Å] and angles [°]: Ga(1)–N(1) 1.955(2), Ga(1)–N(2) 1.976(2), Ga(1)–N(3) 1.852(2), Ga(1)–N(4) 1.847(2), N(3)–H(1) 0.81(2), N(3)–H(2) 0.81(2), N(4)–H(3) 0.82(2), N(4)–H(4) 0.82(2); N(1)–Ga(1)–N(2) 95.4(1), N(1)–Ga(1)–N(3) 116.5(1), N(1)–Ga(1)–N(4) 107.8(1), N(2)–Ga(1)–N(3) 106.4(1), N(2)–Ga(1)–N(4) 118.5(1), N(3)–Ga(1)–N(4) 111.8(1), H(3')–N(3)–H(3'') 108(3), H(4')–N(4)–H(4'') 112(3), H(3')–N(3)–Ga(1) 114(2), H(3'')–N(3)–Ga(1) 115(1), H(4')–N(4)–Ga(1) 115(1), H(4'')–N(4)–Ga(1) 117(2).

We carried out DFT calculations on both $\text{La}(\text{NH}_2)_2$ (**16**) and $\text{LGa}(\text{NH}_2)_2$ (**19**) with the program DMOL.^[186,187] The isosurfaces at $0.05 \text{ e} \cdot \text{\AA}^{-3}$ of the HOMO orbitals show that the electron density is mainly localized at the N atom of the NH_2 groups of both **16** and **19** (Figures S1–S2 in the Supporting materials Section). The LUMOs are constructed from π orbitals of the β -diketiminato ligand. To save calculation time, several models can be used.^[188,189] We obtained the best model by replacing the aryl groups at the nitrogen atoms by phenyl groups, because in such a model all the interactions between the π -orbitals of the phenyl rings with the ligand backbone contribute to the proper symmetry of the HOMO orbital of the ligand. However, due to the omitting the *i*Pr moieties the optimized calculation led to planar $\text{C}_3\text{N}_2\text{M}$ rings. Hence, the coordinates of the metal and the adjacent nitrogen atoms were fixed at the positions given by the experiment and the optimization was performed for the bonding distances and angles between metal and nitrogen atoms as well as within the NH_2 groups (Figures S3–S4 in the Supporting materials Section). The results show,

that the most stable conformation for $\text{LAl}(\text{NH}_2)_2$ has the NH_2 groups slightly twisted towards each other to allow the overlap of the free orbitals on the nitrogen atoms in the HOMO orbital. Similar stabilization can be found in the Ga derivative, with the difference, that the NH_2 groups need to “bend” to allow similar overlap, mainly due to the longer Ga-N(H₂) bonds and thus larger distance between the corresponding nitrogen atoms. This results in planar NH_2 groups in $\text{LAl}(\text{NH}_2)_2$ (both sums of angles $360(1)^\circ$), whereas these groups are almost tetrahedral in $\text{LGa}(\text{NH}_2)_2$ with the sum of angles $339(1)$ and $335(1)^\circ$, respectively. The results are in a good agreement with the experiment (see above). Furthermore, we could observe partial contribution of the d-orbitals of gallium to the HOMO orbital, whereas there is no metal orbital contribution in the aluminum case (Figure S5 in the Supporting materials Section).

Triclinic single crystals of **20** suitable for an X-ray structural analysis were obtained by keeping a saturated toluene solution at -30°C . The colorless blocks of **20** crystallize in the space group $P\bar{1}$ and spontaneously fracture when exposed to temperatures above -5°C . This is due to an irreversible phase change into a monoclinic form under elimination of toluene and crystallizing in the space group $P2_1/n$ with one molecule of **20** in the asymmetric unit. Due to the high disorder of the molecules we were not able to obtain data of satisfactory quality for the monoclinic form. The triclinic form contains two independent molecules of **20** and one molecule of toluene in the asymmetric unit. Different positions of these molecules toward the inversion center result in the formation of two dimers contrasting in the number and kind of hydrogen bonds between the OH units. Dimer **A** is formed by only two equivalent hydrogen bonds $\text{O}(1)\cdots\text{H}(2\text{B})-\text{O}(2\text{B})$ and $\text{O}(1\text{B})\cdots\text{H}(2)-\text{O}(2)$ ($\text{O}\cdots\text{H}$ 2.01 Å, $\text{O}-\text{H}-\text{O}$ angle 174°) having still two free terminal hydrogen atoms $\text{H}(1)$ and $\text{H}(1\text{B})$ of the OH moieties (Figure 24), whereas in dimer **B** there are two nonequivalent kinds of $\text{O}\cdots\text{H}$ interactions. The first one is similar to that in **A**, $\text{O}(2\text{A})\cdots\text{H}(1'\text{A})-\text{O}(1\text{AA})$ and $\text{O}(2\text{AA})\cdots\text{H}(1')-\text{O}(1\text{A})$ ($\text{O}\cdots\text{H}$ 2.51 Å, $\text{O}-\text{H}-\text{O}$ angle 159°), and the second one is formed by two oxygen atoms equivalent by symmetry. Due to this, the hydrogen atoms of these OH groups are disordered into two positions with equal occupancy factors (Figure 25). This $\text{O}(2\text{A})\cdots\text{H}(2'\text{A})-\text{O}(2\text{AA})$ or equivalent $\text{O}(2\text{AA})\cdots\text{H}(2')-\text{O}(2\text{A})$ hydrogen bonds are shorter than the previous one with an $\text{O}\cdots\text{H}$ distance of 2.09 Å and an $\text{O}-\text{H}-\text{O}$ angle of 174° , whereas $\text{H}(2'')$ or $\text{H}(2''\text{A})$, respectively, remains terminal. The Ga–O bond lengths vary (1.777 to 1.820 Å) and are affected by the $\text{O}\cdots\text{H}$ interactions. However, they are very similar to those in $[\text{2,6-(Me}_2\text{NCH}_2)_2\text{C}_6\text{H}_3]\text{Ga}(\text{OH})_2 \cdot 10\text{H}_2\text{O}$ (1.81–1.83 Å)^[121] and are shorter than those of the

bridged hydroxides $[t\text{Bu}_2\text{Ga}(\mu\text{-OH})]_3$ (1.96 Å)^[117,118] and $[\text{Me}_2\text{Ga}(\mu\text{-OH})]_4$ (1.94–1.99 Å).^[190]

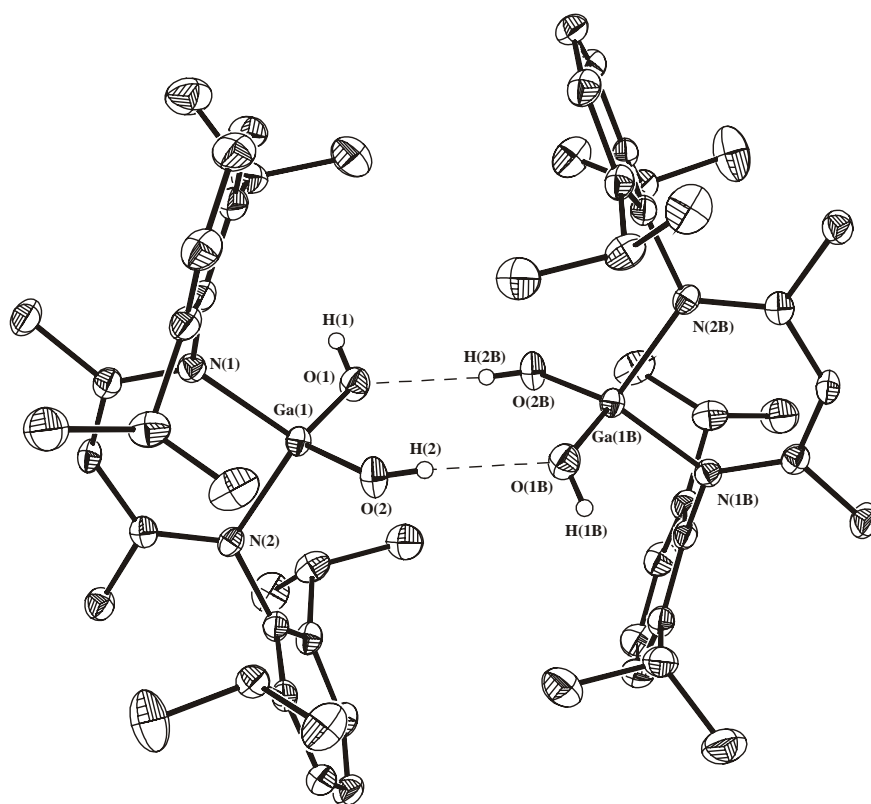


Figure 24: Thermal ellipsoids plot of dimer **A** of **20** showing the 50% probability level. Hydrogen atoms, except O–H, are omitted for clarity. Selected bond lengths [Å] and angles [°]: Ga(1)–N(1) 1.931(1), Ga(1)–N(2) 1.938(1), Ga(1)–O(1) 1.820(1), Ga(1)–O(2) 1.777(1), O(1)–H(1) 0.72(2), O(2)–H(2) 0.74(2); N(1)–Ga(1)–N(2) 98.0(1), N(1)–Ga(1)–O(1) 110.6(1), N(1)–Ga(1)–O(2) 112.0(1), N(2)–Ga(1)–O(1) 107.0(1), N(2)–Ga(1)–O(2) 112.6(1), O(1)–Ga(1)–O(2) 115.3(1), H(1)–O(1)–Ga(1) 114(2), H(2)–O(2)–Ga(1) 113(2).

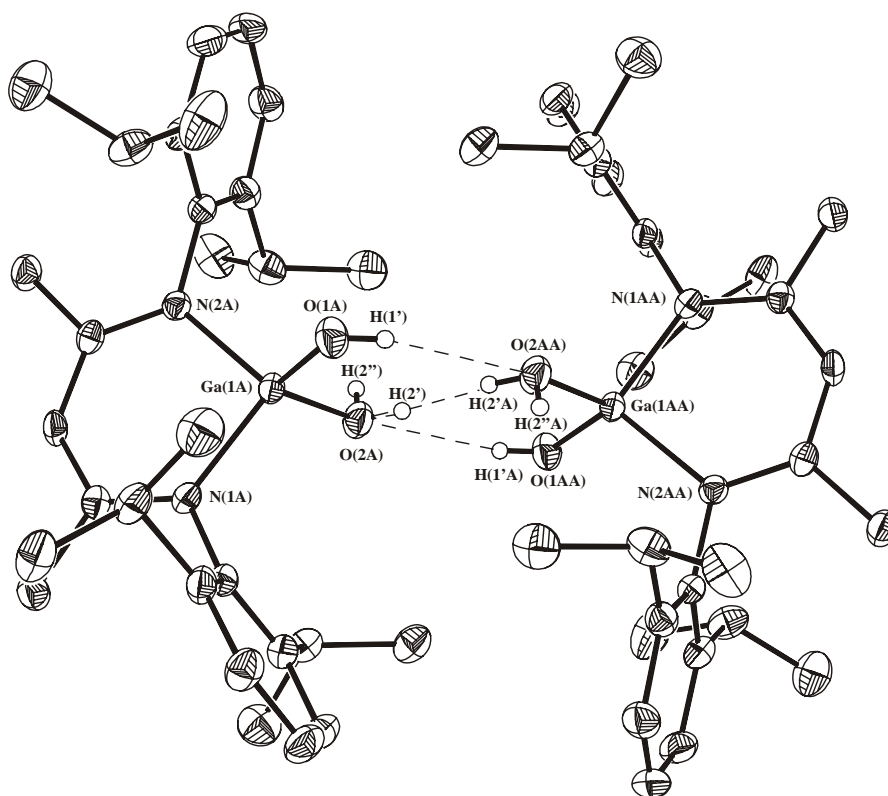


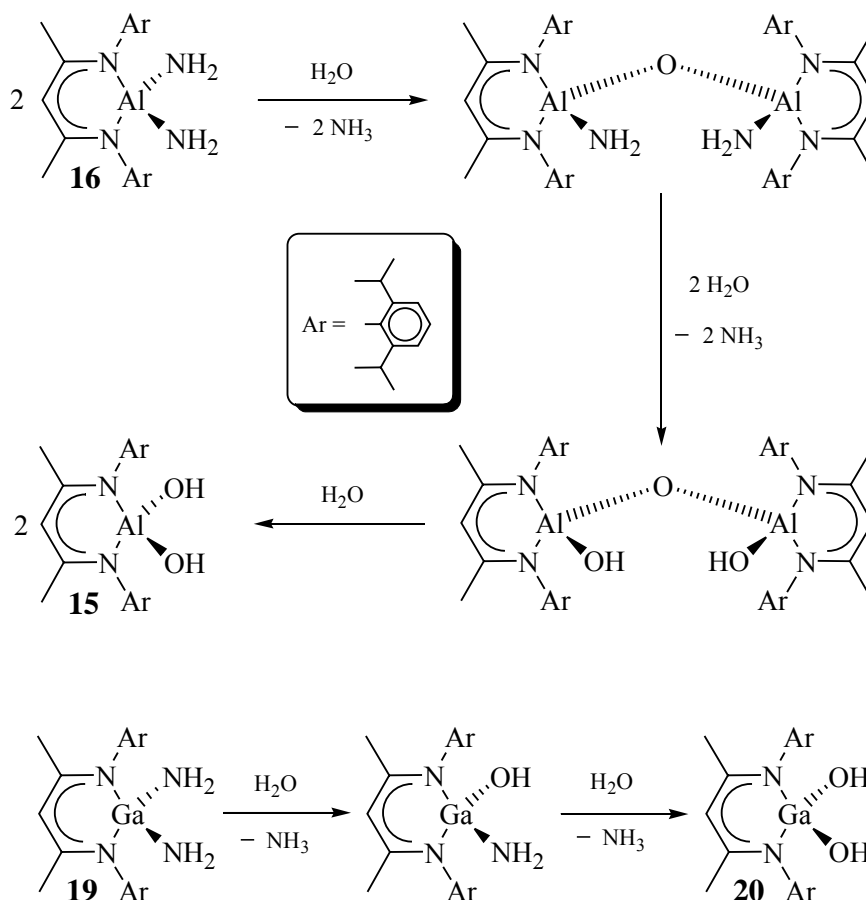
Figure 25: Thermal ellipsoids plot of dimer **B** of **20** showing the 50% probability level. H atoms, except O–H, are omitted for clarity. Only one of the two independent molecules is shown. Selected bond lengths [Å] and angles [°]: Ga(1A)–N(1A) 1.933(1), Ga(1A)–N(2A) 1.933(1), Ga(1A)–O(1A) 1.801(1), Ga(1A)–O(2A) 1.819(1), O(1A)–H(1') 0.72(2), O(2A)–H(2') 0.74(2), O(2A)–H(2'') 0.73(2); N(1A)–Ga(1A)–N(2A) 98.3(1), N(1A)–Ga(1A)–O(1A) 112.3(1), N(1A)–Ga(1A)–O(2A) 110.9(1), N(2A)–Ga(1A)–O(1A) 114.2(1), N(2A)–Ga(1A)–O(2A) 109.0(1), O(1A)–Ga(1A)–O(2A) 111.5(1), H(1')–O(1A)–Ga(1A) 105(2), H(2')–O(2A)–Ga(1A) 98(4), H(2'')–O(2A)–H(2'') 109(7), H(2'')–O(2A)–Ga(1A) 113(6).

2.4. Controlled Degradation of Amides and Sulfides

2.4.1. Controlled Hydrolysis of Amides $LAl(NH_2)_2$ (**16**), $LAl(NH_2)Cl$ (**17**), $LAl(NH_2)Me$ (**18**) and $LGa(NH_2)_2$ (**19**)

It is well known, that the metal amides $M_x(NR_2)_y$ are important synthetic precursor. The NR_2 moiety can be easily replaced by stronger nucleophiles as OR or SR, but the reaction stoichiometries and the conditions have to be carefully controlled to avoid decomposition of the products. Recently, we have shown the successful preparation of molecular Sn-, Pb- and Ge-oxoclusters from bulky silanetriols and the corresponding hexamethyldisilazanides $M[N(SiMe_3)_2]_2$ ($M = Ge, Sn, Pb$).^[191–193] Furthermore, the hydrolysis of amides and thiols of oxo- and carboxylic acids leading to the acids are basic chemical reactions.^[194] We were curious to know, if we can combine these two approaches and hydrolyze selectively amides described in the previous chapter. Compounds $LAl(NH_2)_2$ (**16**), $LAl(NH_2)Me$ (**18**), and $LGa(NH_2)_2$ (**19**) react in toluene cleanly with one (**18**) or two (**16** and **19**) equivalent(s) of water upon formation of NH_3 and the hydroxides $LAl(OH)_2$ (**15**), $LAl(OH)Me$, and $LGa(OH)_2$ (**20**). Only $LAl(NH_2)Cl$ (**17**) decomposed in this reaction due to the presence of a reactive Al–Cl bond. Exact stoichiometries of the reactions are critical, because excess of water leads to decomposition of the hydroxides. The next aim was to determine the mechanism of these reactions to examine whether the reactions proceed *via* bridged intermediates. We focused the hydrolysis on **16** and **19** because of the presence of two NH_2 groups. As determined by 1H NMR spectroscopy for different molar ratios of the amide and water, there is significant difference in their reactivity. Interpretation of the proton NMR spectra obtained of the hydrolysis of **16** with less than 2 equivalents of water revealed the presence of $[LAl(OH)]_2O$ in the product. This compound was isolated in pure form when a 2:3 (**16**: H_2O) molar ratio was used. Further addition of water to this compound leads to the cleavage of the Al–O–Al bridge and formation of **15**. Thus the Al–O–Al bridged species $[LAl(NH_2)]_2O$ is one of the first products in the hydrolysis, but cannot be isolated. Subsequently, the free NH_2 groups are replaced by OH functionalities to form $[LAl(OH)]_2O$. This species has been obtained recently in our group also in the reaction of wet methylhydrazine with LiH_2 .^[195] The steric bulk of the ligand prevents these species of further condensation. Addition of one equivalent of H_2O to $[LAl(OH)]_2O$ led quantitatively to **15**. Compared to **16** the hydrolysis of **19** does not proceed *via* an oxygen bridged species but

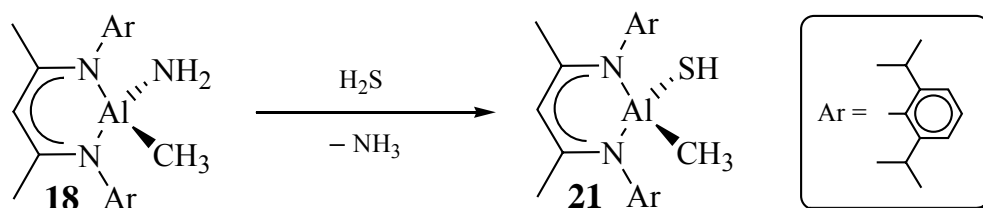
forms the intermediate, $\text{LGa}(\text{NH}_2)(\text{OH})$. The latter one was identified as a byproduct in the preparation of **19**. Currently we are working on its isolation. Scheme 13 shows proposed mechanisms for the hydrolysis of **16** and **19**.



Scheme 13: Proposed mechanisms for the hydrolysis of **16** and **19**.

2.4.2. Reaction of $\text{LAl}(\text{NH}_2)\text{Me}$ (**18**) with H_2S

Furthermore we explored the reaction of **18** with gaseous H_2S in toluene. According to our expectations $\text{LAl}(\text{SH})\text{Me}$ (**21**) was formed as the only product (Scheme 14). The ^1H NMR spectrum clearly shows the presence of two different substituents on the Al center. The SH



Scheme 14: Synthesis of $\text{LAl}(\text{SH})\text{Me}$ (**21**).

proton resonates at $\delta -0.88$ ppm, which has the same value observed for that of $\text{LAl}(\text{SH})_2$. The highest peak in the EI-MS spectrum is at m/z 477 and was assigned to $[\text{M} - \text{Me}]^+$ cation. Compound **21** decomposes similarly like **18** to $\text{LAl}(\text{OH})\text{Me}$ after addition of H_2O or exposure to moisture.

2.4.3. Solid State Structure of $\text{LAl}(\text{SH})\text{Me}$ (**21**)

Single crystals of **21** suitable for a X-ray measurement were obtained by storing a toluene solution at -32 °C. Compound **21** crystallizes in the monoclinic space group $P2_1/n$ with one molecule in the asymmetric unit. As in the case of $\text{LAl}(\text{NH}_2)\text{Cl}$ (**17**) the substituents on Al are disordered. (Figure 26) The preferred conformer (88%) has the SH group in the axial and the

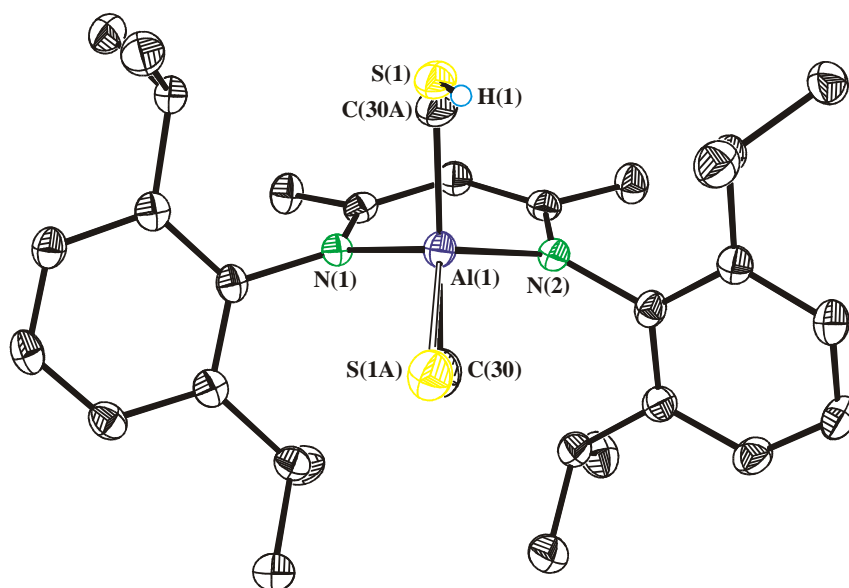


Figure 26: Crystal structure of **21** showing the presence of two conformers (50% probability ellipsoids). Hydrogen atoms except SH proton are omitted for clarity. Proton on S(1A) could not be localized. Selected bond lengths [\AA] and angles [$^\circ$]: $\text{Al}(1)\text{--S}(1)$ 2.234(1), $\text{Al}(1)\text{--C}(30)$ 1.947(6), $\text{S}(1)\text{--H}(1)$ 1.21(4), $\text{Al}(1)\text{--S}(1\text{A})$ 2.122(14), $\text{Al}(1)\text{--C}(30\text{A})$ 1.864(16), $\text{Al}(1)\text{--N}(1)$ 1.910(1), $\text{Al}(1)\text{--N}(2)$ 1.892(1); $\text{N}(1)\text{--Al}(1)\text{--N}(2)$ 97.48(6), $\text{S}(1)\text{--Al}(1)\text{--C}(30)$ 116.8(3), $\text{Al}(1)\text{--S}(1)\text{--H}(1)$ 99(2), $\text{S}(1\text{A})\text{--Al}(1)\text{--C}(30\text{A})$ 113(1).

CH_3 groups in equatorial position. The SH proton of the 12% conformer could not be localized from the electron density map. Due to the low content of the minor conformer the $\text{Al}\text{--S}$ (2.122(14)) \AA and $\text{Al}\text{--C}$ (1.864(16)) \AA bond lengths were determined with larger standard deviations as those for the main component ($\text{Al}\text{--S}$ 2.234(1) \AA and $\text{Al}\text{--C}$ 1.947(6) \AA)

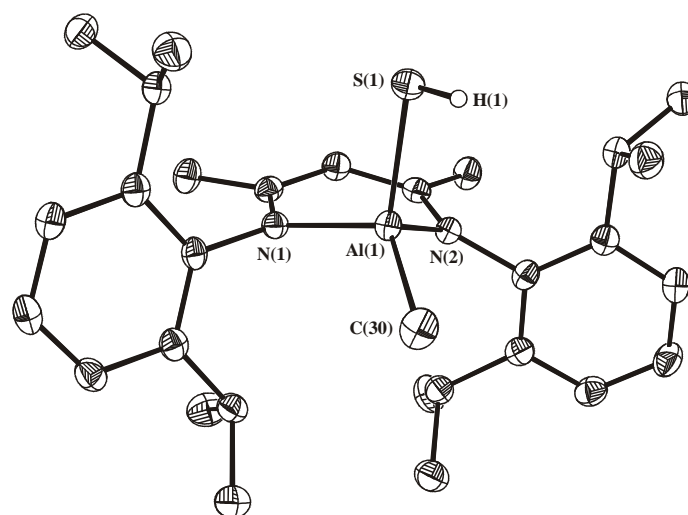
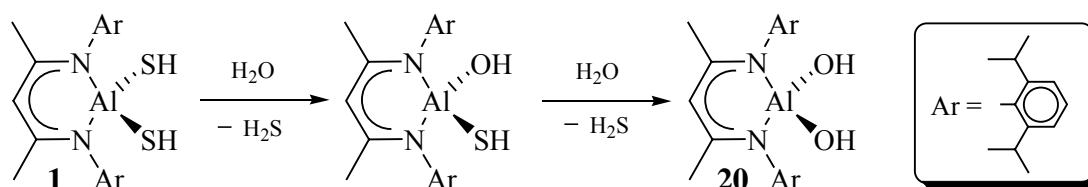


Figure 27: Preferred conformer (88%) of **21**.

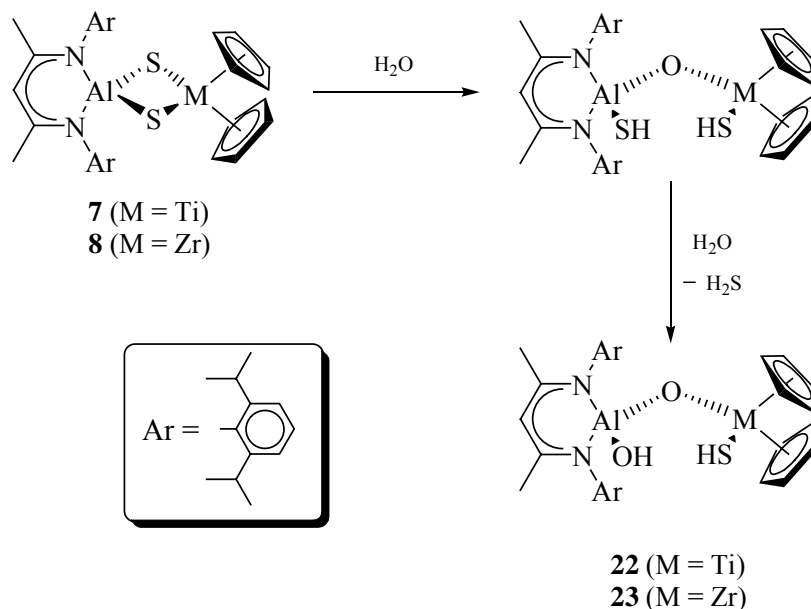
(only standard value for SADI restraint was used for these bonds lengths). A lower limit for the difference between the Al–S and Al–C bond lengths led to an increase of the standard deviations of these bonds for the main component and did not give a better *R*1 factor. Thus, only the bond lengths for the main component will be used for further discussion (Figures 26 and 27). The N₂AlSC core has a distorted tetrahedral geometry with the smallest 97.5° (N–Al–N) and the largest 116.7° (C–Al–S) angle. The Al–S bond length (2.234 Å) is slightly longer than those in LAl(SH)₂ (2.223 and 2.217 Å), but the Al–C distance (1.947 Å) is almost identical with that in LAl(NH₂)Me (**18**) (1.943 Å) and slightly shorter than in LAlMe₂ (1.958, 1.970 Å).^[185]

2.4.4. Controlled Hydrolysis of LAl(SH)₂ (**1**) and LAl(μ-S)₂MCp₂ (**7**, M = Ti; **8**, M = Zr)

After the successful investigations of the hydrolysis of the amides, a similar study on the sulfides was studied next. The preparation of LAl(OH)₂ (**15**) from LAl(SH)₂ would be the easiest way to obtain this species. Addition of two equivalents of water to a toluene solution of **1** at ambient temperature resulted in evolution of H₂S and formation of **15** in 90% yield. ¹H NMR measurements revealed a similar hydrolysis mechanism like that of **19**. The first equivalent of water reacts with **1** to form a stable intermediate LAl(SH)(OH) which reacts further with a second equivalent to **15** (Scheme 15). We are currently working on the isolation of the intermediate. Encouraged by these results, we started to study hydrolysis of the bimetallic sulfide LAl(μ-S)₂MCp₂ (**7**, M = Ti; **8**, M = Zr) in THF. Addition of water to these systems led to the opening of the AlS₂M ring and formation of the oxygen bridged species



Scheme 15: Proposed mechanism for the hydrolysis of **1**.



Scheme 16: Proposed mechanism for the hydrolysis of **7** and **8**.

$\text{LAl}(\text{SH})(\mu\text{-O})\text{M}(\text{SH})\text{Cp}_2$. These intermediates react with a second molecule of water and form under elimination of H_2S under formation of $\text{LAl}(\text{OH})(\mu\text{-O})\text{M}(\text{SH})\text{Cp}_2$ (**22**, $\text{M} = \text{Ti}$; **23**, $\text{M} = \text{Zr}$) (Scheme 16). This mechanism is supported by the presence of ca. 10% of the intermediates in the crystals of **22** and **23** as proven by X-ray structural analysis (see next Section). The presence of the intermediates in the final product can be explained by the low solubility of the bridged species in THF and their crystallization from the mother liquor before the reaction was completed. This problem can be easily overcome by using a THF/ CH_2Cl_2 mixture, due to the higher solubility of **22** and **23** in halogenated solvents such as CH_2Cl_2 or CHCl_3 higher than in THF. Currently, we are focused on the optimization of the ratio between THF and CH_2Cl_2 to obtain pure **22** and **23**. Surprising in these reactions is the higher reactivity of the Al-S bond compared to that of M-S . The hydrolysis of **1** proceeds smoothly, but is relatively slow and needs at least 20 minutes at ambient temperature to reach completion. It has been reported that even traces of moisture in Ti-S and Zr-S systems led to fast hydrolysis of these bonds.^[196–199] As reported earlier, the alumoxane $[\text{LAl}(\text{OH})]_2\text{O}$ ^[109] is

stable, whereas the LAl(OH)_2 (**15**) decomposes even under an inert atmosphere. It seems, that the presence of at least one bridging oxygen atom is necessary for the stabilization of the AlO_2 unit containing species.

2.4.5. Crystal Structure Determinations of $\text{LAl(OH)(}\mu\text{-O)M(SH)Cp}_2$ (**22**, $M = \text{Ti}$; **23**, $M = \text{Zr}$)

The almost isostructural compounds **22** and **23** crystallize in the monoclinic space group $P2_1/n$ with one molecule in the asymmetric unit. As mentioned above, both derivatives are contaminated by ca. 10% of the hydrolysis intermediates, $\text{LAl(SH)(}\mu\text{-O)M(SH)Cp}_2$ (Figures 28–31). The OH moiety on aluminum and the SH groups on Ti (**22**) and Zr (**23**), respectively, are in *cis* conformation and are involved in an intramolecular hydrogen bond $\text{O–H}\cdots\text{S}$ (**22**: 2.54 Å, **23**: 2.77 Å). The Al–O(H) (**22**: 1.715 Å, **23**: 1.716 Å) and Al–O(M)

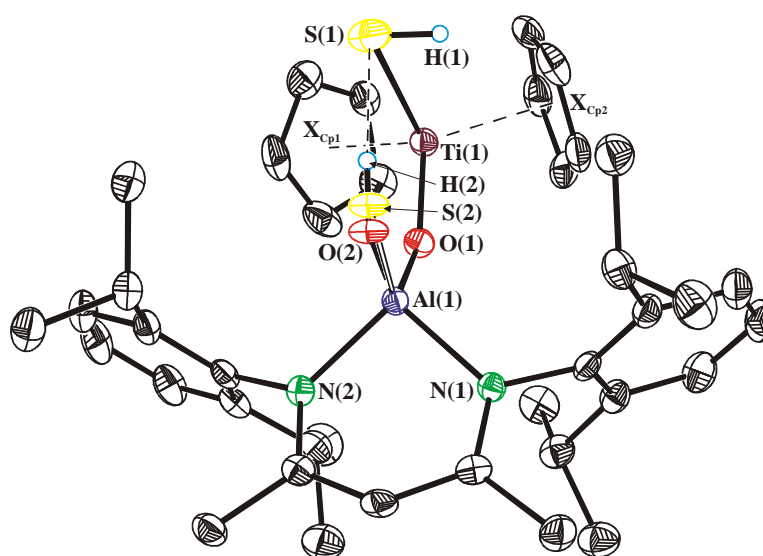


Figure 28: XP plot of **22** (50% probability ellipsoids) showing presence of the reaction intermediate containing SH group on aluminum, whose proton could not be localized. Hydrogen atoms except the Ti–SH and Al–OH protons are omitted for clarity. Selected bond lengths [Å] and angles [°]: Al(1)–N(1) 1.893(2), Al(1)–N(2) 1.899(2), Al(1)–O(1) 1.720(2), Al(1)–S(2) 1.95(3), Al(1)–O(2) 1.716(7), O(2)–H(2) 1.01(6), Ti(1)–O(1) 1.819(2), Ti(1)–S(1) 2.477(1), S(1)–H(1) 1.04(4), Ti(1)–X_{Cp1} 2.107(3), Ti(1)–X_{Cp2} 2.098(3); N(1)–Al(1)–N(2) 97.5(1), O(1)–Al(1)–O(2) 115.3(2), O(1)–Al(1)–S(2) 106.7(9), Al(1)–O(2)–H(2) 114(2), Al(1)–O(1)–Ti(1) 149.3(1), O(1)–Ti(1)–S(1) 97.2(1), Ti(1)–S(1)–H(1) 80(2), X_{Cp1}–Ti(1)–X_{Cp2} 128.6(2).

(**22** – 1.713 Å, **23** – 1.720 Å) bond lengths are similar to those in **15** (1.711 and 1.695 Å),^[38] [Al(OH)]₂O (1.694–1.741 Å)^[109] and in the trimeric alumoxane [(LAl)₂(MeAl)(μ-O)₃] (1.726–1.708 Å),^[109] but considerably shorter than those in the μ-OH derivatives (1.787–1.928 Å).^[111–114] The O–Al–O angles (**22**: 115.3°, **23**: 114.8°) are similar to those of **15**, [Al(OH)]₂O and [(LAl)₂(MeAl)(μ-O)₃] (108.3–115.3°). The Al–O–M angles have values for **22** (149.3°) and **23** (147.2°). The Ti–O (1.819 Å) and Ti–S (2.477 Å) bond lengths and the O–Ti–S angle (97.2°) are similar to those reported in the literature for other Cp₂TiOS fragments: Ti–O (1.845–1.872 Å), Ti–S (2.314–2.467 Å) and O–Ti–S angle (87.7–97.9°).^[157,200–202] Also in the case of the zirconium derivative the Zr–O (1.939 Å) and Zr–S (2.573 Å) bond lengths and the O–Zr–S angle (98.7 Å) are similar to those reported previously for Cp₂ZrOS moiety containing species: Zr–S (2.459–2.554 Å), Zr–S (1.941–2.199 Å) O–Zr–S (92.6–103.3°).^[197,203–206]

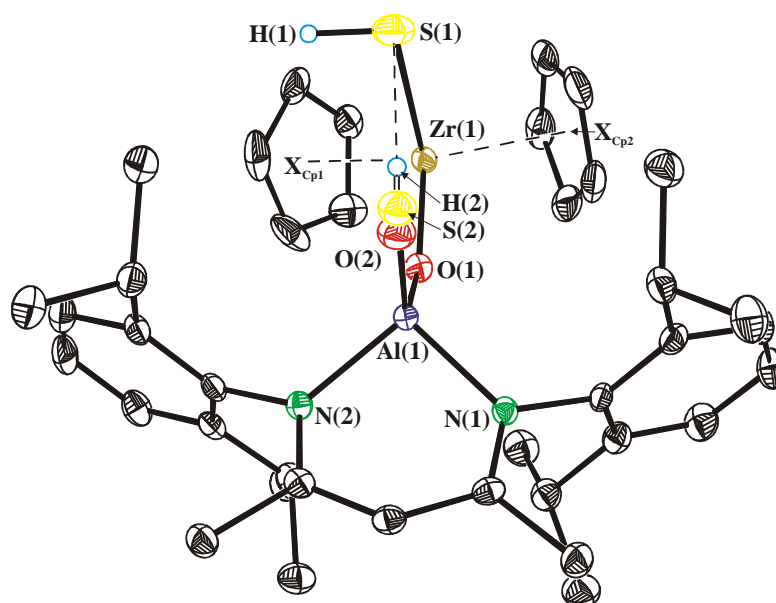


Figure 29: XP plot of **23** (50% probability ellipsoids) showing presence of the reaction intermediate containing an SH group on aluminum, whose proton could not be localized. Hydrogen atoms except the Zr–SH and Al–OH protons are omitted for clarity. Selected bond lengths [Å] and angles [°]: Al(1)–N(1) 1.895(2), Al(1)–N(2) 1.898(2), Al(1)–O(1) 1.713(2), Al(1)–S(2) 2.08(2), Al(1)–O(2) 1.715(8), O(2)–H(2) 0.89(4), Zr(1)–O(1) 1.939(2), Zr(1)–S(1) 2.573(1), S(1)–H(1) 1.19(3), Zr(1)–X_{Cp1} 2.237(3), Zr(1)–X_{Cp2} 2.240(3); N(1)–Al(1)–N(2) 96.1(1), O(1)–Al(1)–O(2) 114.8(3), O(1)–Al(1)–S(2) 112.0(6), Al(1)–O(2)–H(2) 121(2), Zr(1)–S(1)–H(1) 100(2), Al(1)–O(1)–Zr(1) 147.2(1), O(1)–Zr(1)–S(1) 98.7(1), X_{Cp1}–Zr(1)–X_{Cp2} 128.0(2).

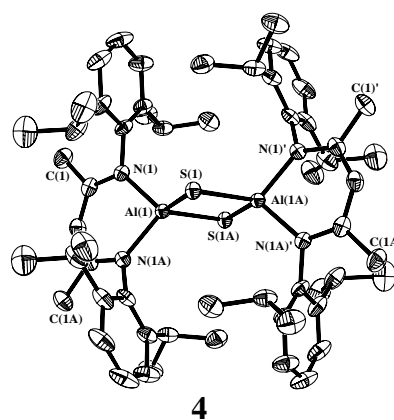
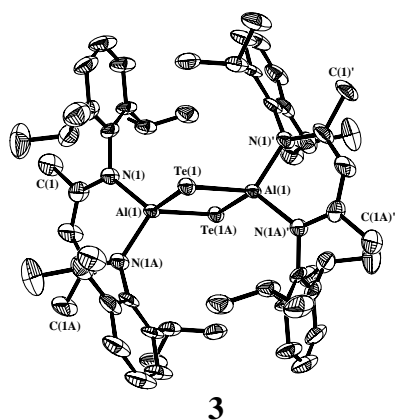
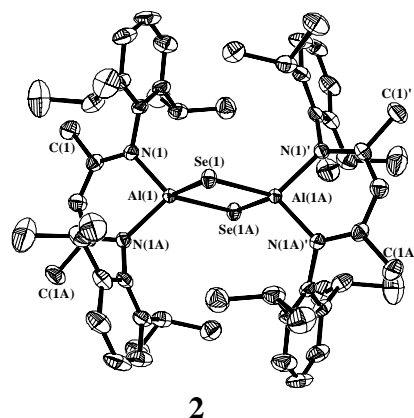
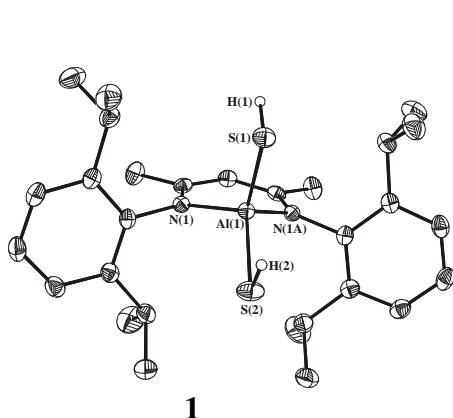


3. Summary and Outlook

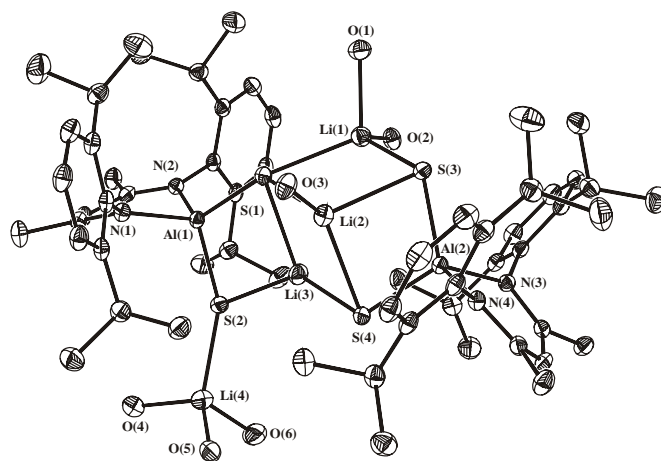
3.1. Summary

The preparation of small organometallic molecules with functional groups, e.g. SH, OH, NH₂ attached to the metal center has not yet been well investigated though these compounds are highly desired. Substitution of the free functionalities is a route to heterobimetallic systems.

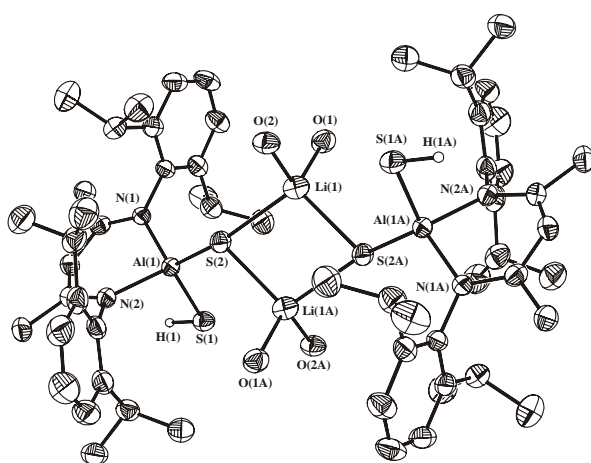
The first part of this work was focused on reactions of elemental sulfur, selenium and tellurium with LAIH₂. Phosphine catalysis has significant influence on the reaction products and such reactions led to the isolation of LAI(μ-Se)₂AIL (2), LAI(μ-Te)₂AIL (3) and unique LAI(SH)₂ (1). The latter one is the first structurally characterized bishydrogensulfide of a main group metal. Reaction of 1 and LAIH₂ produces LAI(μ-S)₂AIL (4) as the only product.



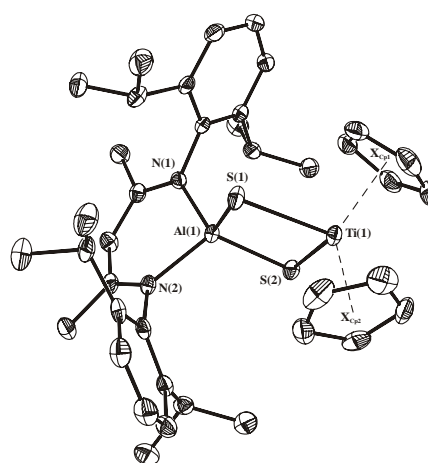
Furthermore, lithiation of **1** with $\text{LiN}(\text{SiMe}_3)_2$ in 1:1 and 1:2 molar ratios gave exclusive mono- and dilithium salts $\text{LAl}(\text{SLi})_2$ (**5**) and $\text{LAl}(\text{SH})(\text{SLi})$ (**6**). Their reactions with Cp_2MCl_2 ($\text{M} = \text{Ti}, \text{Zr}$) resulted in the formation of the first mixed metal sulfides containing aluminum: $\text{LAl}(\mu\text{-S})_2\text{MCp}_2$ (**7** $\text{M} = \text{Ti}$, **8** $\text{M} = \text{Zr}$).



5



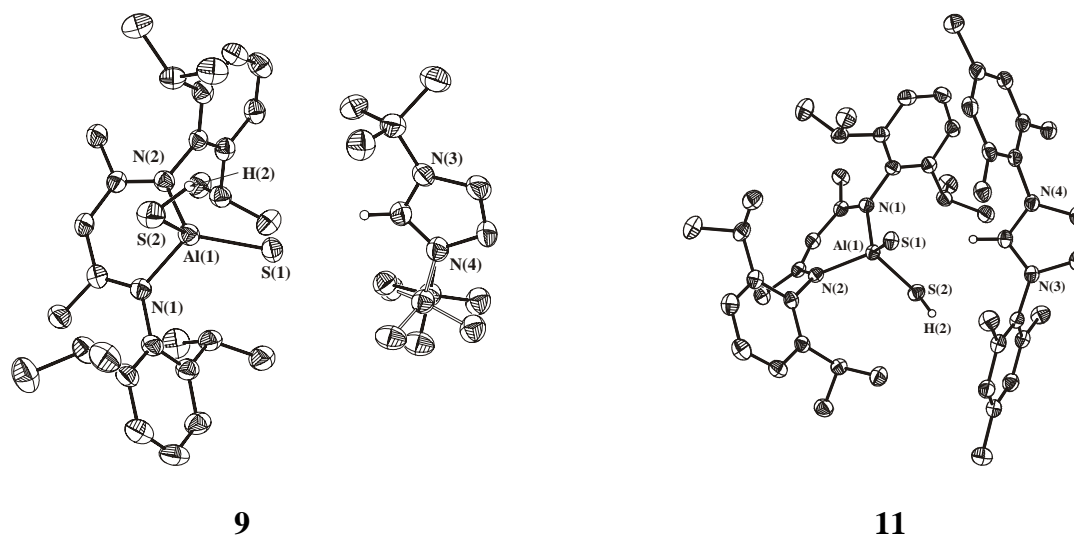
6



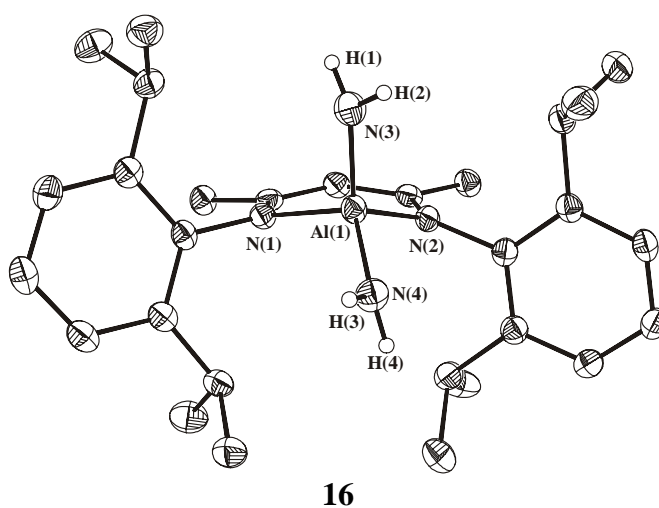
7

Deprotonation of the SH groups in **1** was achieved by use of N-heterocyclic carbenes as bases and generated the mono- and di-carbene salts $\text{C}_6\text{H}^+[\text{LAl}(\text{SH})(\text{S})]^-$ (**9**), $\text{C}_m\text{H}^+_2[\text{LAl}(\text{S})_2]^{2-}$ (**10**) and $\text{C}_m\text{H}^+[\text{LAl}(\text{SH})(\text{S})]^-$ (**11**), respectively. The X-ray crystallographic studies of the salts **9** and **11** revealed the presence of “naked” sulfur centers bound to aluminum and incorporated into two close contacts with hydrogen atoms from two different imidazolium cations. The Al-S^- bonds in **9** and **11** are with 2.114 Å the shortest observed so far.^[49,57,58,61,168–173] These carbene salts showed to be excellent precursor for the formation of mixed sulfides based on aluminum and silicon, $\text{LAl}(\text{SSiMe}_3)_2$ (**12**), $\text{LAl}(\mu\text{-S})_2\text{SiMe}_2$ (**13**), and

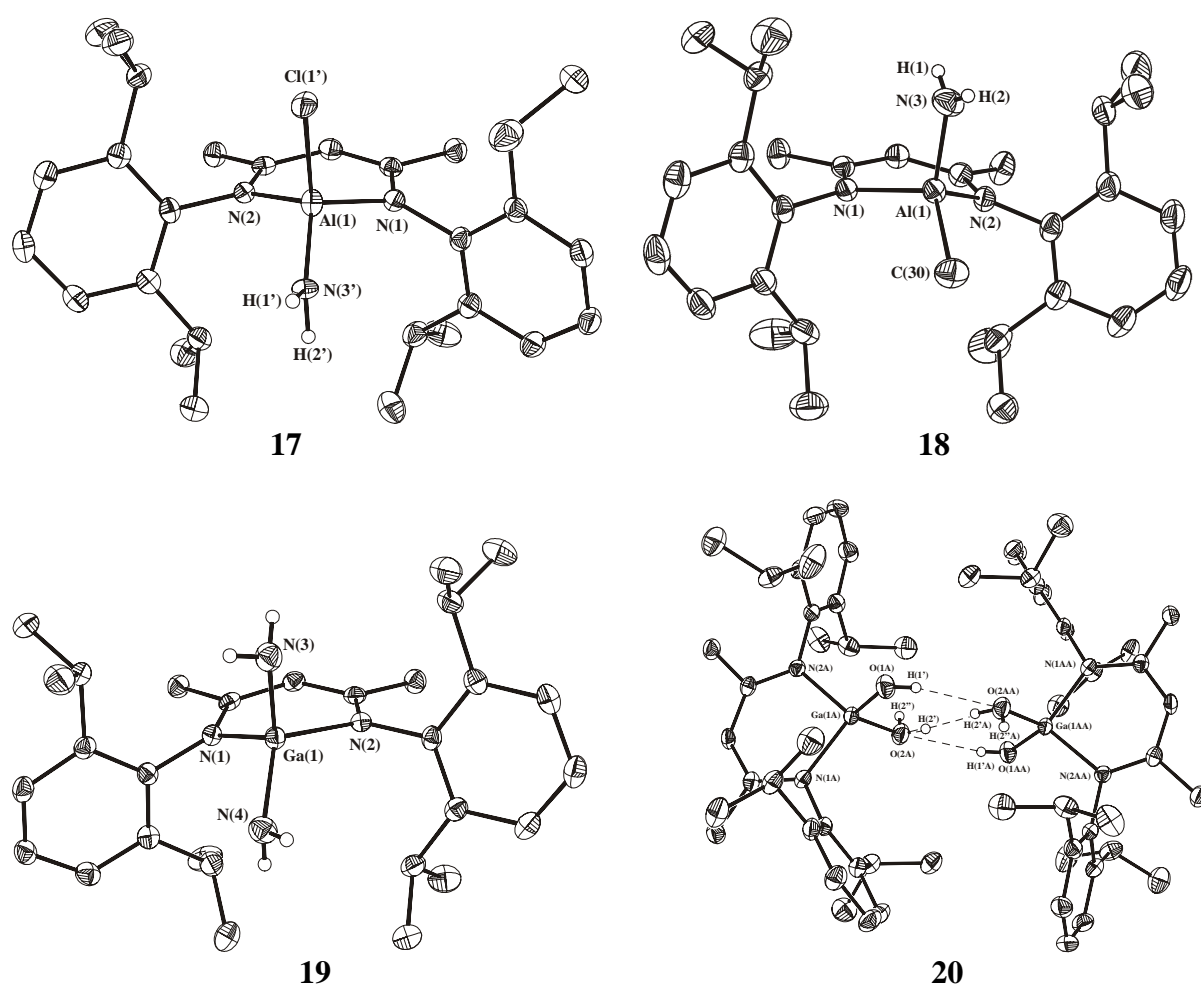
$\text{LAl}(\text{SSiMe}_2)_2\text{O}$ (**15**). Thus, their synthesis was possible only through direct reactions of organoaluminum halides and lithium salts of silanethiols.



In the second part, innovative synthetic routes using N-heterocyclic carbenes as proton scavengers were developed for the conversion of the metal halides to the corresponding hydroxides and amides. Reactions of LAlI_2 with two equivalents of *N,N'*-bis-mesitylimidazolyl carbene and two equivalents of H_2O and NH_3 , respectively, led in the first case to the previously described $\text{LAl}(\text{OH})_2$ (**15**) and $\text{LAl}(\text{NH}_2)_2$ (**16**) containing two terminal NH_2 groups. These are not involved in any kind of hydrogen bonding as proved by crystallographic measurements. Alternatively, LAlCl_2 and *N,N'*-bis-*t*-butylimidazolyl carbene can be used as educts in this reaction. The only byproducts are imidazolium halides, which are very sparingly soluble in hexane, toluene or THF, can be easily separated from the reaction mixtures by filtration. After recrystallization from dichloromethane or acetonitrile the free carbene can be recovered with a strong base such as KO^tBu or NaH .

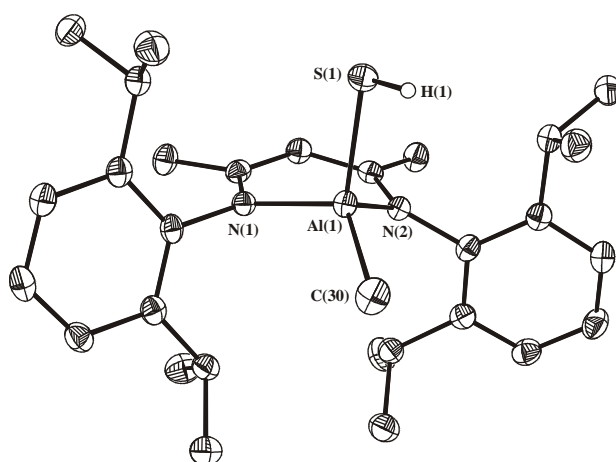


The same methodology was used also for the preparation of hydroxides and amides: $\text{LAl}(\text{NH}_2)\text{Cl}$ (**17**), $\text{LAl}(\text{NH}_2)\text{Me}$ (**18**), $\text{LGa}(\text{NH}_2)_2$ (**19**) and $\text{LGa}(\text{OH})_2$ (**20**). In addition $\text{LGe}(\text{OH})$ – the first stable $\text{Ge}(\text{II})$ hydroxide,^[32] $\text{LAl}(\text{OH})\text{Cl}$,^[207] $\text{LAl}(\text{OH})\text{Me}$,^[184] and $\text{LGa}(\text{OH})\text{Me}$ ^[208] by this method using the corresponding halides. Furthermore, these reagents have been successfully used for the preparation of unprecedented heterobimetallic oxides such as $\text{LAl}(\text{Me})(\mu\text{-O})\text{YbCp}_2\text{THF}$,^[209] $\text{LAlMe}(\mu\text{-O})(\mu\text{-MH}_2)_2(\mu\text{-O})\text{AlMeL}$ ($\text{M} = \text{Al}, \text{Ga}$),^[210] $\text{LGe}(\mu\text{-O})\text{MCp}_2\text{Me}$ ($\text{M} = \text{Zr}, \text{Hf}$)^[211] and $\text{LGaMe}(\mu\text{-O})\text{ZrCp}_2\text{Me}$.^[208] This clearly demonstrates the impact of this method in this field.



The last part of this thesis was focused on reactivity studies of amides, hydrogensulfides, and heterobimetallic sulfides toward H_2O and H_2S . It was suggested that the hydrolysis of $\text{LAl}(\text{NH}_2)_2$ (**16**) proceeds through $(\mu\text{-O})$ bridged binuclear species and can be used in an alternative route for the preparation of $[\text{LAl}(\text{OH})]_2\text{O}$ when a stoichiometric amount of water is used. Addition of one more equivalent of water leads to cleavage of the

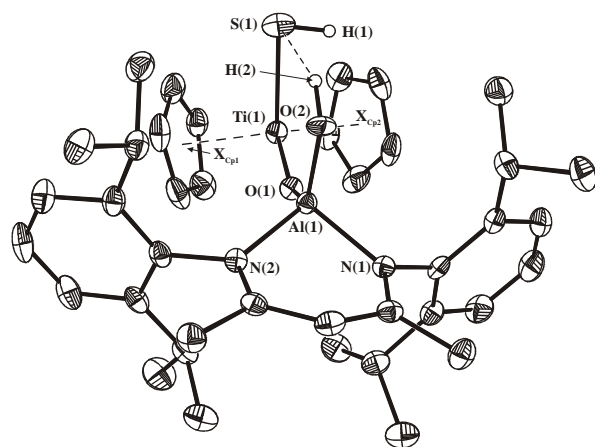
Al–O–Al bridge and formation of LAl(OH)_2 (**15**). This species is highly unstable and decomposes readily under formation of the free ligand LH. The reaction of LAl(SH)_2 (**1**) with water led to the reactive intermediate LAl(OH)(SH) and further to LAl(OH)_2 (**15**). No formation of bridged intermediates was observed. This method of hydrolysis represents the easiest synthetic route to the formation of **15**. Similar behavior during the controlled hydrolysis like in the case of **1** was observed also for $\text{LGa(NH}_2)_2$ (**19**), which decomposes *via* $\text{LGa(OH)(NH}_2)$. Compound **20** is the final product of the hydrolysis. The compound LAl(SH)Me (**21**) was isolated from the reaction of **18** with H_2S in high yield.



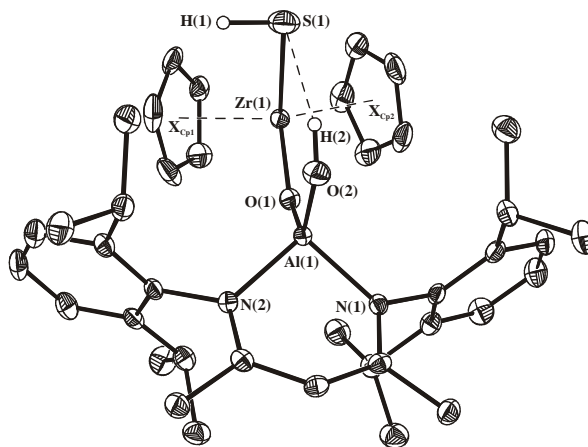
21

Compounds **18** and **21** react with H_2O under formation of LAl(OH)Me . Furthermore, addition of H_2O to the $\text{THF/CH}_2\text{Cl}_2$ solution of $\text{LAl}(\mu\text{-S})_2\text{MCp}_2$ (**7** $\text{M} = \text{Ti}$, **8** $\text{M} = \text{Zr}$) resulted in the formation of unprecedented heterobimetallic oxide-hydroxide-hydrogensulfides $\text{LAl(OH)}(\mu\text{-O})\text{M(SH)Cp}_2$ (**22**, $\text{M} = \text{Ti}$; **23**, $\text{M} = \text{Zr}$).

All substances **1–22** have been fully characterized by analytical and spectroscopic techniques. The solid state structures of the following compounds have been determined by means of X-ray diffraction studies: LAl(SH)_2 (**1**), $\text{LAl}(\mu\text{-Se})_2\text{AIL}$ (**2**), $\text{LAl}(\mu\text{-Te})_2\text{AIL}$ (**3**), $\text{LAl}(\mu\text{-S})_2\text{AIL}$ (**4**), LAl(SLi)_2 (**5**), LAl(SH)(SLi) (**6**), $\text{LAl}(\mu\text{-S})_2\text{TiCp}_2$ (**7**), $\text{C}_4\text{H}^+[\text{LAl(SH)(S)}]^-$ (**9**), $\text{C}_m\text{H}^+[\text{LAl(SH)(S)}]^-$ (**11**), $\text{LAl(NH}_2)_2$ (**16**), $\text{LAl(NH}_2)\text{Cl}$ (**17**), $\text{LAl(NH}_2)\text{Me}$ (**18**), $\text{LGa(NH}_2)_2$ (**19**), LGa(OH)_2 (**20**), LAl(SH)Me (**21**), $\text{LAl(OH)}(\mu\text{-O})\text{Ti(SH)Cp}_2$ (**22**) and $\text{LAl(OH)}(\mu\text{-O})\text{Zr(SH)Cp}_2$ (**23**).



22



23

3.2. Outlook

The thesis presented here has focussed on generating functionalities on aluminum and gallium centers such as SH, OH, NH₂ and studying their reactivity. This resulted in the development of new synthetic strategies for generating of such species. Extension of this work may be the application of the carbene method for conversion of metal halides to the corresponding hydroxides and amides. In summary, generation of such hydroxides has a huge synthetic potential in the field of well-defined heterobimetallic oxides. Moreover, other p-, d- or f- block metals are potential candidates for the generation of heterobimetallic sulfides containing aluminum from carbene and lithium salts obtained from $\text{LiAl}(\text{SH})_2$.

4. Experimental Section

4.1. General Procedures

All reactions and handling of reagents were performed under an atmosphere of dry nitrogen or argon using Schlenk techniques^[212] or a glovebox where the O₂ and H₂O levels were usually kept below 1 ppm. All glassware was oven-dried at 140 °C for at least 24 h, assembled hot and cooled under high vacuum prior to use. Toluene (Na/benzophenone ketyl and diphenylether), benzene (K/benzophenone ketyl and diphenylether), hexane (Na/K/benzophenone ketyl and diphenylether), pentane (Na/K/benzophenone ketyl and diphenylether), tetrahydrofuran (K/benzophenone ketyl), diethylether (Na/benzophenone ketyl), dichloromethane (CaH₂) were dried and distilled prior to use. Ethanol free trichloromethane stabilized with amylene was stirred for three min. with P₄O₁₀ and after filtration stored over molecular sieves in a sealed vessel.

4.2. Physical Measurements

Melting points were measured in sealed glass tubes on a Büchi B-540 melting point apparatus.

NMR spectra were recorded on Bruker Avance 200, Bruker Avance 300, and Bruker Avance 500 NMR spectrometers. Chemical shifts are reported in ppm with reference to SiMe₄ (external) for ¹H, ¹³C and ²⁹Si isotopes, 1M LiCl in D₂O (external) for ⁷Li nuclei, [Al(H₂O)₆]³⁺ (external) for ²⁷Al nuclei, and CH₃NO₂ (external) for ¹⁵N isotope. Downfield shifts from the reference are quoted positive, upfield shifts are assigned negative values. The NMR grade deuterated solvents were dried and in following manners: C₆D₆ – overnight stirring with Na/K alloy followed by vacuum distillation, CDCl₃ – 3 min. stirring with P₄O₁₀ followed by filtration, THF – storing over freshly activated molecular sieves for one week. Heteroatom NMR spectra were recorded ¹H decoupled.

IR spectra were recorded on a Bio-Rad Digilab FTS7 spectrometer in the range 4000–350 cm⁻¹ as KBr pellets. Only the absorption of significant moieties (NH₂, OH, SH) are listed except for compounds **2–4**, where all the absorption (weak to very strong) are reported

as the only method for their identification. IR spectra of compounds **9–11** could not be obtained due to the reaction with available pellet materials.

Mass spectra were obtained with a Finnigan MAT 8230 or a Varian MAT CH5 instrument (70 eV) by EI-MS methods.

Elemental analyses were performed by the Analytisches Labor des Instituts für Anorganische Chemie der Universität Göttingen.

Crystal structure determination: Intensity data for compound **2** were collected on an IPDS II Stoe image-plate diffractometer and compound **18** was measured on a STOE-AED2 four circle diffractometer using graphite monochromated Mo-K α radiation ($\lambda = 0.71073$ Å). The diffraction data for the compounds **1**, **3–7**, **9**, **11**, **16**, **17**, **19–23** were measured on a Bruker three-circle diffractometer equipped with a SMART 6000 CCD detector using mirror monochromated Cu-K α radiation ($\lambda = 1.54178$ Å). The data for all compounds were collected at low temperature (for exact values see Tables in Section 6). The structures were solved by direct methods (SHELXS-97)^[213] and refined with all data by full-matrix least-squares methods on F^2 using SHELXL-97.^[214] The restraints and constraints as AFIX, DELU, EADP, FLAT, SAME, SADI, SIMU were used to treat disordered groups, lattice solvents such as THF, toluene and trichloromethane and the hydrogen atoms. The non-hydrogen atoms were refined anisotropically; the hydrogen atoms of C–H bonds except the ones on γ -C of the ligand were placed in idealized positions, and refined with a riding model, whereas the hydrogen atoms from the NH₂, OH, SH and γ -CH moieties were localized from the difference electron density map and refined isotropically. The crystal data for all compounds along with the final residuals and other pertaining details are tabulated in Section 6.

4.3. Starting Materials

Sulfur (Aldrich), tellurium (Aldrich) and PMe₃ (1 M solution in toluene, Fluka), Cp₂MCl₂ (M = Ti, Zr) (Aldrich), (Me₂SiCl)₂O (Fluka), H₂S (Messer), NH₃ (Messer) were used as received. P(NMe₂)₃ (Aldrich), Me₃SiCl (Acros), and Me₂SiCl₂ (Acros) were freshly distilled prior to use. Elemental red selenium,^[215] LAIH₂,^[26] LAICl₂,^[182] LAI₂,^[27] LAIClMe,^[184] LGaCl₂,^[186] and TePEt₃,^[216] N,N'-bis-*tert*-butylimidazolyl carbene,^[162] N,N'-bis-

mesitylimidazolyl carbene^[167] were prepared by literature procedures. $\text{LiN}(\text{SiMe}_3)_2$ was prepared prior to use from freshly distilled $\text{HN}(\text{SiMe}_3)_2$ and MeLi in pentane. Redistilled H_2O was degassed prior to use.

4.4. Syntheses of Compounds 1–23

4.4.1. Synthesis of $\text{LAl}(\text{SH})_2$ (**1**)

Toluene (50 mL) was added to a mixture of LAlH_2 (3.18 g, 7.12 mmol) and sulfur (0.48 g, 1.87 mmol – calcd. for S_8) and after complete dissolution of the sulfur, $\text{P}(\text{NMe}_2)_3$ (0.03 mL, 0.02 mmol) was added. The reaction mixture was stirred for additional 5 h, concentrated to ~10 mL and stored overnight at $-32\text{ }^\circ\text{C}$. The resulting pale yellow crystals of **1** were filtered off, washed with cold toluene (1 mL) and dried *in vacuo*. Yield 3.27 g (90%). M.p. $218\text{ }^\circ\text{C}$ (decomp.); ^1H NMR (C_6D_6 , 200.13 MHz, $25\text{ }^\circ\text{C}$, TMS): δ -0.88 (s, 2H, SH), 1.10 (d, 12H, $^3J_{\text{H-H}} = 6.8\text{ Hz}$, $\text{CH}(\text{CH}_3)_2$), 1.44 (d, 12H, $^3J_{\text{H-H}} = 6.8\text{ Hz}$, $\text{CH}(\text{CH}_3)_2$), 1.51 (s, 6H, CH_3), 3.47 (sept, 4H, $^3J_{\text{H-H}} = 6.8\text{ Hz}$, $\text{CH}(\text{CH}_3)_2$), 4.88 (s, 1H, $\gamma\text{-CH}$), $7.13\text{--}7.11$ ppm (*m*, *p*- 6H, Ar-*H*); ^{13}C NMR (C_6D_6 , 50.33 MHz): δ $24.0\text{--}24.7$ $\text{CH}(\text{CH}_3)_2$, 25.5 $\text{CH}(\text{CH}_3)_2$, 28.6 (CH_3), 98.7 ($\gamma\text{-C}$), 124.5 , 127.5 , 138.7 , 144.4 (*i*, *o*, *m*, *p*- C of Ar), 171.4 ($\text{C}=\text{N}$); IR (KBr pellet): (cm^{-1}) $\tilde{\nu}$ 2549 (SH); EI-MS: m/z (%): 510 (20, $[\text{M}]^+$), 477 (28, $[\text{M}-\text{SH}]^+$); Elemental analysis calcd. for $\text{C}_{29}\text{H}_{43}\text{AlN}_2\text{S}_2$ ($510.78\text{ g}\cdot\text{mol}^{-1}$): C 68.2, H 8.5, N 5.5; found: C 67.8, H 8.3, N 5.4%.

4.4.2. Synthesis of $\text{LAl}(\mu\text{-Se})_2\text{AlI}$ (**2**)

Toluene (20 mL) was added to a mixture of LAlH_2 (1.00 g, 2.24 mmol) and red selenium (0.18 g, 2.24 mmol) and after dissolving of the reactants, freshly distilled $\text{P}(\text{NMe}_2)_3$ (0.03 mL, 0.02 mmol) was added. The reaction mixture was stirred for additional 16 h and the white insoluble **2** was filtered off, washed with toluene (5 mL) and dried *in vacuo*. Yield 1.07 g (91%). No m.p. above $260\text{ }^\circ\text{C}$ (decomp.); IR (KBr pellet): (cm^{-1}) $\tilde{\nu}$ 2959 st, 2927 w, 2868 w, 1544 vst, 1462 w, 1438 m, 1392 vst, 1317 m, 1249 w, 1177 w, 1101 w, 1024 w, 867 w, 801 m, 763 w, 435 w; EI-MS: m/z (%): 1048 (48, $[\text{M}]^+$), 523 (28, $[\text{M}/2]^+$); Elemental analysis calcd. for $\text{C}_{58}\text{H}_{82}\text{Al}_2\text{N}_4\text{Se}_2$ ($1047.20\text{ g}\cdot\text{mol}^{-1}$): C 66.5, H 7.9, N 5.4; found: C 67.1, H 8.0, N 5.3%.

4.4.3. Synthesis of $LAl(\mu\text{-Te})_2AlL$ (**3**)

Method 1: Toluene (20 mL) was added to a mixture of $LiAlH_4$ (1.00 g, 2.24 mmol) and tellurium (0.29 g, 2.23 mmol) and after complete dissolving $LiAlH_4$, PMe_3 (0.03 mL, 1 M solution in toluene, 0.03 mmol) was added. The reaction mixture was stirred for additional 15 h, the pale yellow insoluble **3** was filtered off, washed with toluene (5 mL) and dried *in vacuo*. Yield 1.15 g (90% based on Te). No m.p. above 260 °C (decomp.); IR (KBr pellet): (cm^{-1}) $\tilde{\nu}$ 3061 w, 2990 w, 2968 vs, 2956 vs, 2930 st, 2866 m, 1587 w, 1543 vs, 1462 vs, 1440 vs, 1394 vs, 1365 sh, 1300 m, 1251 s, 1176 m, 1100 m, 1057 m, 1024 m, 937 m, 942 w, 868 st, 798 vs, 780 m, 761 st, 648 w, 537 w, 417 vst; EI-MS: m/z (%): 1144 (25, $[M]^+$), 574 (60, $[M/2]^+$), 443 (100, $[M/2 - \text{Te} - \text{H}]^+$). Elemental analysis calcd. for $C_{58}H_{82}Al_2N_4Te_2$ (1144.48 $\text{g}\cdot\text{mol}^{-1}$): C 60.9, H 7.2, N 4.9; found: C 60.5, H 7.2, N 4.8%.

Method 2: Toluene (20 mL) was added to a mixture of $LiAlH_4$ (1.00 g, 2.24 mmol) and $TePEt_3$ (0.55 g, 2.24 mmol) and the reaction mixture was stirred for additional 2 h. The pale yellow insoluble **3** was filtered off, washed with toluene (5 mL) and dried *in vacuo*. Yield 1.22 g (95%).

4.4.4. Synthesis of $LAl(\mu\text{-S})_2AlL$ (**4**)

Toluene (20 mL) was added to a mixture of **1** (1.14 g, 2.24 mmol) and $LiAlH_4$ (1.00 g, 2.24 mmol) and the reaction mixture was refluxed over a period of 15 h. Afterwards the mixture was cooled to ambient temperature and a white insoluble product was filtered off, washed with toluene (5 mL), and dried *in vacuo*. Yield 1.96 g (92%). No m.p. above 200 °C (decomp.); IR (KBr pellet): (cm^{-1}) $\tilde{\nu}$ 2959 st, 2924 m, 2866 w, 1547 vst, 1529 sh, 1462 m, 1437 m, 1390 vst, 1317 st, 11249 m, 1176 w, 1024 w, 868 w, 801 m, 775 w, 763 w, 541 w, 516 m, 472 w, 454 m; EI-MS: m/z (%): 952 (100, $[M]^+$), 937 (64, $[M - \text{CH}_3]^+$), 909 (21, $[M - \text{C}_3\text{H}_7]^+$), 477 (58, $[M/2]^+$); Elemental analysis calcd. for $C_{58}H_{82}Al_2N_4S_2$ (953.40 $\text{g}\cdot\text{mol}^{-1}$): C 73.1, H 8.7, N 5.9; found: C 72.6, H 8.5, N 5.9%.

4.4.5. Synthesis of $\{LAl[SLi(thf)_2]\}_2$ (**5'**)

Compound **1** (2.00 g, 3.92 mmol) and $LiN(SiMe_3)_2$ (1.31 g, 7.83 mmol) were mixed as solids in a flask and subsequently cold THF (70 mL, 0 °C) was added. Within a few seconds pale yellow crystals of **5** started to precipitate from the reaction mixture. After 5 min of stirring at 0 °C, the reaction mixture was cooled to –20 °C and maintained at this temperature for 5–10 min under vigorous stirring to support the crystallization. The time allowed for the crystallization is determined by the color of the solution. The original pale yellow color of the solution turned slowly into a dark brown, which indicates decomposition of the product. Thus, the filtration of the microcrystalline product should occur within the first significant color change of the mother liquor. After washing the crude product with cold THF (5 mL) and drying *in vacuo*, **5'** was obtained as a pale yellow powder. Yield 2.19 g (85%). M.p.: 320 °C (decomp.); 1H NMR (500.13 MHz, THF- d_8 , 25 °C, TMS) δ 1.07 (d, $^3J_{H-H} = 6.8$ Hz, 12H, $CH(CH_3)_2$), 1.25 (d, $^3J_{H-H} = 6.8$ Hz, 12H, $CH(CH_3)_2$), 1.51 (s, 6H, CH_3), 1.77 (m, 8H, $O(CH_2CH_2)_2$), 3.62 (m, 8H, $O(CH_2CH_2)_2$), 4.00 (sept, $^3J_{H-H} = 6.8$ Hz, 4H, $CH(CH_3)_2$), 5.01 (s, 1H, γ -CH), 7.00–7.01 ppm (m, 6H, *m*, *p*- Ar-H); 7Li NMR (116.64 MHz, THF- d_8 , 25 °C, LiCl, 1M in D_2O) δ 1.26 (SLi); ^{13}C NMR (125.77 MHz, THF- d_8 , 25 °C, TMS) δ 24.7 ($CH(CH_3)_2$), 24.8 ($CH(CH_3)_2$), 26.4 ($O(CH_2CH_2)_2$), 27.4 ($CH(CH_3)_2$), 28.7 (CH_3), 68.2 ($O(CH_2CH_2)_2$), 98.1 (γ -CH), 124.2, 126.2, 145.1, 146.1 (*i*, *o*, *m*, *p*- C of Ar), 168.1 ppm (C=N); Elemental analysis calcd. for $C_{74}H_{114}Al_2Li_4N_4O_4S_4$ (1333.71 g·mol $^{-1}$): C 66.6, H 8.6, N 4.2; found: C 65.7, H 8.6, N 4.3%.

4.4.6. Synthesis of $\{LAl(SH)[SLi(thf)_2]\}_2$ (**6**)

Compound **1** (1.00 g, 1.96 mmol) and $LiN(SiMe_3)_2$ (0.33 g, 1.96 mmol) were mixed as solids in a flask and subsequently THF (30 mL) was added at ambient temperature. The mixture was stirred for 5 min, all volatiles were removed *in vacuo*. The crude product was washed with cold hexane (5 mL) to remove the remaining $HN(SiMe_3)_2$, yielding **6** as a pale yellow powder. Yield 1.105 g (85%). M.p.: 230 °C (decomp.); 1H NMR (500.13 MHz, THF- d_8 , 25 °C, TMS) δ –1.00 (s, 1H, SH), 1.04 (d, $^3J_{H-H} = 6.8$ Hz, 6H, $CH(CH_3)_2$), 1.21 (d, $^3J_{H-H} = 6.8$ Hz, 6H, $CH(CH_3)_2$), 1.25 (d, $^3J_{H-H} = 6.8$ Hz, 6H, $CH(CH_3)_2$), 1.40 (d, $^3J_{H-H} = 6.8$ Hz, 6H, $CH(CH_3)_2$), 1.69 (s, 6H, CH_3), 1.77 (m, 8H, $O(CH_2CH_2)_2$), 3.62 (m, 8H, $O(CH_2CH_2)_2$), 3.77 (sept, $^3J_{H-H} = 6.8$ Hz, 2H, $CH(CH_3)_2$), 3.85 (sept, $^3J_{H-H} = 6.8$ Hz, 2H, $CH(CH_3)_2$), 5.13 (s, 1H,

γ -CH), 7.06–7.16 ppm (m, 6H, *m*, *p*- Ar-*H*); ^7Li NMR (116.64 MHz, THF- d_8 , 25 °C, LiCl, 1M in D_2O) δ 0.32 (SLi); ^{13}C NMR (125.77 MHz, THF- d_8 , 25 °C, TMS) δ 24.3 ($\text{CH}(\text{CH}_3)_2$), 24.4 ($\text{CH}(\text{CH}_3)_2$), 25.1 ($\text{CH}(\text{CH}_3)_2$), 25.1 ($\text{CH}(\text{CH}_3)_2$), 26.4 ($\text{O}(\text{CH}_2\text{CH}_2)_2$), 28.0 ($\text{CH}(\text{CH}_3)_2$), 28.5 ($\text{CH}(\text{CH}_3)_2$), 29.6 (CH_3), 68.2 ($\text{O}(\text{CH}_2\text{CH}_2)_2$), 97.6 (γ -CH), 124.1, 134.3, 126.4, 143.6, 145.7, 146.0 (*i*, *o*, *m*, *p*- C of Ar), 169.0 ppm ($\text{C}=\text{N}$); IR (KBr pellet): $\tilde{\nu}$ 2552 vw (SH) cm^{-1} ; Elemental analysis calcd. for $\text{C}_{74}\text{H}_{116}\text{Al}_2\text{Li}_2\text{N}_4\text{O}_4\text{S}_4$ ($1321.84 \text{ g}\cdot\text{mol}^{-1}$): C 67.2, H 8.9, N 4.2; found: C 66.5, H 8.5, N 4.5%.

4.4.7. Synthesis of $\text{LAl}(\mu\text{-S})_2\text{TiCp}_2$ (**7**)

A solution of Cp_2TiCl_2 (0.22 g, 0.90 mmol) in THF (20 mL) was added dropwise to a solution of **5'** (0.60 g, 0.45 mmol) in THF (40 mL) at -20°C . During the addition, the color of the solution changed to deep brown-green. After the addition was complete, the reaction mixture was stirred for additional 5 min at -20°C and then allowed to warm to ambient temperature. The solvent was removed *in vacuo* and the crude product was extracted twice with cold toluene (15 mL, 5°C). After filtration, removal of the toluene, washing of the product with cold toluene:pentane (5 mL, 1:4) mixture and drying *in vacuo*, **7** was obtained as a brown-green powder. Yield 0.55 g (89%). No m.p. above 270°C (decomp.); ^1H NMR (500.13 MHz, C_6D_6 , 25°C , TMS) δ 1.06 (d, $^3J_{\text{H-H}} = 6.8 \text{ Hz}$, 12H, $\text{CH}(\text{CH}_3)_2$), 1.64 (s, 6H, CH_3), 1.88 (d, $^3J_{\text{H-H}} = 6.8 \text{ Hz}$, 12H, $\text{CH}(\text{CH}_3)_2$), 3.57 (sept, $^3J_{\text{H-H}} = 6.8 \text{ Hz}$, 4H, $\text{CH}(\text{CH}_3)_2$), 4.84 (s, 1H, CH), 5.71 (s, 10H, Cp-*H*), 7.30–7.37 ppm (m, 6H, *m*, *p*- Ar-*H*); ^{27}Al NMR (78.20 MHz, C_6D_6 , 25°C , $[\text{Al}(\text{H}_2\text{O})_6]^{3+}$) δ 94 ppm; ^{13}C NMR (125.77 MHz, C_6D_6 , 25°C , TMS) δ 24.0 ($\text{CH}(\text{CH}_3)_2$), 25.7 ($\text{CH}(\text{CH}_3)_2$), 25.7 ($\text{CH}(\text{CH}_3)_2$), 29.1 (CH_3), 94.9 (γ -CH), 118.3 (C of Cp), 125.0, 128.0, 140.6, 146.0 (*i*, *o*, *m*, *p*- C of Ar), 170.2 ppm ($\text{C}=\text{N}$); EI-MS (70 eV): m/z (%): 686 (8, $[\text{M}]^+$), 621 (100, $[\text{M} - \text{Cp}]^+$). Elemental analysis calcd. for $\text{C}_{39}\text{H}_{51}\text{AlN}_2\text{S}_2\text{Ti}$ ($686.83 \text{ g}\cdot\text{mol}^{-1}$): C 68.2, H 7.5, N 4.1; found: C 67.6, H 7.5, N 4.0%.

4.4.8. Synthesis of $\text{LAl}(\mu\text{-S})_2\text{ZrCp}_2$ (**8**)

It has been prepared like **7** from Cp_2ZrCl_2 (0.26 g, 0.90 mmol) and **5'** (0.60 g, 0.45 mmol). The product was isolated as a deep yellow powder. Yield 0.56 g (85%). No m.p. above 180°C (decomp.); ^1H NMR (500.13 MHz, C_6D_6 , 25°C , TMS) δ 1.06 (d, $^3J_{\text{H-H}} = 6.8$

Hz, 12H, CH(CH₃)₂), 1.65 (s, 6H, CH₃), 1.82 (d, ³J_{H-H} = 6.8 Hz, 12H, CH(CH₃)₂), 3.59 (sept, ³J_{H-H} = 6.8 Hz, 4H, CH(CH₃)₂), 4.87 (s, 1H, γ-CH), 5.65 (s, 10H, Cp-H), 7.22–7.32 ppm (m, 6H, *m*, *p*- Ar-H); ¹³C NMR (125.77 MHz, C₆D₆, 25 °C, TMS) δ 24.4 (CH(CH₃)₂), 25.7 (CH(CH₃)₂), 25.7 (CH(CH₃)₂), 29.0 (CH₃), 95.1 (γ-CH), 114.4 (C of Cp), 124.9, 128.0, 140.1, 146.1 (*i*, *o*, *m*, *p*- C of Ar), 170.6 ppm (C=N); ²⁷Al NMR (78.20 MHz, C₆D₆, 25 °C, [Al(H₂O)₆]³⁺) δ 101 ppm; MS (70 eV): *m/z* (%): 728 (58, [M]⁺), 663 (100, [M – Cp]⁺); Elemental analysis calcd. for C₃₉H₅₁AlN₂S₂Zr (730.17 g·mol⁻¹): C 64.2, H 7.0, N 3.8; found: C 63.4, H 7.3, N 3.8%.

4.4.9. Synthesis of C_tH⁺[LAl(SH)(S)]⁻ (**9**)

Compound **1** (0.30 g, 0.59 mmol) and N,N'-bis-*t*-butylimidazolyl carbene (0.11 g, 0.59 mmol) were mixed as solids in a flask and subsequently THF (20 mL) was added at ambient temperature. The mixture was stirred for 5 min and all volatiles were removed *in vacuo*. The crude product was washed with cold hexane/toluene (3 mL, 1:1) and dried *in vacuo* yielding **9** as a pale yellow powder. Yield 0.39 g (95%). M.p.: 230 °C (decomp.); The NMR spectra were not properly resolved and thus are not reported; An elemental analysis was not performed due to the very high reactivity of **9**.

4.4.10. Synthesis of C_mH⁺₂[LAl(S)₂]²⁻ (**10**)

Compound **1** (0.30 g, 0.59 mmol) and N,N'-bis-mesitylimidazolyl carbene (0.36 g, 1.18 mmol) were mixed as solids in a flask and subsequently THF (20 mL) was added at ambient temperature. The mixture was stirred for 5 min and all volatiles were removed *in vacuo*. The crude product was washed with cold hexane/toluene (3 mL, 1:1) and dried *in vacuo* yielding **10** as a pale yellow powder. Yield 0.63 g (95%). M.p.: 230 °C (decomp.); ¹H NMR (200.13 MHz, C₆D₆, 25 °C, TMS) δ 1.21 (d, ³J_{H-H} = 6.8 Hz, 12H, CH(CH₃)₂), 1.35 (d, ³J_{H-H} = 6.8 Hz, 12H, CH(CH₃)₂), 1.55 (s, 6H, CH₃), 1.92 (s, 24H, Ar-CH₃), 2.21 (s, 12H, Ar-CH₃), 3.90 (sept, ³J_{H-H} = 6.8 Hz, 4H, CH(CH₃)₂), 4.90 (s, 1H, γ-CH), 6.66 (s, 4H, Ar(H)-N-CH-CH), 6.72 (s, 8H, Ar(H)-N-CH-CH), 6.90–7.20 (m, 6H, *m*, *p*- Ar-H), the SH and N-CH-N proton resonances were not observed; ¹³C NMR (50.33 MHz, C₆D₆, 25 °C, TMS) δ 18.1, 21.1 (Ar-CH₃), 24.4, 24.6 (CH(CH₃)₂), 26.5 (CH(CH₃)₂), 28.5 (CH₃), 97.7 (γ-CH), 123.7, 126.1, 129.5, 132.9, 134.7, 136.1, 139.4, 143.0, 145.3 (*i*, *o*, *m*, *p*- C of Ar,

Ar–N–CH–CH), 168.3 ppm (C=N), the N–CH–N carbon resonance was not observed; An elemental analysis was not performed due to the very high reactivity of **10**.

4.4.11. Synthesis of $C_mH^+[LAl(SH)(S)]^-$ (**11**)

Compound **1** (0.30 g, 0.59 mmol) and N,N'-bis-mesitylimidazolyl carbene (0.18 g, 0.59 mmol) were mixed as solids in a flask and subsequently THF (20 mL) was added at ambient temperature. The mixture was stirred for 5 min and all volatiles were removed *in vacuo*. The crude product was washed with cold hexane/toluene mixture (3 mL, 1:1) and dried *in vacuo*, yielding **11** as a pale yellow powder. Yield 0.456 g (95%). M.p.: 230 °C (decomp.); 1H NMR (200.13 MHz, C_6D_6 , 25 °C, TMS) δ 1.23 (d, $^3J_{H-H} = 6.8$ Hz, 12H, $CH(CH_3)_2$), 1.36 (d, $^3J_{H-H} = 6.8$ Hz, 12H, $CH(CH_3)_2$), 1.57 (s, 6H, CH_3), 1.97 (s, 12H, Ar– CH_3), 2.18 (s, 6H, Ar– CH_3), 3.98 (sept, $^3J_{H-H} = 6.8$ Hz, 4H, $CH(CH_3)_2$), 4.91 (s, 1H, γ -CH), 6.68 (s, 2H, Ar(H)–N–CH–CH), 6.74 (s, 4H, Ar(H)–N–CH–CH), 6.90–7.20 (m, 6H, *m*, *p*- Ar–H), the N–CH–N proton resonance was not observed; ^{13}C NMR (50.33 MHz, C_6D_6 , 25 °C, TMS) δ 18.1, 21.1 (Ar– CH_3), 24.0, 24.6 ($CH(CH_3)_2$), 26.5 ($CH(CH_3)_2$), 28.6 (CH_3), 97.7 (γ -CH), 123.7, 126.1, 129.6, 132.9, 134.7, 136.1, 139.4, 143.0, 145.3 (*i*, *o*, *m*, *p*- C of Ar, Ar–N–CH–CH), 168.4 ppm (C=N), the N–CH–N carbon resonance was not observed; Elemental analysis was not performed due to very high reactivity of **11**.

4.4.12. Synthesis of $LAl(SSiMe_3)_2$ (**12**)

Compound **1** (0.300 g, 0.587 mmol) and N,N'-bis-mesitylimidazolyl carbene (0.360 g, 1.175 mmol) were mixed as solids in a flask and subsequently THF (20 mL) was added at ambient temperature and stirred for further 5 min. Finally, Me_3SiCl (15 mL, 1.185 mmol) was added dropwise. Immediately a thick slurry of N,N'-bis-mesitylimidazolium chloride was formed. All volatiles were removed *in vacuo* and the crude product was extracted with dichloromethane (15 mL), and the solution filtered over celite. After removal of the dichloromethane, washing of the product with cold toluene/pentane (5 mL, 1:1), and drying *in vacuo*, **12** was obtained as a white powder. Yield 0.29 g (75%). M.p.: 160 °C; 1H NMR (200.13 MHz, C_6D_6 , 25 °C, TMS) δ 0.29 (s, 18H, $Si(CH_3)_3$), 1.17 (d, $^3J_{H-H} = 6.8$ Hz, 12H, $CH(CH_3)_2$), 1.50 (s, 6H, CH_3), 1.55 (d, $^3J_{H-H} = 6.8$ Hz, 12H, $CH(CH_3)_2$), 3.54 (sept, $^3J_{H-H} = 6.8$ Hz, 4H, $CH(CH_3)_2$), 4.96 (s, 1H, γ -CH), 7.10–7.18 ppm (m, 6H, *p*+*m* Ar–H); ^{13}C NMR

(50.33 MHz, C₆D₆, 25 °C, TMS) δ 5.2 (Si(CH₃)₃), 24.3, 25.0 (CH(CH₃)₂), 26.0 (CH(CH₃)₂), 28.6 (CH₃), 99.9 (γ -CH), 125.1, 129.3, 136.1, 144.9 (*i*, *o*, *m*, *p*- Ar-H), 171.0 ppm (C=N); EI-MS (70 eV): *m/z* (%): 654 (1, [M]⁺), 639 (5, [M - Me]⁺), 549 (100, [M -SSi(Me)₃]⁺); Elemental analysis calcd. for C₃₅H₅₉AlN₂S₂Si₂ (655.14 g·mol⁻¹): C 64.2, H 9.1, N 4.3; found: C 64.5, H 8.5, N 4.4%.

4.4.13. Synthesis of LAl(μ -S)₂SiMe₂ (**13**)

It has been prepared like **12** from **1** (1.00 g, 1.96 mmol), N,N'-bis-mesitylimidazolyl carbene (1.20 g, 3.94 mmol) and Me₂SiCl₂ (0.24 mL, 1.99 mmol). The product was isolated as a white powder. Yield 0.94 g (85%). M.p.: 170 °C; ¹H NMR (200.13 MHz, C₆D₆, 25 °C, TMS) δ 0.28 (s, 6H, Si(CH₃)₂), 1.10 (d, ³J_{H-H} = 6.8 Hz, 12H, CH(CH₃)₂), 1.56 (s, 6H, CH₃), 1.58 (d, ³J_{H-H} = 6.8 Hz, 12H, CH(CH₃)₂), 3.38 (sept, ³J_{H-H} = 6.8 Hz, 4H, CH(CH₃)₂), 4.87 (s, 1H, γ -CH), 5.65 (s, 10H, C₅H₅), 7.10–7.20 ppm (m, 6H, *p+m* Ar-H); ¹³C NMR (50.33 MHz, C₆D₆, 25 °C, TMS) δ 8.1 (Si(CH₃)₂), 24.7, 25.5 (CH(CH₃)₂), 25.6 (CH(CH₃)₂), 28.8 (CH₃), 98.9 (γ -CH), 124.9, 129.3, 138.3, 144.8 (*i*, *o*, *m*, *p*- C of Ar), 172.3 ppm (C=N); EI-MS (70 eV): *m/z* (%): 566 (25, [M]⁺), 551 (100, [M - Me]⁺); Elemental analysis calcd. for C₃₁H₄₇AlN₂S₂Si (566.91 g·mol⁻¹): C 65.7, H 8.4, N 4.9; found: C 65.1, H 8.3, N 5.1%.

4.4.14. Synthesis of LAl(SSiMe₂)₂O (**14**)

It has been prepared like **12** and **13** from **1** (0.30 g, 0.59 mmol), N,N'-bis-mesitylimidazolyl carbene (0.36 g, 1.18 mmol) and (Me₂SiCl)₂O (0.12 mL, 0.59 mmol). The product was isolated as a white powder. Yield 0.30 g (80%). M.p. 190 °C; ¹H NMR (200.13 MHz, C₆D₆, 25 °C, TMS) δ 0.15 (Si(CH₃)₂), 1.12 (d, ³J_{H-H} = 6.8 Hz, 12H, CH(CH₃)₂), 1.52 (s, 6H, CH₃), 1.57 (d, ³J_{H-H} = 6.8 Hz, 12H, CH(CH₃)₂), 3.63 (sept, ³J_{H-H} = 6.8 Hz, 4H, CH(CH₃)₂), 4.84 (s, 1H, γ -CH), 6.90–7.20 ppm (m, 6H, *p+m* Ar-H); ¹³C NMR (50.33 MHz, C₆D₆, 25 °C, TMS) δ 6.3 (Si(CH₃)₃), 24.1, 25.1 (CH(CH₃)₂), 25.8 (CH(CH₃)₂), 28.9 (CH₃), 98.4 (γ -CH), 124.9, 129.3, 140.1, 145.2 (*i*, *o*, *m*, *p*- C of Ar), 170.9 ppm (C=N); EI-MS (70 eV): *m/z* (%): 640 (90, [M]⁺), 625 (100, [M - Me]⁺); Elemental analysis calcd. for C₃₃H₅₃AlN₂OS₂Si (641.07 g·mol⁻¹): C 61.8, H 8.3, N 4.4; found: C 61.4, H 8.1, N 4.2%.

4.4.15. Synthesis of $LAl(OH)_2$ (**15**)

Method 1: H_2O (180 μL , 9.99 mmol) was added quickly in a solution of $LAlCl_2$ (2.56 g, 4.97 mmol) and N,N' -*bis*-*t*butylimidazolyl carbene (1.79 g, 9.93 mmol) in benzene (60 mL) cooled to 10 °C. Immediately a thick slurry of N,N' -*bis*-*t*butylimidazolium chloride was formed. The suspension was vigorously stirred for additional 10 min. and then filtered. The precipitate was washed twice with benzene (5 mL) and all volatiles were removed *in vacuo*. The solid residue was treated twice with cold pentane (5 mL), after filtration and drying *in vacuo* **15** was obtained as a white powder. Yield 1.55 g (65%). 1H NMR (200.13 MHz, C_6D_6 , 25 °C, TMS) δ 0.22 (s, 2H, OH), 1.16 (d, $^3J_{H-H} = 6.8$ Hz, 12H, $CH(CH_3)_2$), 1.42 (d, $^3J_{H-H} = 6.8$ Hz, 12H, $CH(CH_3)_2$), 1.58 (s, 6H, CH_3), 3.47 (sept, $^3J_{H-H} = 6.8$ Hz, 4H, $CH(CH_3)_2$), 4.92 (s, 1H, γ -CH), 7.14–7.16 ppm (m, 6H, *m*, *p*- Ar-H); IR (KBr pellet): $\tilde{\nu}$ 3458 wbr (OH) cm^{-1} ; EI-MS (70 eV): m/z (%): 478 (38, $[M]^+$), 460 (10, $[M-H_2O]^+$), 445 (100, $[M-H_2O-CH_3]^+$). For further spectral characterization see ref. 38.

Method 2: As method 1 starting from H_2O (180 μL , 9.99 mmol), $LAlI_2$ (3.47 g, 4.97 mmol) and N,N' -*bis*-mesitylimidazolyl carbene (3.02 g, 9.93 mmol). Yield 1.55 g (65%).

Method 3: H_2O (21 μL , 1.16 mmol) was added quickly to a solution of **1** (0.30 g, 0.59 mmol) in THF (30 mL) at ambient temperature. The solution was stirred for additional 10 min. and all volatiles were removed *in vacuo*. The solid residue was treated twice with cold pentane (5 mL), and after filtration, and drying *in vacuo*, **15** was obtained as a white powder. Yield 0.21 g (75%).

Method 4: H_2O (23 μL , 1.26 mmol) was added quickly in a solution of **16** (0.30 g, 0.63 mmol) in THF (30 mL) at ambient temperature. The solution was stirred for additional 10 min. and all the volatiles were removed *in vacuo*. The solid residue was triturated twice with cold pentane (5 mL) and after filtration and drying *in vacuo*, **15** was obtained as a white powder. Yield 0.226 g (75%).

4.4.16. Synthesis of $LAl(NH_2)_2$ (**16**)

Dry $NH_3(g)$ was vigorously passed into a solution of $LAlCl_2$ (2.41 g, 4.68 mmol) and N,N' -*bis*-*t*butylimidazolyl carbene (1.69 g, 9.35 mmol) in toluene (60 mL) cooled to –20 °C. Immediately a thick slurry of the N,N' -*bis*-*t*butylimidazolium chloride was formed. After 10 min. the NH_3 supply was shut off, the suspension was removed from the cold bath and

vigorously stirred for additional 10 min. Excess ammonia was released *via* a mineral oil bubbler attached to the flask. The precipitate was filtered off, washed twice with 10 mL of toluene, and all volatiles were removed *in vacuo*. The oily residue was treated twice with cold pentane (5 mL), after filtration and drying *in vacuo*, **16** was obtained as a white microcrystalline powder. Yield 1.67 g (75%). M.p.: 180 °C (decomp.); ^1H NMR (500.13 MHz, C_6D_6 , 25 °C, TMS) δ -0.52 (br s, $^1J_{\text{N-H}} = 64$ Hz 4H, NH_2), 1.17 (d, $^3J_{\text{H-H}} = 6.9$ Hz, 12H, $\text{CH}(\text{CH}_3)_2$), 1.37 (d, $^3J_{\text{H-H}} = 6.9$ Hz, 12H, $\text{CH}(\text{CH}_3)_2$), 1.58 (s, 6H, CH_3), 3.47 (sept, $^3J_{\text{H-H}} = 6.9$ Hz, 4H, $\text{CH}(\text{CH}_3)_2$), 4.88 (s, 1H, $\gamma\text{-CH}$), 7.05–7.20 ppm (m, 6H, *m*, *p*- Ar-*H*); ^{13}C NMR (125.77 MHz, C_6D_6 , 25 °C, TMS) δ 23.4, 24.8 ($\text{CH}(\text{CH}_3)_2$), 25.4 ($\text{CH}(\text{CH}_3)_2$), 28.5 (CH_3), 96.5 ($\gamma\text{-CH}$), 124.3, 127.0, 141.2, 144.5 (*i*, *o*, *m*, *p*- C of Ar), 169.2 ppm ($\text{C}=\text{N}$); ^{15}N NMR (50.70 MHz, C_6D_6 , 25 °C, CH_3NO_2) δ -378 (NH_2); -205 ppm ($\text{C}=\text{N}$); ^{27}Al NMR (78.20 MHz, C_6D_6 , 25 °C, $[\text{Al}(\text{OH}_2)_6]^{3+}$) δ 102 ppm ($\nu_{1/2} = 4031$ Hz); IR (KBr pellet): $\tilde{\nu}$ 3468 vw, 3396 vw (NH) cm^{-1} ; EI-MS (70 eV): *m/z* (%): 476 (16, $[\text{M}]^+$), 459 (20, $[\text{M} - \text{NH}_3]^+$), 444 (100, $[\text{M} - 2 \text{NH}_2]^+$); An elemental analysis did not give satisfactory results due to very high reactivity of **16** toward moisture.

4.4.17. Synthesis of $\text{LAl}(\text{NH}_2)\text{Cl}$ (**17**)

A solution of *N,N'*-*bis*-*t*-butylimidazolyl carbene (0.44 g, 2.42 mmol) in toluene (60 mL) cooled to -20 °C and saturated with dry $\text{NH}_3(\text{g})$ was added dropwise to a solution of LAlCl_2 (1.00 g, 1.94 mmol) in toluene (30 mL) at -35 °C. Immediately a precipitate of *N,N'*-*bis*-*t*-butylimidazolium chloride started to form. After the addition was complete the cold bath was removed and the suspension was stirred for additional 10 min. Excess ammonia was released *via* a mineral oil bubbler attached to the flask. The precipitate was filtered off, washed twice with toluene (10 mL), and all volatiles were removed *in vacuo*. The oily residue was treated twice with cold pentane (5 mL), after filtration, and drying *in vacuo*, **17** was obtained as a white microcrystalline powder. Yield 0.67 g (70%). M.p.: 170 °C (decomp.); ^1H NMR (200.13 MHz, C_6D_6 , 25 °C, TMS) δ -0.31 (br s, 2H, NH_2), 1.08 (d, $^3J_{\text{H-H}} = 6.7$ Hz, 6H, $\text{CH}(\text{CH}_3)_2$), 1.17 (d, $^3J_{\text{H-H}} = 6.8$ Hz, 6H, $\text{CH}(\text{CH}_3)_2$), 1.29 (d, $^3J_{\text{H-H}} = 6.7$ Hz, 6H, $\text{CH}(\text{CH}_3)_2$), 1.51 (d, $^3J_{\text{H-H}} = 6.8$ Hz, 6H, $\text{CH}(\text{CH}_3)_2$), 1.53 (s, 6H, CH_3), 3.27 (sept, $^3J_{\text{H-H}} = 6.8$ Hz, 2H, $\text{CH}(\text{CH}_3)_2$), 3.61 (sept, $^3J_{\text{H-H}} = 6.7$ Hz, 2H, $\text{CH}(\text{CH}_3)_2$), 4.90 (s, 1H, $\gamma\text{-CH}$), 6.95–7.20 ppm (m, 6H, *m*, *p*- Ar-*H*); ^{13}C NMR (125.77 MHz, C_6D_6 , 25 °C, TMS) δ 23.5, 24.7, 24.8, 24.8

(CH(CH₃)₂), 26.1, 28.4 (CH(CH₃)₂), 28.9 (CH₃), 98.0 (γ -CH), 124.2, 125.0, 127.6, 139.7, 144.0, 145.4 (*i*, *o*, *m*, *p*- C of Ar), 170.9 ppm (C=N); ²⁷Al NMR (78.21 MHz, C₆D₆, 25 °C, [Al(OH₂)₆]³⁺) δ 100 ppm ($\nu_{1/2}$ = 235 Hz); IR (KBr pellet): $\tilde{\nu}$ 3420 vw, 3370 vw (NH) cm⁻¹; EI-MS (70 eV): *m/z* (%): 495 (15, [M]⁺), 460 (100, [M-Cl]⁺); An elemental analysis was not performed due to the presence of LAl(NH₂)₂ and LAlCl₂ in the final sample.

4.4.18. Synthesis of LAl(NH₂)Me (**18**)

Compound **18** was synthesized in similar manner as **17** from N,N'-bis-*t*-butylimidazolyl carbene (0.12 g, 0.67 mmol) and LAlClMe (0.30 g, 0.61 mmol). Yield 0.21 g (72%). M.p.: 170 °C (decomp.); ¹H NMR (200.13 MHz, C₆D₆, 25 °C, TMS) δ -0.88 (s, 3H, Al-CH₃), -0.20 (br s, 2H, NH₂), 1.09 (d, ³J_{H-H} = 6.8 Hz, 6H, CH(CH₃)₂), 1.24 (d, ³J_{H-H} = 6.8 Hz, 6H, CH(CH₃)₂), 1.35 (d, ³J_{H-H} = 6.8 Hz, 12H, CH(CH₃)₂), 1.59 (s, 6H, CH₃), 3.32 (sept, ³J_{H-H} = 6.8 Hz, 2H, CH(CH₃)₂), 3.63 (sept, ³J_{H-H} = 6.8 Hz, 2H, CH(CH₃)₂), 4.88 (s, 1H, γ -CH), 6.90–7.20 ppm (m, 6H, *m*, *p*- Ar-*H*); ¹³C NMR (50.33 MHz, C₆D₆, 25 °C, TMS) δ -13.7 (Al-CH₃), 23.2, 24.1, 24.3, 24.9 (CH(CH₃)₂), 26.3 (CH(CH₃)₂), 28.9 (CH₃), 97.5 (γ -CH), 124.0, 124.8, 127.1, 140.7, 143.4, 145.4 (*i*, *o*, *m*, *p*- C of Ar), 169.4 ppm (C=N), ²⁷Al NMR (78.21 MHz, C₆D₆, 25 °C, [Al(OH₂)₆]³⁺) δ 113 ppm ($\nu_{1/2}$ = 4223 Hz); IR (KBr pellet): $\tilde{\nu}$ 3445 vw, 3375 vw (NH) cm⁻¹; EI-MS (70 eV): *m/z* (%): 460 (100, [M-Me]⁺); An elemental analysis did not give satisfactory results due to very high reactivity of **18** with traces of water.

4.4.19. Synthesis of LGa(NH₂)₂ (**19**)

A solution of N,N'-bis-*t*-butylimidazolyl carbene (0.81 g, 4.51 mmol) in toluene (40 mL) cooled to -20 °C and saturated with dry NH₃(g) was added dropwise to a solution of LGaCl₂ (1.50 g, 2.15 mmol) in toluene (30 mL) at -35 °C. Immediately a precipitate of N, N'-bis-*t*-butylimidazolium chloride started to form. After complete addition, the cold bath was removed and the suspension was stirred for additional 25 min. Excess ammonia was released *via* a mineral oil bubbler attached to the flask. The precipitate was filtered off, washed twice with toluene (10 mL) and all volatiles were removed *in vacuo*. The oily residue was treated twice with cold pentane (5 mL), after filtration and drying *in vacuo*, **19** was obtained as a white microcrystalline powder. Yield 0.78 g (70%). M.p.: 175 °C (decomp.); ¹H NMR

(500.13 MHz, C₆D₆, 25 °C, TMS) δ -0.58 (br s, $^1J_{\text{N-H}} = 65$ Hz, 4H, NH₂), 1.16 (d, $^3J_{\text{H-H}} = 6.9$ Hz, 12H, CH(CH₃)₂), 1.37 (d, $^3J_{\text{H-H}} = 6.9$ Hz, 12H, CH(CH₃)₂), 1.60 (s, 6H, CH₃), 3.49 (sept, $^3J_{\text{H-H}} = 6.9$ Hz, 4H, CH(CH₃)₂), 4.76 (s, 1H, γ -CH), 7.05–7.10 ppm (m, 6H, *m*, *p*- Ar-H); ¹³C NMR (125.77 MHz, C₆D₆, 25 °C, TMS) δ 23.5, 24.8 (CH(CH₃)₂), 25.3 (CH(CH₃)₂), 28.4 (CH₃), 95.1 (γ -CH), 124.3, 126.9, 141.3, 144.3 (*i*, *o*, *m*, *p*- C of Ar), 168.6 ppm (C=N); IR (KBr pellet): $\tilde{\nu}$ 3460 vw, 3373 vw (NH) cm⁻¹; EI-MS (70 eV): *m/z* (%): 518 (8, [M]⁺), 501 (60, [M -NH₃]⁺), 486 (100, [M -2 NH₂]⁺); An elemental analysis did not give satisfactory results due to very high reactivity of **19** with traces of water.

4.4.20. Synthesis of LGa(OH)₂ (**20**)

H₂O (97 μ L, 5.37 mmol) was added quickly to a solution of LGaCl₂ (1.50 g, 2.69 mmol) and N,N'-bis-*t*-butylimidazolyl carbene (1.02 g, 5.64 mmol) in toluene (45 mL) cooled to -5 °C. Immediately after the addition of water a slurry of the N,N'-bis-*t*-butylimidazolium chloride was formed. The suspension was vigorously stirred for additional 10 min and filtered. The precipitate was washed twice with toluene (5 mL) and all the volatiles were removed *in vacuo*. The solid residue was treated twice with cold pentane (5 mL) and after filtration and drying *in vacuo*, **20** was obtained as a white powder. Yield 1.12 g (80%). M.p.: 200 °C (decomp.); ¹H NMR (200.13 MHz, C₆D₆, 25 °C, TMS) δ -0.27 (s, 2H, OH), 1.14 (d, $^3J_{\text{H-H}} = 6.8$ Hz, 12H, CH(CH₃)₂), 1.43 (d, $^3J_{\text{H-H}} = 6.8$ Hz, 12H, CH(CH₃)₂), 1.57 (s, 6H, CH₃), 3.45 (sept, $^3J_{\text{H-H}} = 6.8$ Hz, 4H, CH(CH₃)₂), 4.79 (s, 1H, γ -CH), 7.04–7.10 ppm (m, 6H, *m*, *p*- Ar-H); ¹³C NMR (125.77 MHz, C₆D₆, 25 °C, TMS) δ 23.3, 24.8 (CH(CH₃)₂), 25.0 (CH(CH₃)₂), 28.4 (CH₃), 95.1 (γ -CH), 124.5, 127.5, 139.9, 144.6 (*i*, *o*, *m*, *p*- C of Ar), 170.1 ppm (C=N); IR (KBr pellet): $\tilde{\nu}$ 3465 vbr (OH) cm⁻¹; EI-MS (70 eV): *m/z* (%): 520 (5, [M]⁺), 502 (22, [M -H₂O]⁺), 487 (100, [M -H₂O -CH₃]⁺); Elemental analysis calcd. for C₂₉H₄₃GaN₂O₂ (521.39): C 66.7, H 8.2, N 5.4; found: C 66.8, H 8.3, N 5.4%.

4.4.21. Synthesis of LAl(SH)Me (**21**)

Gaseous H₂S was dried by passing through two traps cooled to -50 °C and bubbled slowly in a toluene (20 mL) solution of **18** (0.50 g, 1.05 mmol). After 10 min. the H₂S supply was shut off and the solution was stirred for additional 10 min. Removing of all volatiles *in*

vacuo, washing of the product with cold pentane (5 mL) and drying of the product *in vacuo* gave **21** as a pale yellow microcrystalline solid. Yield 0.47 g (90%). M.p.: 196 °C (decomp.); ^1H NMR (200.13 MHz, C_6D_6 , 25 °C, TMS) δ -0.88 (s, 1H, SH), -0.63 (s, 3H, Al-CH₃), 1.04 (d, $^3J_{\text{H-H}} = 6.8$ Hz, 6H, CH(CH₃)₂), 1.18 (d, $^3J_{\text{H-H}} = 6.7$ Hz, 6H, CH(CH₃)₂), 1.30 (d, $^3J_{\text{H-H}} = 6.8$ Hz, 6H, CH(CH₃)₂), 1.46 (d, $^3J_{\text{H-H}} = 6.7$ Hz, 6H, CH(CH₃)₂), 1.53 (s, 6H, CH₃), 3.27 (sept, $^3J_{\text{H-H}} = 6.8$ Hz, 2H, CH(CH₃)₂), 3.73 (sept, $^3J_{\text{H-H}} = 6.7$ Hz, 2H, CH(CH₃)₂), 4.90 (s, 1H, γ -CH), 7.05–7.20 ppm (m, 6H, *m*, *p*- Ar-H); ^{13}C NMR (125.77 MHz, C_6D_6 , 25 °C, TMS) δ -10.0 (Al-CH₃), 23.6, 24.4, 24.6, 24.9 (CH(CH₃)₂), 27.1, 28.4 (CH(CH₃)₂), 28.9 (CH₃), 98.4 (γ -CH), 124.1, 125.3, 127.6, 140.2, 143.7, 145.8 (*i*, *o*, *m*, *p*- C of Ar), 170.4 ppm (C=N); IR (KBr pellet): $\tilde{\nu}$ 2567 vw (SH) cm^{-1} ; EI-MS (70 eV): *m/z* (%): 477 (100, [M - Me]⁺), 459 (16, [M - SH]⁺), 443 (20, [M - H₂S - Me]⁺); Elemental analysis calcd. for C₃₀H₄₅AlN₂S (492.74 g·mol⁻¹): C 73.1, H 9.2, N 5.7; found: C 72.9, H 9.1, N 5.7%.

4.4.22. Synthesis of LAl(OH)(μ -O)Ti(SH)Cp₂ (**22**)

H₂O (26 μL , 1.46 mmol) was added quickly to a solution of **7** (0.50 g, 0.73 mmol) in THF/CH₂Cl₂ (45 mL, 1:1) at ambient temperature. The suspension was stirred for additional 10 h and filtered. All the volatiles were removed *in vacuo* resulting in a brown solid residue that was treated twice with cold toluene (5 mL). After filtration and drying *in vacuo*, **22** was obtained as a light brown powder. Yield 0.31 g (60%). M.p.: 227 °C (decomp.); ^1H NMR (500.13 MHz, CDCl₃, 25 °C, TMS) δ 1.07 (s, 1H, OH), 1.10 (d, $^3J_{\text{H-H}} = 6.9$ Hz, 6H, CH(CH₃)₂), 1.20 (d, $^3J_{\text{H-H}} = 6.7$ Hz, 6H, CH(CH₃)₂), 1.37 (d, $^3J_{\text{H-H}} = 6.9$ Hz, 6H, CH(CH₃)₂), 1.44 (d, $^3J_{\text{H-H}} = 6.7$ Hz, 6H, CH(CH₃)₂), 1.77 (s, 6H, CH₃), 2.08 (s, 1H, SH), 3.03 (sept, $^3J_{\text{H-H}} = 6.9$ Hz, 2H, CH(CH₃)₂), 3.49 (sept, $^3J_{\text{H-H}} = 6.7$ Hz, 2H, CH(CH₃)₂), 5.20 (s, 1H, γ -CH), 5.36 (s, 10H, Cp-H), 7.04–7.20 ppm (m, 6H, *m*, *p*- Ar-H); ^{13}C NMR (125.77 MHz, CDCl₃, 25 °C, TMS) δ 23.6, 24.2, 24.4, 24.7 (CH(CH₃)₂), 26.1, 27.5 (CH(CH₃)₂), 28.7 (CH₃), 97.5 (γ -CH), 113.9 (C of Cp) 124.0, 125.2, 127.3, 140.9, 142.9, 145.6 (*i*, *o*, *m*, *p*- C of Ar), 170.6 ppm (C=N); IR (KBr pellet): $\tilde{\nu}$ 3551 br (OH), 2574 vw (SH) cm^{-1} ; EI-MS (70 eV): *m/z* (%): 623 (10, [M - Cp]⁺), 605 (50, [M - Cp - H₂O]⁺); An elemental analysis was not performed due to the presence of LAl(SH)(μ -O)Ti(SH)Cp₂ in the final sample.

4.4.23. Synthesis of $\text{LAl}(\text{OH})(\mu\text{-O})\text{Zr}(\text{SH})\text{Cp}_2$ (23**)**

Compound **23** was synthesized in similar manner as **22** from H_2O (25 μL , 1.37 mmol) and **8** (0.50 g, 0.69 mmol) as a pale yellow powder. Yield 0.31 g (62%). ^1H NMR (500.13 MHz, CDCl_3 , 25 $^\circ\text{C}$, TMS) δ 0.36 (s, 1H, OH), 1.11 (d, $^3J_{\text{H-H}} = 6.8$ Hz, 6H, $\text{CH}(\text{CH}_3)_2$), 1.21 (d, $^3J_{\text{H-H}} = 6.8$ Hz, 6H, $\text{CH}(\text{CH}_3)_2$), 1.38 (d, $^3J_{\text{H-H}} = 6.8$ Hz, 6H, $\text{CH}(\text{CH}_3)_2$), 1.39 (d, $^3J_{\text{H-H}} = 6.8$ Hz, 6H, $\text{CH}(\text{CH}_3)_2$), 1.65 (s, 1H, SH), 1.77 (s, 6H, CH_3), 3.04 (sept, $^3J_{\text{H-H}} = 6.8$ Hz, 2H, $\text{CH}(\text{CH}_3)_2$), 3.50 (sept, $^3J_{\text{H-H}} = 6.8$ Hz, 2H, $\text{CH}(\text{CH}_3)_2$), 5.20 (s, 1H, $\gamma\text{-CH}$), 5.46 (s, 10H, Cp-H), 7.04–7.20 ppm (m, 6H, *m*, *p*- Ar-H); ^{13}C NMR (125.77 MHz, CDCl_3 , 25 $^\circ\text{C}$, TMS) δ 23.5, 24.4, 24.5, 24.6 ($\text{CH}(\text{CH}_3)_2$), 27.5, 28.6 ($\text{CH}(\text{CH}_3)_2$), 28.7 (CH_3), 97.4 ($\gamma\text{-CH}$), 111.8 (C of Cp) 124.0, 125.1, 127.3, 140.6, 143.2, 145.5 (*i*, *o*, *m*, *p*- C of Ar), 170.6 ppm (C=N); IR (KBr pellet); $\tilde{\nu}$ 3560 br (OH), 2562 vw (SH) cm^{-1} ; EI-MS (70 eV): *m/z* (%): 665 (5, $[\text{M} - \text{Cp}]^+$), 647 (50, $[\text{M} - \text{Cp} - \text{H}_2\text{O}]^+$); An elemental analysis was not performed due to the presence of $\text{LAl}(\text{SH})(\mu\text{-O})\text{Zr}(\text{SH})\text{Cp}_2$ in the final sample.

4.4.24. Alternative preparation of $[\text{LAl}(\text{OH})]_2\text{O}$

H_2O (28 μL , 1.672 mmol) was added quickly to a solution of **16** (0.500 g, 1.105 mmol) in THF (30 mL) at ambient temperature. The solution was stirred for additional 10 min. and all volatiles were removed *in vacuo*. The solid residue was triturated twice with cold pentane (5 mL) and after filtration and drying *in vacuo*, $[\text{LAl}(\text{OH})]_2\text{O}$ was obtained as a white powder. Yield 0.463 g (80%). ^1H NMR (500.13 MHz, C_6D_6 , 25 $^\circ\text{C}$, TMS) δ -0.30 (s, 2H, OH), 0.73 (d, $^3J_{\text{H-H}} = 6.6$ Hz, 6H, $\text{CH}(\text{CH}_3)_2$), 0.82 (d, $^3J_{\text{H-H}} = 6.6$ Hz, 6H, $\text{CH}(\text{CH}_3)_2$), 1.13 (d, $^3J_{\text{H-H}} = 6.8$ Hz, 6H, $\text{CH}(\text{CH}_3)_2$), 1.14 (d, $^3J_{\text{H-H}} = 6.8$ Hz, 6H, $\text{CH}(\text{CH}_3)_2$), 1.35 (d, $^3J_{\text{H-H}} = 6.8$ Hz, 6H, $\text{CH}(\text{CH}_3)_2$), 1.36 (d, $^3J_{\text{H-H}} = 6.8$ Hz, 6H, $\text{CH}(\text{CH}_3)_2$), 1.46 (s, 6H, CH_3), 1.47 (d, $^3J_{\text{H-H}} = 6.8$ Hz, 6H, $\text{CH}(\text{CH}_3)_2$), 1.51 (s, 6H, CH_3), 1.55 (d, $^3J_{\text{H-H}} = 6.86$ Hz, 6H, $\text{CH}(\text{CH}_3)_2$), 2.10 (s, 3H, $\text{C}_6\text{H}_5\text{CH}_3$), 3.12 (sept, $^3J_{\text{H-H}} = 6.6$ Hz, 2H, $\text{CH}(\text{CH}_3)_2$), 3.24 (sept, $^3J_{\text{H-H}} = 6.8$ Hz, 2H, $\text{CH}(\text{CH}_3)_2$), 3.56 (sept, $^3J_{\text{H-H}} = 6.8$ Hz, 2H, $\text{CH}(\text{CH}_3)_2$), 3.73 (sept, $^3J_{\text{H-H}} = 6.8$ Hz, 2H, $\text{CH}(\text{CH}_3)_2$), 4.87 (s, 2H, $\gamma\text{-CH}$), 6.90–7.20 ppm (m, 17H, *m*, *p*- Ar-H, $\text{C}_6\text{H}_5\text{CH}_3$). For further spectral characterization see ref 109.

5. Handling and Disposal of Solvents and Residual Waste

1. The recovered solvents were distilled or condensed into a cold-trap under vacuum and collected in halogen-free or halogen-containing solvent containers, and stored for disposal.
2. Used NMR solvents were classified into halogen-free and halogen-containing solvents and were disposed as selenium and tellurium containing wastes and halogen-containing wastes, respectively.
3. The selenium and tellurium residues were dissolved in nitric acid and after neutralization stored in containers for heavy element wastes.
4. Drying agents such as KOH, CaCl_2 and P_4O_{10} were hydrolyzed and disposed as acid or base wastes.
5. Whenever possible, sodium metal used for drying solvents was collected for recycling.^[217] The non-reusable sodium metal was carefully hydrolyzed in cold ethanol and poured into the base-bath used for cleaning glassware.
6. Ethanol and acetone used for cold-baths (with solid CO_2 or liquid N_2) were subsequently used for cleaning glassware.
7. The acid-bath used for cleaning glassware was neutralized with Na_2CO_3 and the resulting NaCl solution was washed-off in the communal water drainage.
8. The residue of the base-bath used for glassware cleaning was poured into container for base wastes.

Amounts of various types of disposable wastes generated during the work:

Heavy elements containing wastes	2 L
Halogen-containing solvent wastes	7 L
Halogen-free solvent wastes	40 L
Acid wastes	10 L
Base wastes	20 L

6. Crystal Data and Refinement Details

Table CD1. Crystal Data and Structure Refinement Details for $\text{LaI}(\text{SH})_2$ (1).

Empirical formula	$\text{C}_{29}\text{H}_{43}\text{AlN}_2\text{S}_2$
Formula weight	510.75
Temperature	100(2) K
Wavelength	1.54178 Å
Crystal system	Orthorhombic
Space group	<i>Pnma</i>
Unit cell dimensions	$a = 12.685(2)$ Å $b = 22.058(3)$ Å $c = 10.448(2)$ Å
Volume	$2924(1)$ Å ³
<i>Z</i>	4
Density (calculated)	1.160 Mg/m ³
Absorption coefficient	2.072 mm ⁻¹
<i>F</i> (000)	1104
Crystal size	0.31 x 0.12 x 0.10 mm ³
θ range for data collection	4.68 to 59.61°.
Index ranges	$-13 \leq h \leq 14$, $-24 \leq k \leq 23$, $-11 \leq l \leq 10$
Reflections collected	13243
Independent reflections	2190 ($R_{\text{int}} = 0.0252$)
Completeness to $\theta = 59.61^\circ$	98.8%
Refinement method	Full-matrix least-squares on F^2
Data / restraints / parameters	2190 / 1 / 171
Goodness-of-fit on F^2	1.045
Final <i>R</i> indices ($I > 2\sigma(I)$)	$R1 = 0.0292$, $wR2 = 0.0786$
<i>R</i> indices (all data)	$R1 = 0.0320$, $wR2 = 0.0805$
Largest difference peak and hole	0.281 and -0.237 e ⁻ Å ⁻³

Table CD2. Crystal Data and Structure Refinement Details for $\text{LAl}(\mu\text{-Se})_2\text{AlL} \cdot \text{C}_7\text{H}_8 \cdot 2\text{CHCl}_3$ (2).

Empirical formula	$\text{C}_{67}\text{H}_{92}\text{Al}_2\text{Cl}_6\text{N}_4\text{Se}_2$
Formula weight	1378.03
Temperature	200(2) K
Wavelength	0.71073 Å
Crystal system	Monoclinic
Space group	$C2/m$
Unit cell dimensions	$a = 18.329(4)$ Å $b = 19.161(5)$ Å $\beta = 125.54(2)^\circ$ $c = 11.984(3)$ Å
Volume	$3425(1)$ Å ³
Z	2
Density (calculated)	1.336 Mg/m ³
Absorption coefficient	1.381 mm^{-1}
$F(000)$	1436
Crystal size	0.50 x 0.40 x 0.30 mm ³
θ range for data collection	3.51 to 24.99° .
Index ranges	$-21 \leq h \leq 21$, $-4 \leq k \leq 22$, $-14 \leq l \leq 14$
Reflections collected	4065
Independent reflections	3111 ($R_{\text{int}} = 0.0307$)
Completeness to $\theta = 24.99^\circ$	99.6%
Refinement method	Full-matrix least-squares on F^2
Data / restraints / parameters	3111 / 111 / 258
Goodness-of-fit on F^2	1.076
Final R indices ($I > 2\sigma(I)$)	$R1 = 0.0435$, $wR2 = 0.1083$
R indices (all data)	$R1 = 0.0546$, $wR2 = 0.1171$
Largest diff. peak and hole	0.881 and $-0.614 \text{ e} \cdot \text{Å}^{-3}$

Table CD3. Crystal Data and Structure Refinement Details for $\text{LAl}(\mu\text{-Te})_2\text{Al} \cdot 0.27\text{C}_7\text{H}_8 \cdot 2.73\text{CHCl}_3$ (3).

Empirical formula	$\text{C}_{62.63}\text{H}_{86.90}\text{Al}_2\text{Cl}_{8.18}\text{N}_4\text{Te}_2$
Formula weight	1495.14
Temperature	100(2) K
Wavelength	1.54178 Å
Crystal system	Monoclinic
Space group	$C2/m$
Unit cell dimensions	$a = 17.972(2)$ Å $b = 19.125(2)$ Å $\beta = 124.84(2)^\circ$. $c = 11.923(2)$ Å
Volume	$3364(1)$ Å ³
Z	2
Density (calculated)	1.476 Mg/m ³
Absorption coefficient	10.399 mm ⁻¹
$F(000)$	1520
Crystal size	0.4 x 0.4 x 0.2 mm ³
θ range for data collection	3.78 to 58.10°.
Index ranges	$-19 \leq h \leq 19, -18 \leq k \leq 20, -12 \leq l \leq 12$
Reflections collected	6352
Independent reflections	2314 ($R_{\text{int}} = 0.0356$)
Completeness to $\theta = 58.10^\circ$	95.0%
Refinement method	Full-matrix least-squares on F^2
Data / restraints / parameters	2314 / 405 / 332
Goodness-of-fit on F^2	1.126
Final R indices ($I > 2\sigma(I)$)	$R1 = 0.0510, wR2 = 0.1174$
R indices (all data)	$R1 = 0.0535, wR2 = 0.1187$
Largest diff. peak and hole	1.661 and -0.878 e.Å ⁻³

Table CD4. Crystal Data and Structure Refinement Details for $\text{LAl}(\mu\text{-S})_2\text{AlL} \cdot 0.68\text{C}_7\text{H}_8 \cdot 2.32\text{CHCl}_3$ (4).

Empirical formula	$\text{C}_{65.08}\text{H}_{89.78}\text{Al}_2\text{Cl}_{6.96}\text{N}_4\text{S}_2$
Formula weight	1293.08
Temperature	100(2) K
Wavelength	1.54178 Å
Crystal system	Monoclinic
Space group	$C2/m$
Unit cell dimensions	$a = 18.021(3)$ Å $b = 19.107(3)$ Å $\beta = 125.22(2)^\circ$ $c = 11.920(2)$ Å
Volume	$3353(1)$ Å ³
Z	2
Density (calculated)	1.281 Mg/m ³
Absorption coefficient	3.844 mm^{-1}
$F(000)$	1369
Crystal size	$0.3 \times 0.2 \times 0.2 \text{ mm}^3$
θ range for data collection	3.79 to 57.76° .
Index ranges	$-19 \leq h \leq 19$, $-20 \leq k \leq 15$, $-13 \leq l \leq 13$
Reflections collected	7081
Independent reflections	2370 ($R_{\text{int}} = 0.0224$)
Completeness to $\theta = 57.76^\circ$	98.5%
Refinement method	Full-matrix least-squares on F^2
Data / restraints / parameters	2370 / 285 / 295
Goodness-of-fit on F^2	1.146
Final R indices ($I > 2\sigma(I)$)	$R1 = 0.0398$, $wR2 = 0.0989$
R indices (all data)	$R1 = 0.0451$, $wR2 = 0.1017$
Largest diff. peak and hole	0.436 and $-0.416 \text{ e} \cdot \text{Å}^{-3}$

Table CD5. Crystal Data and Structure Refinement Details for of $\{\text{LAl}[(\text{SLi})_2(\text{thf})_3]\}_2 \cdot 2\text{THF}$ (5).

Empirical formula	$\text{C}_{90}\text{H}_{146}\text{Al}_2\text{Li}_4\text{N}_4\text{O}_8\text{S}_4$
Formula weight	1622.07
Temperature	100(2) K
Wavelength	1.54178 Å
Crystal system	Monoclinic
Space group	$P2_1/n$
Unit cell dimensions	$a = 22.746(1)$ Å $b = 16.414(1)$ Å $c = 26.111(1)$ Å
	$\beta = 106.45(1)^\circ$
Volume	$9350(1)$ Å ³
Z	4
Density (calculated)	1.152 Mg/m ³
Absorption coefficient	1.525 mm ⁻¹
$F(000)$	3520
Crystal size	0.30 x 0.20 x 0.10 mm ³
θ range for data collection	2.28 to 60.04°.
Index ranges	$-25 \leq h \leq 25$, $-18 \leq k \leq 18$, $-29 \leq l \leq 29$
Reflections collected	50734
Independent reflections	13682 ($R_{\text{int}} = 0.0214$)
Completeness to $\theta = 60.04^\circ$	98.3%
Refinement method	Full-matrix least-squares on F^2
Data / restraints / parameters	13682 / 400 / 1109
Goodness-of-fit on F^2	1.016
Final R indices ($I > 2\sigma(I)$)	$R1 = 0.0298$, $wR2 = 0.0753$
R indices (all data)	$R1 = 0.0318$, $wR2 = 0.0767$
Largest diff. peak and hole	0.356 and -0.218 e·Å ⁻³

Table CD6. Crystal Data and Structure Refinement Details for {LAl(SH)[SLi(thf)₂]}₂ (6).

Empirical formula	C ₇₄ H ₁₁₆ Al ₂ Li ₂ N ₄ O ₄ S ₄
Formula weight	1321.78
Temperature	100(2) K
Wavelength	1.54178 Å
Crystal system	Monoclinic
Space group	<i>P</i> 2 ₁ / <i>n</i>
Unit cell dimensions	<i>a</i> = 12.558(1) Å <i>b</i> = 19.423(1) Å <i>β</i> = 111.29(1)° <i>c</i> = 16.862(1) Å
Volume	3832(1) Å ³
<i>Z</i>	2
Density (calculated)	1.145 Mg/m ³
Absorption coefficient	1.721 mm ⁻¹
<i>F</i> (000)	1432
Crystal size	0.20 x 0.10 x 0.10 mm ³
<i>θ</i> range for data collection	3.62 to 59.01°.
Index ranges	-13 ≤ <i>h</i> ≤ 12, -21 ≤ <i>k</i> ≤ 21, -15 ≤ <i>l</i> ≤ 18
Reflections collected	14831
Independent reflections	5403 (<i>R</i> _{int} = 0.0567)
Completeness to <i>θ</i> = 59.01°	97.9%
Refinement method	Full-matrix least-squares on <i>F</i> ²
Data / restraints / parameters	5403 / 166 / 461
Goodness-of-fit on <i>F</i> ²	0.999
Final <i>R</i> indices (<i>I</i> > 2σ(<i>I</i>))	<i>R</i> 1 = 0.0441, <i>wR</i> 2 = 0.1058
<i>R</i> indices (all data)	<i>R</i> 1 = 0.0765, <i>wR</i> 2 = 0.1219
Largest diff. peak and hole	0.277 and -0.238 e·Å ⁻³

Table CD7. Crystal Data and Structure Refinement Details for $\text{LaI}(\mu\text{-S})_2\text{TiCp}_2$ (7).

Empirical formula	$\text{C}_{39}\text{H}_{51}\text{AlN}_2\text{S}_2\text{Ti}$
Formula weight	686.82
Temperature	100(2) K
Wavelength	1.54178 Å
Crystal system	Monoclinic
Space group	$P2_1$
Unit cell dimensions	$a = 11.831(1)$ Å $b = 8.727(1)$ Å $\beta = 99.10(1)^\circ$ $c = 17.776(1)$ Å
Volume	$1812(1)$ Å ³
Z	2
Density (calculated)	1.259 Mg/m^3
Absorption coefficient	3.525 mm^{-1}
$F(000)$	732
Crystal size	$0.50 \times 0.20 \times 0.20 \text{ mm}^3$
θ range for data collection	4.20 to 56.84° .
Index ranges	$-11 \leq h \leq 12$, $-9 \leq k \leq 7$, $-17 \leq l \leq 18$
Reflections collected	6417
Independent reflections	3178 ($R_{\text{int}} = 0.0189$)
Completeness to $\theta = 56.84^\circ$	95.6%
Refinement method	Full-matrix least-squares on F^2
Data / restraints / parameters	3178 / 1 / 419
Goodness-of-fit on F^2	1.059
Final R indices ($I > 2\sigma(I)$)	$R1 = 0.0235$, $wR2 = 0.0588$
R indices (all data)	$R1 = 0.0241$, $wR2 = 0.0591$
Absolute structure parameter	$0.013(5)$
Largest diff. peak and hole	0.250 and $-0.199 \text{ e} \cdot \text{Å}^{-3}$

Table CD8. Crystal Data and Structure Refinement Details for $C_4H_7[LAI(SH)(S)]^- \cdot THF$ (9).

Empirical formula	$C_{44}H_{71}AlN_4OS_2$
Formula weight	763.15
Temperature	100(2) K
Wavelength	1.54178 Å
Crystal system	Orthorhombic
Space group	$P2_12_12_1$
Unit cell dimensions	$a = 12.390(1)$ Å $b = 14.271(1)$ Å $c = 25.320(2)$ Å
Volume	$4477(1)$ Å ³
Z	4
Density (calculated)	1.132 Mg/m ³
Absorption coefficient	1.533 mm ⁻¹
$F(000)$	1664
Crystal size	0.3 x 0.2 x 0.2 mm ³
θ range for data collection	3.49 to 59.05°.
Index ranges	$-13 \leq h \leq 13$, $-14 \leq k \leq 15$, $-27 \leq l \leq 28$
Reflections collected	21027
Independent reflections	6317 ($R_{int} = 0.0479$)
Completeness to $\theta = 59.05^\circ$	99.1%
Data / restraints / parameters	6317 / 226 / 551
Goodness-of-fit on F^2	1.034
Final R indices ($I > 2\sigma(I)$)	$R1 = 0.0348$, $wR2 = 0.0823$
R indices (all data)	$R1 = 0.0449$, $wR2 = 0.0872$
Absolute structure parameter	0.011(14)
Largest diff. peak and hole	0.170 and -0.140 e·Å ⁻³

Table CD9. Crystal Data and Structure Refinement Details for $C_mH^+[LAl(SH)(S)]^- \cdot THF$ (11).

Empirical formula	$C_{54}H_{75}AlN_4OS_2$
Formula weight	887.28
Temperature	100(2) K
Wavelength	1.54178 Å
Crystal system	Monoclinic
Space group	$P2_1/c$
Unit cell dimensions	$a = 19.443(1)$ Å $b = 17.610(1)$ Å $\beta = 95.53(1)^\circ$. $c = 15.226(1)$ Å
Volume	$5189(1)$ Å ³
Z	4
Density (calculated)	1.136 Mg/m ³
Absorption coefficient	1.392 mm ⁻¹
$F(000)$	1920
Crystal size	0.2 x 0.2 x 0.1 mm ³
θ range for data collection	2.28 to 59.00°.
Index ranges	$-21 \leq h \leq 20$, $-19 \leq k \leq 19$, $-15 \leq l \leq 15$
Reflections collected	22645
Independent reflections	7274 ($R_{int} = 0.0474$)
Completeness to $\theta = 59.00^\circ$	97.4%
Refinement method	Full-matrix least-squares on F^2
Data / restraints / parameters	7274 / 184 / 628
Goodness-of-fit on F^2	1.021
Final R indices ($I > 2\sigma(I)$)	$R1 = 0.0364$, $wR2 = 0.0850$
R indices (all data)	$R1 = 0.0537$, $wR2 = 0.0926$
Largest diff. peak and hole	0.225 and -0.249 e·Å ⁻³

Table CD10. Crystal Data and Structure Refinement Details for $\text{LAl}(\text{NH}_2)_2$ (16).

Empirical formula	$\text{C}_{29}\text{H}_{45}\text{AlN}_4$
Formula weight	476.67
Temperature	100(2) K
Wavelength	1.54178 Å
Crystal system	Monoclinic
Space group	$P2_1/c$
Unit cell dimensions	$a = 16.995(2)$ Å $b = 13.057(2)$ Å $\beta = 109.26(2)^\circ$ $c = 13.565(2)$ Å
Volume	$2842(1)$ Å ³
Z	4
Density (calculated)	1.114 Mg/m ³
Absorption coefficient	0.781 mm ⁻¹
$F(000)$	1040
Crystal size	$0.30 \times 0.10 \times 0.10$ mm ³
θ range for data collection	4.37 to 58.10° .
Index ranges	$-18 \leq h \leq 16$, $-14 \leq k \leq 13$, $-14 \leq l \leq 14$
Reflections collected	17547
Independent reflections	3915 ($R_{\text{int}} = 0.0356$)
Completeness to $\theta = 58.10^\circ$	98.5%
Refinement method	Full-matrix least-squares on F^2
Data / restraints / parameters	3915 / 6 / 334
Goodness-of-fit on F^2	1.044
Final R indices ($I > 2\sigma(I)$)	$R1 = 0.0390$, $wR2 = 0.1004$
R indices (all data)	$R1 = 0.0425$, $wR2 = 0.1033$
Extinction coefficient	$0.0012(2)$
Largest diff. peak and hole	0.227 and -0.281 e·Å ⁻³

Table CD11. Crystal Data and Structure Refinement Details for $\text{LAl}(\text{NH}_2)\text{Cl}$ (17)
(Contains 4% of 16).

Empirical formula	$\text{C}_{29}\text{H}_{43.07}\text{AlCl}_{0.96}\text{N}_{3.04}$
Formula weight	495.41
Temperature	100(2) K
Wavelength	1.54178 Å
Crystal system	Monoclinic
Space group	$P2_1/c$
Unit cell dimensions	$a = 17.003(3)$ Å $b = 13.075(3)$ Å $\beta = 108.66(2)^\circ$ $c = 13.582(3)$ Å
Volume	$2861(1)$ Å ³
Z	4
Density (calculated)	1.150 Mg/m ³
Absorption coefficient	1.594 mm ⁻¹
$F(000)$	1071
Crystal size	0.2 x 0.15 x 0.15 mm ³
θ range for data collection	2.74 to 58.01°.
Index ranges	$-18 \leq h \leq 18, -14 \leq k \leq 14, -14 \leq l \leq 13$
Reflections collected	18732
Independent reflections	3939 ($R_{\text{int}} = 0.0409$)
Completeness to $\theta = 58.01^\circ$	98.6%
Refinement method	Full-matrix least-squares on F^2
Data / restraints / parameters	3939 / 22 / 345
Goodness-of-fit on F^2	1.077
Final R indices ($I > 2\sigma(I)$)	$R1 = 0.0348, wR2 = 0.0848$
R indices (all data)	$R1 = 0.0355, wR2 = 0.0853$
Largest diff. peak and hole	0.269 and -0.307 e·Å ⁻³

Table CD12. Crystal Data and Structure Refinement Details for $\text{LAl}(\text{NH}_2)\text{Me}$ (18).

Empirical formula	$\text{C}_{30}\text{H}_{46}\text{AlN}_3$
Formula weight	475.68
Temperature	133(2) K
Wavelength	0.71073 Å
Crystal system	Monoclinic
Space group	$P2_1/c$
Unit cell dimensions	$a = 8.903(2)$ Å $b = 9.812(2)$ Å $\beta = 91.92(3)^\circ$ $c = 33.541(7)$ Å
Volume	$2928(1)$ Å ³
<i>Z</i>	4
Density (calculated)	1.079 Mg/m ³
Absorption coefficient	0.090 mm ⁻¹
<i>F</i> (000)	1040
Crystal size	0.60 x 0.50 x 0.50 mm ³
θ range for data collection	2.16 to 27.52°.
Index ranges	$-11 \leq h \leq 11, -12 \leq k \leq 12, -33 \leq l \leq 43$
Reflections collected	39501
Independent reflections	6708 ($R_{\text{int}} = 0.0325$)
Completeness to $\theta = 27.52^\circ$	99.5%
Refinement method	Full-matrix least-squares on F^2
Data / restraints / parameters	6708 / 1 / 331
Goodness-of-fit on F^2	1.035
Final <i>R</i> indices ($I > 2\sigma(I)$)	$R1 = 0.0421, wR2 = 0.1079$
<i>R</i> indices (all data)	$R1 = 0.0495, wR2 = 0.1128$
Extinction coefficient	0.0023(6)
Largest diff. peak and hole	0.298 and -0.251 e·Å ⁻³

Table CD13. Crystal Data and Structure Refinement Details for LGa(NH₂)₂ (19).

Empirical formula	C ₂₉ H ₄₅ GaN ₄
Formula weight	519.41
Temperature	100(2) K
Wavelength	1.54178 Å
Crystal system	Monoclinic
Space group	<i>P</i> 2 ₁ / <i>c</i>
Unit cell dimensions	<i>a</i> = 17.016(1) Å <i>b</i> = 13.101(1) Å <i>β</i> = 109.14(1)° <i>c</i> = 13.494(1) Å
Volume	2842(1) Å ³
<i>Z</i>	4
Density (calculated)	1.214 Mg/m ³
Absorption coefficient	1.481 mm ⁻¹
<i>F</i> (000)	1112
Crystal size	0.10 x 0.05 x 0.05 mm ³
<i>θ</i> range for data collection	2.75 to 58.93°.
Index ranges	-17 ≤ <i>h</i> ≤ 18, -14 ≤ <i>k</i> ≤ 13, -14 ≤ <i>l</i> ≤ 13
Reflections collected	12292
Independent reflections	4002 (<i>R</i> _{int} = 0.0392)
Completeness to <i>θ</i> = 58.93°	97.8%
Refinement method	Full-matrix least-squares on <i>F</i> ²
Data / restraints / parameters	4002 / 6 / 336
Goodness-of-fit on <i>F</i> ²	1.035
Final <i>R</i> indices (<i>I</i> > 2σ(<i>I</i>))	<i>R</i> 1 = 0.0282, <i>wR</i> 2 = 0.0722
<i>R</i> indices (all data)	<i>R</i> 1 = 0.0320, <i>wR</i> 2 = 0.0745
Largest diff. peak and hole	0.226 and -0.285 e·Å ⁻³

Table CD14. Crystal Data and Structure Refinement Details for $\text{LGa}(\text{NH}_2)_2 \cdot 0.5\text{C}_7\text{H}_8$ (19).

Empirical formula	$\text{C}_{32.50}\text{H}_{47}\text{GaN}_2\text{O}_2$	
Formula weight	567.44	
Temperature	100(2) K	
Wavelength	1.54178 Å	
Crystal system	Triclinic	
Space group	$P\bar{1}$	
Unit cell dimensions	$a = 13.332(1)$ Å	$\alpha = 99.08(1)^\circ$
	$b = 14.432(1)$ Å	$\beta = 95.01(1)^\circ$
	$c = 18.190(1)$ Å	$\gamma = 114.00(1)^\circ$
Volume	3112(1) Å ³	
<i>Z</i>	4	
Density (calculated)	1.211 Mg/m ³	
Absorption coefficient	1.426 mm ⁻¹	
<i>F</i> (000)	1212	
Crystal size	0.30 x 0.20 x 0.20 mm ³	
θ range for data collection	2.50 to 58.98°.	
Index ranges	$-14 \leq h \leq 14, -15 \leq k \leq 15, -19 \leq l \leq 19$	
Reflections collected	23915	
Independent reflections	8679 ($R_{\text{int}} = 0.0299$)	
Completeness to $\theta = 58.98^\circ$	97.2%	
Refinement method	Full-matrix least-squares on F^2	
Data / restraints / parameters	8679 / 10 / 726	
Goodness-of-fit on F^2	1.030	
Final <i>R</i> indices ($I > 2\sigma(I)$)	$R1 = 0.0261, wR2 = 0.0678$	
<i>R</i> indices (all data)	$R1 = 0.0274, wR2 = 0.0687$	
Extinction coefficient	0.00018(6)	
Largest diff. peak and hole	0.274 and $-0.368 \text{ e} \cdot \text{Å}^{-3}$	

Table CD15. Crystal Data and Structure Refinement Details for LAl(SH)Me (21).

Empirical formula	C ₃₀ H ₄₅ AlN ₂ S
Formula weight	492.72
Temperature	100(2) K
Wavelength	1.54178 Å
Crystal system	Monoclinic
Space group	<i>P</i> 2 ₁ / <i>n</i>
Unit cell dimensions	<i>a</i> = 12.659(1) Å <i>b</i> = 19.516(1) Å <i>β</i> = 117.50(1)° <i>c</i> = 13.291(1) Å
Volume	2913(1) Å ³
<i>Z</i>	4
Density (calculated)	1.124 Mg/m ³
Absorption coefficient	1.409 mm ⁻¹
<i>F</i> (000)	1072
Crystal size	0.10 x 0.05 x 0.05 mm ³
<i>θ</i> range for data collection	3.99 to 58.96°.
Index ranges	-14 ≤ <i>h</i> ≤ 14, -21 ≤ <i>k</i> ≤ 21, -14 ≤ <i>l</i> ≤ 14
Reflections collected	12520
Independent reflections	4070 (<i>R</i> _{int} = 0.0302)
Completeness to <i>θ</i> = 58.96°	97.3%
Refinement method	Full-matrix least-squares on <i>F</i> ²
Data / restraints / parameters	4070 / 2 / 333
Goodness-of-fit on <i>F</i> ²	1.053
Final <i>R</i> indices (<i>I</i> > 2σ(<i>I</i>))	<i>R</i> 1 = 0.0321, <i>wR</i> 2 = 0.0838
<i>R</i> indices (all data)	<i>R</i> 1 = 0.0356, <i>wR</i> 2 = 0.0864
Largest diff. peak and hole	0.255 and -0.219 e·Å ⁻³

Table CD16. Crystal Data and Structure Refinement Details for $\text{LaI}(\text{OH})(\mu\text{-O})\text{Ti}(\text{SH})\text{Cp}_2$ (22) (Contains 10% of $\text{LaI}(\text{SH})(\mu\text{-O})\text{Ti}(\text{SH})\text{Cp}_2$).

Empirical formula	$\text{C}_{39}\text{H}_{53}\text{AlN}_2\text{O}_{1.90}\text{S}_{1.10}\text{Ti}$
Formula weight	690.30
Temperature	100(2) K
Wavelength	1.54178 Å
Crystal system	Monoclinic
Space group	$P2_1/n$
Unit cell dimensions	$a = 10.907(1)$ Å $b = 20.560(2)$ Å $\beta = 98.91(1)^\circ$ $c = 16.208(1)$ Å
Volume	$3591(1)$ Å ³
Z	4
Density (calculated)	1.277 Mg/m ³
Absorption coefficient	3.122 mm^{-1}
$F(000)$	1475
Crystal size	$0.10 \times 0.10 \times 0.05 \text{ mm}^3$
θ range for data collection	3.50 to 59.03° .
Index ranges	$-11 \leq h \leq 12$, $-22 \leq k \leq 22$, $-17 \leq l \leq 17$
Reflections collected	15644
Independent reflections	5091 ($R_{\text{int}} = 0.0486$)
Completeness to $\theta = 59.03^\circ$	98.6%
Refinement method	Full-matrix least-squares on F^2
Data / restraints / parameters	5091 / 0 / 440
Goodness-of-fit on F^2	1.033
Final R indices ($I > 2\sigma(I)$)	$R1 = 0.0415$, $wR2 = 0.1042$
R indices (all data)	$R1 = 0.0621$, $wR2 = 0.1149$
Largest diff. peak and hole	0.621 and $-0.364 \text{ e} \cdot \text{\AA}^{-3}$

Table CD17. Crystal Data and Structure Refinement Details for $\text{LaI}(\text{OH})(\mu\text{-O})\text{Zr}(\text{SH})\text{Cp}_2$ (23) (Contains 14% of $\text{LaI}(\text{SH})(\mu\text{-O})\text{Zr}(\text{SH})\text{Cp}_2$).

Empirical formula	$\text{C}_{39}\text{H}_{53}\text{AlN}_2\text{O}_{1.86}\text{S}_{1.14}\text{Zr}$
Formula weight	734.34
Temperature	100(2) K
Wavelength	1.54178 Å
Crystal system	Monoclinic
Space group	$P2_1/n$
Unit cell dimensions	$a = 11.064(1)$ Å $b = 20.627(1)$ Å $\beta = 97.76(1)^\circ$ $c = 16.242(1)$ Å
Volume	$3673(1)$ Å ³
Z	4
Density (calculated)	1.328 Mg/m ³
Absorption coefficient	3.555 mm^{-1}
$F(000)$	1548
Crystal size	0.1 x 0.1 x 0.05 mm ³
θ range for data collection	3.48 to 58.97° .
Index ranges	$-12 \leq h \leq 12$, $-22 \leq k \leq 22$, $-18 \leq l \leq 18$
Reflections collected	15708
Independent reflections	5150 ($R_{\text{int}} = 0.0351$)
Completeness to $\theta = 58.97^\circ$	97.5%
Refinement method	Full-matrix least-squares on F^2
Data / restraints / parameters	5150 / 0 / 440
Goodness-of-fit on F^2	1.046
Final R indices ($I > 2\sigma(I)$)	$R1 = 0.0291$, $wR2 = 0.0725$
R indices (all data)	$R1 = 0.0368$, $wR2 = 0.0762$
Largest diff. peak and hole	0.396 and $-0.445 \text{ e} \cdot \text{Å}^{-3}$

7. Supporting Materials

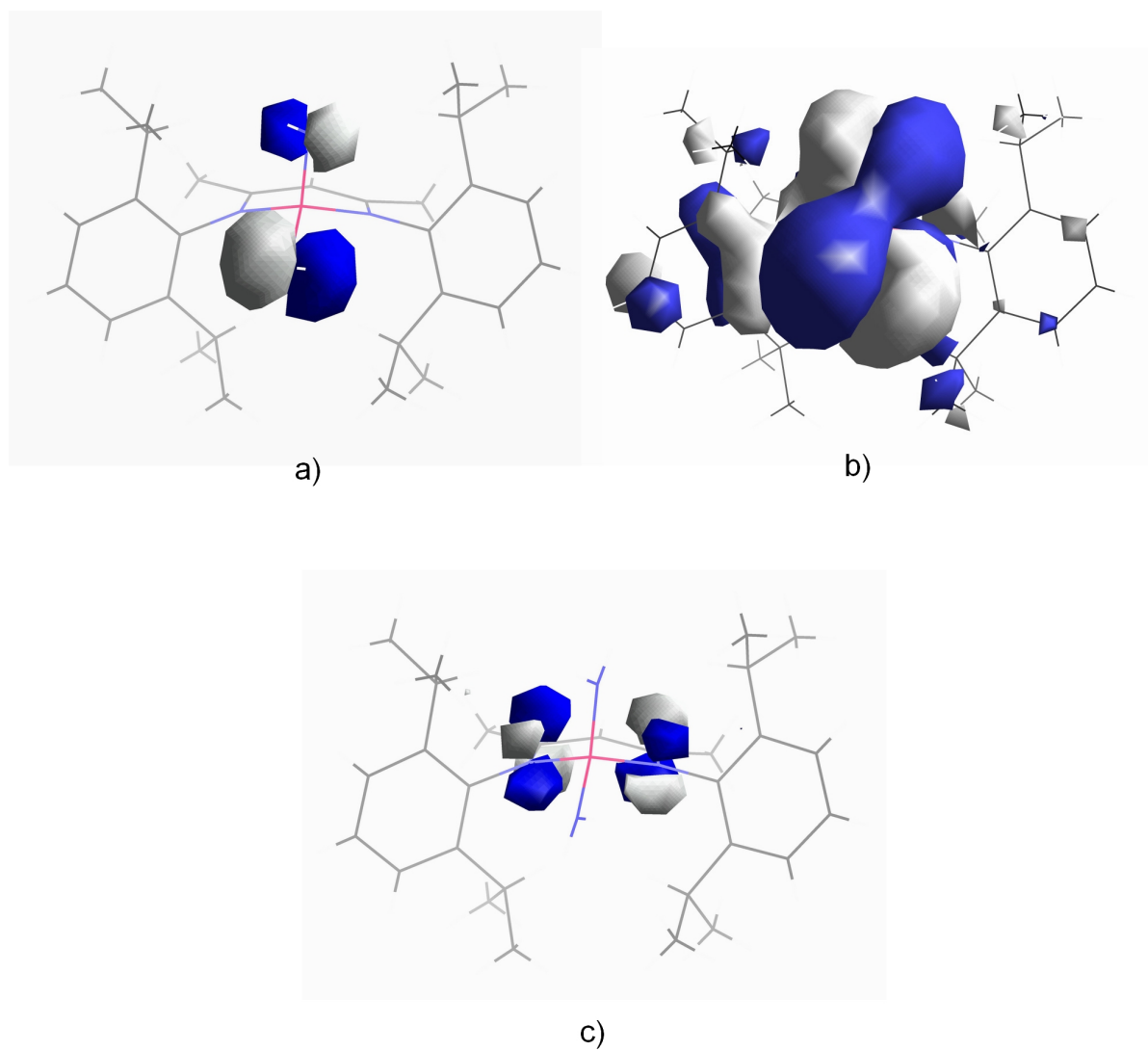


Figure S1: LAl(NH₂)₂ (**16**): HOMO (at about 0.05 (a) and 0.01 (b) e·Å⁻³) and LUMO (c) orbitals at about 0.05 e·Å⁻³.

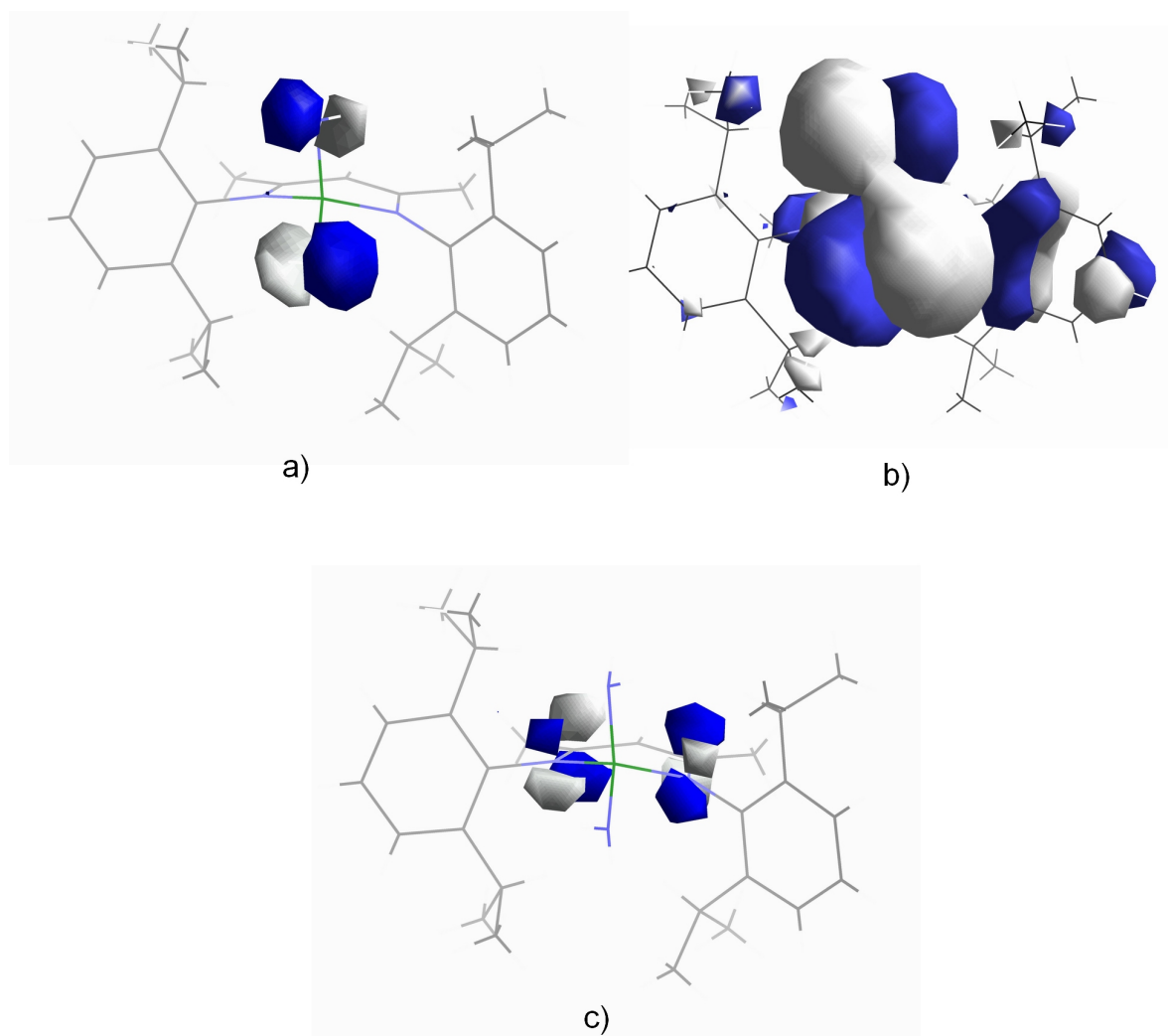


Figure S2: LGa(NH₂)₂ (**19**): HOMO (at about 0.05 (a) and 0.01 (b) e·Å⁻³) and LUMO (c) orbitals at about 0.05 e·Å⁻³.

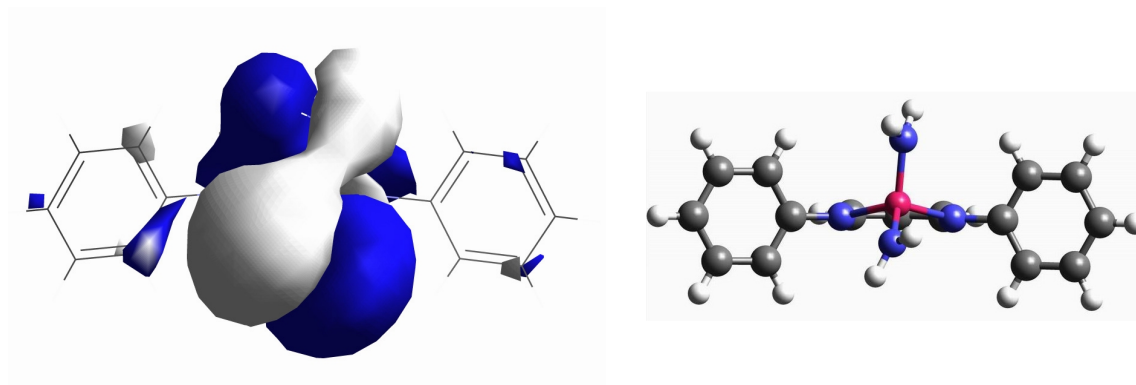


Figure S3: Calculation model of L'Al(NH₂)₂: HOMO orbital (at about 0.01 e·Å⁻³) and ball&stick model (L' = CH[C(Me)N(Ph)]₂).

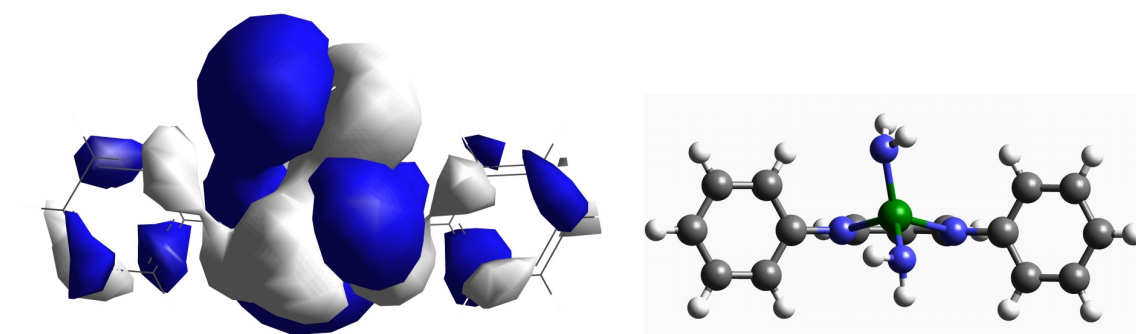


Figure S4: Calculation model of L'Ga(NH₂)₂: HOMO orbital (at about 0.01 e·Å⁻³) and ball&stick model (L' = CH[C(Me)N(Ph)]₂).

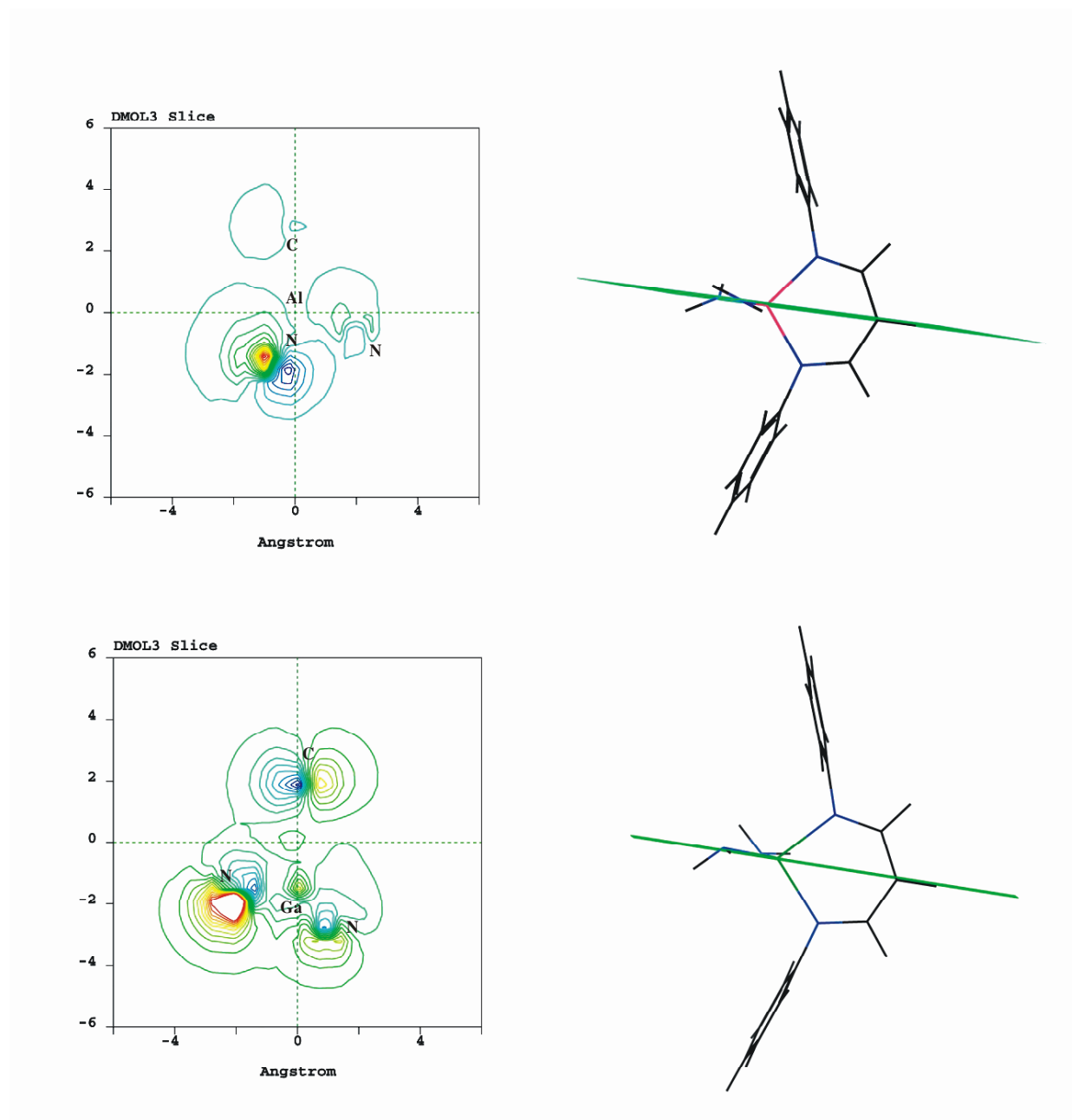


Figure S5: Electron density map (at about $0.01 \text{ e} \cdot \text{\AA}^{-3}$) in the plane $C_3-M-N(H_2)$.

8. References

- [1] R. H. Holm, G. W. Everett, A. Chakravorty, *Prog. Inorg. Chem.* **1966**, 7, 83.
- [2] S. G. McGeachin, *Can. J. Chem.* **1968**, 46, 1903.
- [3] L. C. Dorman, *Tetrahedron Lett.* **1966**, 4, 459.
- [4] W. J. Barry, I. Finar, E. F. Mooney, *Spectrochim. Acta* **1965**, 21, 1095.
- [5] R. Bonnett, D. C. Bradley, K. J. Fisher, *J. Chem. Soc., Chem. Commun.* **1968**, 886.
- [6] R. Bonnett, D. C. Bradley, K. J. Fisher, I. F. Rendall, *J. Chem. Soc. (A)* **1971**, 1622.
- [7] J. E. Parks, R. H. Holm, *Inorg. Chem.* **1968**, 7, 1408.
- [8] C. P. Richards, G. A. Webb, *J. Inorg. Nucl. Chem.* **1969**, 31, 3459.
- [9] N. M. Tsybina, V. G. Vinkurov, T. V. Protopopova, A. P. Skoldinov *J. Gen. Chem., USSR* **1966**, 36, 1383; *Zh. Obshh. Khimii* **1966**, 36, 1372.
- [10] F. A. Cotton, B. G. DeBoer, J. R. Pipal, *Inorg. Chem.* **1970**, 9, 783.
- [11] M. Elder, B. R. Penfold, *J. Chem. Soc. (A)* **1969**, 2556.
- [12] C. L. Honeybourne, G. A. Webb, *Mol. Phys.* **1969**, 17, 17.
- [13] C. L. Honeybourne, G. A. Webb, *Chem. Phys. Lett.* **1968**, 2, 426.
- [14] P. B. Hitchcock, M. F. Lappert, D.-S. Liu, *J. Chem. Soc., Chem. Commun.* **1994**, 1699.
- [15] V. C. Gibson, P. J. Maddox, C. Newton, C. Redshaw, G. Solan, A. J. P. White, D. J. Williams, *J. Chem. Soc., Chem. Commun.* **1998**, 1651.
- [16] D. S. Richeson, J. F. Mitchell, K. H. Theopold, *Organometallics* **1989**, 8, 2570.
- [17] A. C. Filippou, C. Völkl, R. D. Rogers, *J. Organomet. Chem.* **1993**, 463, 135.
- [18] V. C. Gibson, C. Newton, C. Redshaw, G. A. Solan, A. J. P. White, D. J. Williams. *Eur. J. Inorg. Chem.* **2001**, 1895.
- [19] B. J. O'Keefe, M. A. Hillmeyer, W. B. Tolman, *J. Chem. Soc., Dalton Trans.* **2001**, 2215.
- [20] J. Feldman, S. J. McLain, A. Parthasarathy. W. J. Marshall, C. J. Calabrese, S. D. Arthur, *Organometallics* **1997**, 16, 1514.
- [21] P. H. M. Budzelaar, A. B. van Oort, A. G. Orpen, *Eur. J. Inorg. Chem.* **1998**, 1485.
- [22] K. H. Theopold, W.-K. Kim, *Int. Pat. Appl. WO 99/41290* **1999**; *Chem. Abstr.* 131:170748.
- [23] M. Rahim, N. J. Taylor, S. Xin, S. Collins, *Organometallics* **1998**, 17, 1315.
- [24] P. L. Holland, W. B. Tolman, *J. Am. Chem. Soc.* **1999**, 121, 7270.

- [25] D. W. Randall, G. S. DeBeer, P. L. Holland, B. Hedman, K. O. Hodgson, W. B. Tolman, E. I. Solomon, *J. Am. Chem. Soc.* **2000**, *122*, 11632.
- [26] C. Cui, H. W. Roesky, H. Hao, H.-G. Schmidt, M. Noltemeyer, *Angew. Chem.* **2000**, *112*, 1885; *Angew. Chem. Int. Ed.* **2000**, *39*, 1815.
- [27] C. Cui, H. W. Roesky, H.-G. Schmidt, M. Noltemeyer, H. Hao, F. Cimpoesu, *Angew. Chem.* **2000**, *112*, 4444; *Angew. Chem. Int. Ed.* **2000**, *39*, 4274.
- [28] J. M. Smith, R. L. Lachicotte, P. L. Holland, *J. Chem. Soc., Chem. Commun.* **2001**, 1542.
- [29] J. M. Smith, R. L. Lachicotte, K. A. Pittard, T. R. Cundari, G. Lukat-Rodgers, K. R. Rodgers, P. L. Holland, *J. Am. Chem. Soc.* **2001**, *123*, 9222.
- [30] N. J. Hardman, B. E. Eichler, P. P. Power, *J. Chem. Soc., Chem. Commun.* **2000**, 1991.
- [31] B. Rake, F. Zulch, Y. Ding, J. Prust, H. W. Roesky, M. Noltemeyer, H.-G. Schmidt, *Z. Anorg. Allg. Chem.* **2001**, 627, 836.
- [32] L. W. Pineda, V. Jancik, H. W. Roesky, D. Neculai, A. M. Neculai, *Angew. Chem.* **2004**, *116*, 1443; *Angew. Chem. Int. Ed.* **2004**, *43*, 1419.
- [33] H. Hao, C. Cui, H. W. Roesky, G. Bai, H.-G. Schmidt, M. Noltemeyer, *Chem. Commun.* **2001**, 1118.
- [34] S. S. Malhotra, M. C. Whiting, *J. Chem. Soc. Abstr.* **1960**, 3812.
- [35] G. Scheibe, *Ber. Dtsch. Chem. Ges.* **1923**, *56*, 137.
- [36] P. J. Bailey, R. A. Coxall, C. M. E. Dick, S. Fabre, S. Parsons, *Organometallics* **2001**, *20*, 798.
- [37] Y. Ding, H. Hao, H. W. Roesky, M. Noltemeyer, H.-G. Schmidt, *Organometallics* **2001**, *20*, 4806.
- [38] G. Bai, Y. Peng, H. W. Roesky, J. Li, H.-G. Schmidt, M. Noltemeyer, *Angew. Chem.* **2003**, *115*, 1168; *Angew. Chem. Int. Ed.* **2003**, *42*, 1132.
- [39] J. Prust, H. Hohmeister, A. Stasch, H. W. Roesky, J. Magull, E. Alexopoulos, I. Us3n, H.-G. Schmidt, M. Noltemeyer, *Eur. J. Inorg. Chem.* **2002**, 2156.
- [40] Y.-L. Huang, B.-H. Huang, B.-T. Ko, C.-C. Lin, *J. Chem. Soc., Dalton Trans.* **2001**, 2409.
- [41] L. Bourget-Merle, M. F. Lappert, J. R. Severn, *Chem. Rev.* **2002**, *102*, 3031.
- [42] C. Cui, H. W. Roesky, H.-G. Schmidt, M. Noltemeyer, *Organometallics* **1999**, *18*, 5120.

- [43] C. Cui, H. W. Roesky, H.-G. Schmidt, M. Noltemeyer, *Inorg. Chem.* **2000**, 39, 3678.
- [44] W. J. Grigsby, C. L. Raston, V.-A. Tolhurst, B. W. Skelton, A. H. White, *J. Chem. Soc., Dalton Trans.* **1998**, 2547.
- [45] M. G. Gardiner, C. L. Raston, V.-A. Tolhurst, *J. Chem. Soc., Chem. Commun.* **1995**, 2501.
- [46] P. D. Godfrey, C. L. Raston, B. W. Skelton, V.-A. Tolhurst, A. H. White, *J. Chem. Soc., Chem. Commun.* **1997**, 2235.
- [47] C. Schnitter, A. Klemp, H. W. Roesky, H.-G. Schmidt, C. Röpken, R. Herbst-Irmer, M. Noltemeyer, *Eur. J. Inorg. Chem.* **1998**, 2033.
- [48] A. Ecker, R. Köppe, C. Üffing, H. Schnöckel, *Z. Anorg. Allg. Chem.* **1998**, 624, 817.
- [49] R. J. Wehmschulte, P. P. Power, *J. Chem. Soc., Chem. Commun.* **1998**, 335.
- [50] H. Zhu, J. Chai, H. W. Roesky, M. Noltemeyer, H.-G. Schmidt, D. Vidovic, J. Magull, *Eur. J. Inorg. Chem.* **2003**, 3113.
- [51] K. S. Klimek, J. Prust, H. W. Roesky, M. Noltemeyer, H.-G. Schmidt, *Organometallics* **2001**, 20, 2047.
- [52] C. F. Harlan, E. G. Gillan, S. G. Bott, A. R. Barron, *Organometallics* **1996**, 15, 5479.
- [53] S. Schulz, H. W. Roesky, H. J. Koch, G. M. Sheldrick, D. Stalke, A. Kuhn, *Angew. Chem.* **1993**, 105, 1828; *Angew. Chem. Int. Ed. Engl.* **1993**, 32, 1729.
- [54] A. H. Cowley, R. A. Jones, P. R. Harris, D. A. Atwood, L. Contreras, C. J. Burek, *Angew. Chem.* **1991**, 103, 1164; *Angew. Chem. Int. Ed. Engl.* **1991**, 30, 1143.
- [55] T. Hirabayashi, K. Inoue, K. Yokota, Y. Ishii, *J. Organomet. Chem.* **1975**, 92, 139.
- [56] G. H. Robinson, M. F. Self, W. T. Pennington, S. A. Sangokoya, *Organometallics* **1988**, 7, 2424.
- [57] R. J. Wehmschulte, P. P. Power, *J. Am. Chem. Soc.* **1997**, 119, 9566.
- [58] W. Uhl, A. Vester, W. Hiller, *J. Organomet. Chem.* **1993**, 443, 9.
- [59] W. Uhl, R. Gerding, I. Hahn, S. Pohl, W. Saak, H. Reuter, *Polyhedron* **1996**, 15, 3987.
- [60] W. Uhl, U. Schuetz, *Z. Naturforsch.* **1994**, 49b, 931.
- [61] W. Zheng, H. Hohmeister, N. C. Mösch-Zanetti, H. W. Roesky, M. Noltemeyer, H.-G. Schmidt, *Inorg. Chem.* **2001**, 40, 2363.

- [62] W. Zheng, N. C. Mösch-Zanetti, H. W. Roesky, M. Noltemeyer, M. Hewitt, H.-G. Schmidt, T. R. Schneider, *Angew. Chem.* **2000**, *112*, 4446; *Angew. Chem. Int. Ed.* **2000**, *39*, 4276.
- [63] Review: M. Witt, H. W. Roesky, *Curr. Sci.* **2000**, *78*, 410.
- [64] D. A. Neumayer, J. G. Ekerdt, *Chem. Mater.* **1996**, *8*, 9, and references cited therein.
- [65] A. C. Jones, P. O'Brien (Eds.) in *CVD of Compound Semiconductors: Precursor Synthesis, Development and Application*, VCH, Weinheim, FRG, **1997**.
- [66] *Chemistry of Aluminum, Gallium, Indium and Thallium* (Ed.: A. J. Downs), Blackie, Glasgow, UK, **1993**.
- [67] D. C. Boyd, R. T. Haasch, P. R. Mantell, R. K. Schulze, J. F. Evans, W. L. Gladfelter, *Chem. Mater.* **1989**, *1*, 119.
- [68] A. Ochi, H. K. Bowen, W. E. Rhine, *Mater. Res. Soc. Symp. Proc.* **1988**, *121*, 663.
- [69] F. N. Tebbe, *Int. Pat. Appl. U.S. 4696968* **1987**. *Chem. Abstr.* 108:1087473.
- [70] L. V. Interrante, L. E. Carpenter, C. Whitmarsh, W. Lee, G. A. Slack, *Mater. Res. Soc. Symp. Proc.* **1986**, *73*, 359.
- [71] L. V. Interrante, W. Lee, M. McConnel, N. Lewis, E. Hall, *J. Electrochem. Soc.* **1989**, *136*, 472.
- [72] A. Rabineau in: *Compounds Semiconductors* (Eds.: R. K. Willardson, H. L. Goerring), Reinhold Publishing Corp., New York, USA, **1962**, Vol. 1, Chapter 19, 174.
- [73] L. V. Interrante, G. A. Siegel, M. Garbaskas, C. Hejna, G. A. Slack, *Inorg. Chem.* **1989**, *28*, 252.
- [74] F. C. Sauls, C. L. Czekaj, L. V. Interrante, *Inorg. Chem.* **1990**, *29*, 4688.
- [75] J. F. Janik, E. N. Duesler, R. T. Paine, *Inorg. Chem.* **1988**, *27*, 4335.
- [76] J. F. Janik, E. N. Duesler, R. T. Paine, *Inorg. Chem.* **1987**, *26*, 4341.
- [77] C.-C. Chang, M.-D. Li, M. Y. Chiang, S.-M. Peng, Y. Wang, G.-H. Lee, *Inorg. Chem.* **1997**, *36*, 1955.
- [78] J. Müller, U. Ruschewitz, O. Indris, H. Hartwig, W. Stahl, *J. Am. Chem. Soc.* **1999**, *121*, 4647.
- [79] W. Watt, J. L. Hall, G. R. Chopin, *J. Phys. Chem.* **1953**, *57*, 567.
- [80] W. L. Taylor, E. Griswold, J. Kleinberg, *J. Am. Chem. Soc.* **1955**, *77*, 294.
- [81] J.-W. Hwang, S. A. Hanson, D. Britton, J. F. Evans, K. F. Jensen, W. L. Gladfelter, *Chem. Mater.* **1990**, *2*, 342.

- [82] J.-W. Hwang, J. P. Campbell, J. Kozubowski, S. A. Hanson, J. F. Evans, W. L. Gladfelter, *Chem. Mater.* **1995**, 7, 515.
- [83] M. J. Almond, M. G. B. Drew, C. E. Jenkins, D. A. Rice, *J. Chem. Soc., Dalton Trans.* **1992**, 5.
- [84] D. Sengupta, *J. Phys. Chem. B* **2003**, 107, 291.
- [85] H. S. Park, S. D. Waezada, A. H. Cowley, H. W. Roesky, *Chem. Mater.* **1998**, 10, 2251.
- [86] D. A. Atwood, A. H. Cowley, P. R. Harris, R. A. Jones, S. U. Koschmieder, C. M. Nunn, J. L. Atwood, S. G. Bott, *Organometallics* **1993**, 12, 24.
- [87] F. A. Ponce, D. P. Bour, *Nature* **1997**, 386, 351.
- [88] T. Someya, R. Werner, A. Forchel, M. Catalano, R. Cingolani, Y. Arakawa, *Science* **1999**, 285, 1905.
- [89] S. Y. Bae, H. W. Seo, J. Park, H. Yang, H. Kim, S. Kim, *Appl. Phys. Lett.* **2003**, 82, 4564.
- [90] G. Fasol, *Science* **1996**, 272, 1751.
- [91] S. Nakamura, *Science* **1998**, 281, 956.
- [92] C. H. Wallace, S. H. Kim, G. A. Rose, L. Rao, J. R. Heath, M. Nicol, R. B. Kaner, *Appl. Phys. Lett.* **1998**, 72, 596.
- [93] W. Q. Han, S. S. Fan, Q. Q. Li, Y. D. Hu, *Science* **1997**, 277, 1287.
- [94] X. F. Duan, C. M. Lieber, *J. Am. Chem. Soc.* **2000**, 122, 188.
- [95] S. Y. Bae, H. W. Seo, J. Park, H. Yang, J. C. Park, S. Y. Lee, *Appl. Phys. Lett.* **2002**, 81, 126.
- [96] J. Goldberger, R. R. He, Y. F. Zhang, S. K. Lee, H. Q. Yan, H.-J. Choi, P. D. Yang, *Nature* **2003**, 422, 599.
- [97] J. Q. Hu, Y. Bando, D. Golberg, Q. L. Liu, *Angew. Chem.* **2003**, 115, 3617; *Angew. Chem. Int. Ed.* **2003**, 42, 3493.
- [98] X. Sun, Y. Li, *Angew. Chem.* **2004**, 116, 3915; *Angew. Chem. Int. Ed.* **2004**, 43, 3827.
- [99] J. I. Pankove, T. D. Moustakas (Eds.), *Semiconductors and Semimetals: Gallium Nitride (GaN) II*, Vol. 57, Academic Press: New York, USA, **1999**, and references cited therein.
- [100] G. B. Stringfellow, M. G. Craford (Eds.), *Semiconductors and Semimetals: High Brightness Light Emitting Diodes*, Vol. 48, Academic Press: New York, USA, **1995**, and references cited therein.

- [101] C. Coperèt, M. Chabanas, R. P. Sait-Arroman, J.-M. Basset, *Angew. Chem.* **2003**, *115*, 164; *Angew. Chem. Int. Ed.* **2003**, *42*, 156.
- [102] H. W. Roesky, I. Haiduc, N. S. Hosmane, *Chem. Rev.* **2003**, *103*, 2579.
- [103] T. Carofiglio, C. Floriani, M. Rosi, A. Chiesi-Villa, C. Rizzoli, *Inorg. Chem.* **1991**, *30*, 3245.
- [104] M. S. Rau, C. M. Kretz, G. L. Geoffroy, A. L. Rheingold, B. S. Haggerty, *Organometallics* **1994**, *13*, 1624.
- [105] G. Erker, M. Albrecht, S. Werner, C. Krüger, *Z. Naturforsch.* **1990**, *45b*, 1205.
- [106] S. Bansal, Y. Singh, A. Singh, *Heteroatom Chem.* **2004**, 21.
- [107] H. Dorn, H. W. Roesky, *Inorg. Synth.* **2002**, *33*, 230.
- [108] C. Ackerhans, H. W. Roesky, T. Labahn, J. Magull, *Organometallics* **2002**, *21*, 3671.
- [109] G. Bai, H. W. Roesky, J. Li, M. Noltemeyer, H.-G. Schmidt, *Angew. Chem.* **2003**, *115*, 5660; *Angew. Chem. Int. Ed.* **2003**, *42*, 5502.
- [110] J. Janssen, J. Magull, H. W. Roesky, *Angew. Chem.* **2002**, *114*, 1425; *Angew. Chem. Int. Ed.* **2002**, *41*, 1365.
- [111] M. Veith, M. Jarczyk, V. Huch, *Angew. Chem.* **1997**, *109*, 140; *Angew. Chem. Int. Ed. Engl.* **1997**, *36*, 117.
- [112] J. Storre, A. Klemp, H. W. Roesky, H.-G. Schmidt, M. Noltemeyer, R. Fleischer, D. Stalke, *J. Am. Chem. Soc.* **1996**, *118*, 1380.
- [113] C. Schnitter, H. W. Roesky, T. Albers, H.-G. Schmidt, C. Röpken, E. Parisini, G. M. Sheldrick, *Chem. Eur. J.* **1997**, *3*, 1783.
- [114] Y. Koide, A. R. Barron, *Organometallics* **1995**, *14*, 4026.
- [115] N. M. Boag, K. M. Coward, A. C. Jones, M. E. Pemble, J. R. Thompson, *Acta Crystallogr. Sect. C* **2000**, *56*, 1438.
- [116] W. Uhl, I. Hahn, M. Koch, M. Layh, *Inorg. Chim. Acta* **1996**, *249*, 33.
- [117] D. A. Atwood, A. H. Cowley, P. R. Harris, R. A. Jones, S. U. Koschmieder, C. M. Nunn, J. L. Atwood, S. G. Bott, *Organometallics* **1993**, *12*, 24.
- [118] A. A. Naiini, V. Young, Y. Han, M. Akinc, J. G. Verkade, *Inorg. Chem.* **1993**, *32*, 3781.
- [119] P. J. Nichols, S. Papadopoulos, C. L. Raston, *J. Chem. Soc., Chem. Commun.* **2000**, 1227.
- [120] N. Wiberg, K. Amelunxen, H.-W. Lerner, H. Nöth, W. Ponikwar, H. Schwenk, *J. Organomet. Chem.* **1999**, *574*, 246.

- [121] A. H. Cowley, F. P. Gabbaï, D. A. Atwood, C. J. Carrano, L. M. Mokry, M. R. Bond, *J. Am. Chem. Soc.* **1994**, *116*, 1559.
- [122] J. C. Goodwin, S. J. Teat, S. L. Heath, *Angew. Chem.* **2004**, *116*, 4129; *Angew. Chem. Int. Ed. Engl.* **2004**, *43*, 4037.
- [123] S. J. Rettig, M. Sandercock, A. Storr, J. Trotter, *Can. J. Chem.* **1990**, *68*, 59.
- [124] K. Inami, K. Oka, K. Daimon, *J. Imaging Sci. Technol.* **1995**, *39*, 298.
- [125] G. Linti, R. Frey, W. Köstler, H. Urban, *Chem. Ber.* **1996**, *129*, 561.
- [126] C. Cui, *Ph.D. Thesis*. Universität Göttingen, **2001**.
- [127] M. L. Steigerwald, C. R. Sprinkle, *Organometallics* **1988**, *7*, 245.
- [128] L.-B. Han, F. Mirzaei, M. Tanaka, *Organometallics* **2000**, *19*, 722.
- [129] N. Kuhn, G. Henkel, H. Schumann, R. Fröhlich, *Z. Naturforsch.* **1990**, *45b*, 1010.
- [130] H. Tolkmith, *J. Am. Chem. Soc.* **1963**, *85*, 3246.
- [131] Spartan '02 program: W. J. Hehre, R. F. Stewart, J. A. Pople, *J. Chem. Phys.* **1969**, *51*, 2657.
- [132] N. J. Hardman, P. P. Power, *Inorg. Chem.* **2001**, *40*, 2474.
- [133] C. Jones, G. A. Koutsantonis, C. L. Raston, *Polyhedron* **1993**, *12*, 1829.
- [134] C. L. Raston, *J. Organomet. Chem.* **1994**, *475*, 15.
- [135] M. G. Gardiner, C. L. Raston, V.-A. Tolhurst, *J. Chem. Soc., Chem. Commun.* **1995**, 1457.
- [136] J. E. Huheey, *Inorganic Chemistry: Principles of Structure and Reactivity*, Harper Collins College Publishers, New York, USA, **1993**, 292.
- [137] M. Khorasani-Motlag, N. Safari, C. B. Pamplin, B. O. Patrick, B. R. James, *Inorg. Chim. Acta* **2001**, *320*, 184.
- [138] F. Bottomley, D. F. Drummond, G. O. Egharevba, P. S. White, *Organometallics* **1986**, *5*, 1620.
- [139] P. G. Jessop, C.-L. Lee, G. Rastar, B. R. James, C. J. L. Lock, R. Faggiani, *Inorg. Chem.* **1992**, *31*, 4601.
- [140] F. Brisse, F. Bélanger-Gariépy, B. Zacharie, Y. Gareau, K. Steliou, *Nouv. J. Chim.* **1983**, *7*, 391.
- [141] T. S. Zyubina, O. P. Charkin, *Zh. Neorg. Chem.* **1991**, *36*, 3083; *Russ. J. Inorg. Chem.* **1991**, *36*, 1731.
- [142] T. S. Zyubina, O. P. Charkin, *Zh. Neorg. Chem.* **1991**, *36*, 752; *Russ. J. Inorg. Chem.* **1991**, *36*, 425.
- [143] J. Knizek, H. Nöth, A. Schlegel, *Eur. J. Inorg. Chem.* **2001**, 181.

- [144] M. Aslam, R. A. Bartlett, E. Block, M. M. Olmstead, P. P. Power, G. E. Sigel, *J. Chem. Soc., Chem. Commun.* **1985**, 1674.
- [145] M. Niemeyer, P. P. Power, *Inorg. Chem.* **1996**, 35, 7264.
- [146] A. Gebauer, J. A. R. Schmidt, J. Arnold, *Inorg. Chem.* **2000**, 39, 3424.
- [147] F. Pauer, P. P. Power, *Lithium Chemistry: A Theoretical and Experimental Overview*, (Eds. A. M. Sapse, P. v. R. Schleyer), Wiley, New York, USA, **1995**, ch. 9, p. 295.
- [148] S. Chadwick, U. Englich, K. Ruhlandt-Senge, *Organometallics* **1997**, 16, 5792.
- [149] W.-Y. Chen, C. Eaborn, I. B. Gorrell, P. B. Hitchcock, J. D. Smith, *J. Chem. Soc., Dalton Trans.* **2000**, 2313.
- [150] S. C. Lee, J. Li, J. C. Mitchell, R. H. Holm, *Inorg. Chem.* **1992**, 31, 4333.
- [151] K. Tatsumi, Y. Inoue, H. Kawaguchi, M. Kohsaka, A. Nakamura, R. E. Cramer, W. VanDoorne, G. J. Taogoshi, P. N. Richmann, *Organometallics* **1993**, 12, 352.
- [152] H. Kawaguchi, K. Tatsumi, R. E. Cramer, *Inorg. Chem.* **1996**, 35, 4391.
- [153] J. Knizek, H. Nöth, *J. Organomet. Chem.* **2000**, 614, 168.
- [154] J. Francis, S. G. Bott, A. R. Barron, *J. Organomet. Chem.* **2000**, 597, 29, and references cited therein.
- [155] C. J. Harlan, A. R. Barron, *J. Cluster Sci.* **1996**, 7, 455.
- [156] N. N. Greenwood, A. Earnshaw, *Chemistry of the Elements*; Butterworths-Heinemann: Oxford, UK, **2002**, 1205.
- [157] F. Bottomley, R. W. Day, *Can. J. Chem.* **1992**, 70, 1250.
- [158] P. G. Maué, D. Fenske, *Z. Naturforsch.* **1988**, 43b, 1213.
- [159] S. Kabashima, S. Kuwata, M. Hidai, *J. Am. Chem. Soc.* **1999**, 121, 7837.
- [160] D. M. Giolando, T. B. Rauchfuss, G. M. Clark, *Inorg. Chem.* **1987**, 26, 3082.
- [161] A. M. Magill, K. J. Cavell, B. F. Yates, *J. Am. Chem. Soc.* **2004**, 126, 8717.
- [162] A. J. Arduengo III, H. Bock, H. Chen, M. Denk, D. A. Dixon, J. C. Green, W. A. Herrmann, N. L. Jones, M. Wagner, R. West, *J. Am. Chem. Soc.* **1994**, 116, 6641.
- [163] W. Chen, F. Liu, X. You, *J. Solid State Chem.* **2002**, 167, 119.
- [164] F. Liu, W. Chen, X. You, *J. Chem. Crystallogr.* **2002**, 32, 27.
- [165] A. J. Arduengo III, R. L. Harlow, M. Kline, *J. Am. Chem. Soc.* **1991**, 113, 361.
- [166] M. Niehues, G. Kehr, G. Erker, B. Wibbeling, R. Fröhlich, O. Blacque, H. Berke, *J. Organomet. Chem.* **2002**, 663, 192.
- [167] A. J. Arduengo, III, H. V. R. Dias, R. L. Harlow, M. Kline, *J. Am. Chem. Soc.* **1992**, 114, 5530.

- [168] C. Paek, S. O. Kang, J. Ko, P. J. Carroll, *Organometallics* **1997**, *16*, 2110.
- [169] H. Nöth, P. Konrad, *Chem. Ber.* **1983**, *116*, 3552.
- [170] S. Daniel, D. M. Hoffmann, *Inorg. Chem.* **2002**, *41*, 3843.
- [171] K. Ruhlandt-Senge, P. P. Power, *Inorg. Chem.* **1991**, *30*, 2633.
- [172] N. D. Reddy, S. S. Kumar, H. W. Roesky, D. Vidovic, J. Magull, M. Noltemeyer, H.-G. Schmidt, *Eur. J. Inorg. Chem.* **2003**, 442.
- [173] R. J. Wehmschulte, K. Ruhlandt-Senge, P. P. Power, *Inorg. Chem.* **1995**, *34*, 2593.
- [174] M. Taghiof, M. J. Heeg, M. Bailey, D. G. Dick, R. Kumar, D. G. Hendershot, H. Rahbarnoohi, J. P. Oliver, *Organometallics* **1995**, *14*, 2903.
- [175] V. Jancik, J. Prust, H. W. Roesky, *unpublished results*.
- [176] D. Bourissou, O. Guerret, F. P. Gabbaï, G. Bertrand, *Chem. Rev.* **2000**, *100*, 39.
- [177] D. B. Collum, *Acc. Chem. Res.* **1993**, *26*, 227, and references cited therein.
- [178] W. F. Lappert, P. P. Power, A. R. Sanger, R. C. Srivastava (Eds.), *Metal and Metalloid Amides*; Ellis-Horwood: Chichester, UK, **1980**, and references cited therein.
- [179] A. Greenberg, C. M. Breneman, J. F. Liebman (Eds.), *The Amide Linkage: Structural Significance in Chemistry, Biochemistry, and Materials Science*; Wiley-Interscience: New York, USA, **1999**, and references cited therein.
- [180] E. Brady, J. R. Telford, G. Mitchell, W. Lukens, *Acta Crystallogr. Sect. C* **1995**, *51*, 558.
- [181] K. Wraage, H.-G. Schmidt, M. Noltemeyer, H. W. Roesky, *Eur. J. Inorg. Chem.* **1999**, 863.
- [182] M. Stender, B. E. Eichler, N. J. Hardman, P. P. Power, J. Prust, M. Noltemeyer, H. W. Roesky, *Inorg. Chem.* **2001**, *40*, 2794.
- [183] Regine Herbst-Irmer, *private communication*.
- [184] G. Bai, S. Singh, V. Jancik, H. W. Roesky, *Pat. Appl. pending*.
- [185] B. Qian, D. L. Ward, M. R. Smith III, *Organometallics* **1998**, *17*, 3070.
- [186] B. Delley, *J. Chem. Phys.* **1990**, *92*, 508.
- [187] Density functional methods were applied using the program DMOL,^[186] as implemented in the Cerius program suite.^[218] To take into account the density distribution within the extended ligand systems of the investigated compounds in a suitable way, the nonlocal density functionals for exchange and correlation interactions according to Becke^[219] and Lee, Yang and Parr^[220] (BLYP) were chosen. Double numerical basis sets were used for all elements and extended by

- polarization functions for Al, Ga and N. The complex geometries were taken from the experimental data.
- [188] Y. Peng, H. Fan, V. Jancik, H. W. Roesky, R. Herbst-Irmer, *Angew. Chem.* **2004**, *116*, 6316; *Angew. Chem. Int. Ed.* **2004**, *43*, 6190.
- [189] Another model compound for this ligand has been recently used. B. F. Gherman, C. J. Cramer, *Inorganic chemistry* **2004**, *43*, 7281.
- [190] G. S. Smith, J. L. Hoard, *J. Am. Chem. Soc.* **1959**, *81*, 3907.
- [191] U. Nehete, *unpublished results*.
- [192] U. N. Nehete, V. Chandrasekhar, G. Anantharaman, H. W. Roesky, D. Vidovic, J. Magull, *Angew. Chem.* **2004**, *116*, 3930; *Angew. Chem. Int. Ed.* **2004**, *43*, 3842.
- [193] U. Nehete, V. Chandrasekhar, V. Jancik, H. W. Roesky, R. Herbst-Irmer *Organometallics* **2004**, *accepted for publication*.
- [194] J. McMurry, *Organic Chemistry 3rd ed.*, (Ed. N. Miaoulis), Brooks/Cole Publishing, Pacific Grove, USA. **1992**, ch. 21.
- [195] S. S. Kumar, *unpublished results*.
- [196] G. A. Zank, C. A. Jones, T. B. Rauchfuss, A. L. Rheingold, *Inorg. Chem.* **1986**, *25*, 1886.
- [197] D. Coucouvanis, A. Hadjikyriacou, R. Lester, M. G. Kanatzidis, *Inorg. Chem.* **1994**, *33*, 3645.
- [198] F. Bottomley, D. F. Drummond, G. O. Egharevba, P. S. White, *Organometallics* **1986**, *5*, 1620.
- [199] M. A. F. Hernandez-Gruel, J. J. Pérez-Torrente, M. A. Ciriano, J. A. López, F. J. Lahoz, L. A. Oro, *Eur. J. Inorg. Chem.* **1999**, 2047.
- [200] G. A. Zank, T. B. Rauchfuss, S. R. Wilson, A. L. Rheingold, *J. Am. Chem. Soc.* **1984**, *106*, 7621.
- [201] Z. K. Sweeney, J. L. Polse, R. A. Anderson, R. G. Bergman, *J. Am. Chem. Soc.* **1998**, *120*, 7825.
- [202] R. Steudel, A. Prenzel, J. Pickardt, *Angew. Chem.* **1991**, *103*, 586; *Angew. Chem., Int. Ed. Engl.* **1991**, *30*, 550.
- [203] W. E. Piers, L. Koch, D. S. Ridge, L. R. MacGillivray, M. Zaworotko, *Organometallics* **1992**, *11*, 3148.
- [204] J. L. Petersen, *J. Organomet. Chem.* **1979**, *166*, 179.
- [205] V. W.-W. Yam, G.-Z. Qi, K.-K. Cheung, *J. Organomet. Chem.* **1997**, *548*, 289.

- [206] H.-M. Gau, Ch.-A. Chen, S.-J. Chang, W.-E. Shih, T.-K. Yang, T.-T. Jong, M.-Y. Chien, *Organometallics* **1993**, *12*, 1314.
- [207] H. Zhu, J. Chai, C. He, H. W. Roesky, V. Jancik, H.-G. Schmidt, M. Noltemeyer, *Organometallics* **2004**, *submitted for publication*.
- [208] S. Singh, *unpublished results*.
- [209] J. Chai, H. Zhu, C. He, H. W. Roesky, V. Jancik, S. Singh, *Angew. Chem.* **2004**, *submitted for publication*.
- [210] S. Singh, S. S. Kumar, V. Chandrasekhar, H.-J. Ahn, M. Biadene, H. W. Roesky, N. S. Hosmane, M. Noltemeyer, H.-G. Schmidt, *Angew. Chem.* **2004**, *116*, 5048; *Angew. Chem., Int. Ed. Engl.* **2004**, *43*, 4940.
- [211] L. W. Pineda, V. Jancik, H. W. Roesky, R. Herbst-Irmer, *J. Am. Chem. Soc.* **2004**, *submitted for publication*.
- [212] D. F. Shriver, M. A. Drezdon, *The manipulation of Air-Sensitive Compounds*, 2nd ed., McGraw-Hill, New York, USA, **1969**.
- [213] "SHELXS-97, Program for Structure Solution": G. M. Sheldrick, *Acta Crystallogr. Sect. A* **1990**, *46*, 467.
- [214] G. M. Sheldrick, SHELXL-97, *Program for Crystal Structure Refinement*, Universität Göttingen, Göttingen, FRG, **1997**.
- [215] J. Meyer, *Ber.* **1913**, *46*, 308.
- [216] R. A. Zingaro, B. H. Steeves, K. Irgolic, *J. Organomet. Chem.* **1965**, *4*, 320.
- [217] B. Hübler-Blank, M. Witt, H. W. Roesky, *J. Chem. Educ.* **1993**, *70*, 408.
- [218] Cerius² program suite, Accelrys Inc. **2001**.
- [219] A. D. Becke, *Phys. Rev. A* **1988**, *38*, 3098.
- [220] C. Lee, W. Yang, R. G. Parr, *Phys. Rev. B* **1988**, *37*, 785.

List of Publications

- [1] *The First Structurally Characterized Aluminum Compound with Two SH Groups: [LAl(SH)₂] [L = HC{C(Me)N(Ar)}₂, Ar = 2,6-*i*Pr₂C₆H₃] and the Catalytic Properties of the Sulfur P(NMe₂)₃ System.* **Vojtech Jancik**, Ying Peng, Herbert W. Roesky, Jiyang Li, Dante Neculai, Ana M. Neculai, Regine Herbst-Irmer, *J. Am. Chem. Soc.* **2003**, 125, 1452-1453.
- [2] *Molecular Hydroxides and Hydrides of Aluminum.* Herbert W. Roesky, Guangcai Bai, **Vojtech Jancik**, Andreas Stasch. Abstracts of Papers, 225th ACS National Meeting, New Orleans, LA, United States, March 23-27, **2003**.
- [3] *Preparation of Mixed-Metal Chalcogenide Compounds Containing Aluminum.* **Vojtech Jancik**, Herbert W. Roesky, Dante Neculai, Ana M. Neculai. 8th Seminar of PhD Students on Organometallic Chemistry, Abstracts of Papers, Hrubá Skála near Turnov, Czech Republic, September 29 - October 3 **2003**.
- [4] *Preparation and Structure of the First Germanium(II) Hydroxide: The Congener of an Unknown Low-valent Carbon Analogue.* Leslie W. Pineda, **Vojtech Jancik**, Herbert W. Roesky, Dante Neculai, Ana M. Neculai, *Angew. Chem. Int. Ed.* **2004**, 43, 1419-1421.
- [5] *Preparation of Monomeric [LAl(NH₂)₂] - a Main-group Metal Diamide Containing Two Terminal NH₂ Groups [L = HC(CMeNAr)₂, Ar = 2,6-*i*Pr₂C₆H₃].* **Vojtech Jancik**, Leslie W. Pineda, Jiri Pinkas, Herbert W. Roesky, Dante Neculai, Ana M. Neculai, Regine Herbst-Irmer, *Angew. Chem. Int. Ed.* **2004**, 43, 2142-2145.
- [6] *Renaissance of Aluminum Chemistry.* Herbert W. Roesky, Andreas Stasch, Guangcai Bai, **Vojtech Jancik**, S. Shravan Kumar, Hongping Zhu, Ying Peng, Abstracts of Papers, 227th ACS National Meeting, Anaheim, CA, United States, March 28-April 1, **2004**.
- [7] *A Seven-Membered Aluminum Sulfur Allenyl Heterocycle Arising from the Conversion of an Aluminacyclopentene with CS₂.* Hongping Zhu, Jianfang Chai, Qingjun Ma,

Vojtech Jancik, Herbert W. Roesky, Hongjun Fan, Regine Herbst-Irmer, *J. Am. Chem. Soc.* **2004**, *126*, 10194-10195.

- [8] *Phosphane-Catalyzed Reactions of $LiAlH_2$ with Elemental Chalcogens; Preparation of $[LiAl(\mu-E)_2Al]$ [$E = S, Se, Te, L = HC(CMeNAr)_2, Ar = 2,6-iPr_2C_6H_3$].* **Vojtech Jancik**, Monica M. Moya Cabrera, Herbert W. Roesky, Regine Herbst-Irmer, Dante Neculai, Ana M. Neculai, Mathias Noltemeyer, Hans-Georg Schmidt, *Eur. J. Inorg. Chem.* **2004**, 3508-3512.
- [9] *Control of Molecular Topology and Metal Nuclearity in Multimetallic Assemblies: Designer Metallosiloxanes Derived from Silanetriols.* Herbert W. Roesky, Ganapathi Anantharaman, Vadapalli Chandrasekhar, **Vojtech Jancik**, Sanjay Singh, *Chem. Eur. J.* **2004**, *10*, 4106-4114.
- [10] *Germacarboxylic Acid: An Organic-Acid Analogue Based on a Heavier Group 14 Element.* Leslie W. Pineda, **Vojtech Jancik**, Herbert W. Roesky, Regine Herbst-Irmer, *Angew. Chem. Int. Ed.* **2004**, *43*, 5534-5536.
- [11] *Synthesis and Structure of Allyl and Alkynyl Complexes of Manganese(II) Supported by a Bulky β -Diketiminato Ligand.* Jianfang Chai, Hongping Zhu, Herbert W. Roesky, Zhi Yang, **Vojtech Jancik**, Regine Herbst-Irmer, Hans-Georg Schmidt, Mathias Noltemeyer, *Organometallics* **2004**, *23*, 5003-5006.
- [12] *Methyl Substitution of Aluminum-Hydride Bonds in a Carbaalane and an Aluminum Imide.* Andreas Stasch, S. Shravan Kumar, **Vojtech Jancik**, Herbert W. Roesky, Jörg Magull, Mathias Noltemeyer, *Eur. J. Inorg. Chem.* **2004**, 4056-4060.
- [13] *Heavy Metal Containing Polyhedral Metallasiloxane Derived from an Aminosilanetriol: Synthesis and Structural Characterization of $[(PbO)_6(R_2Si_2O_3)_2]$ ($R = (2,6-iPr_2C_6H_3)N(SiMe_3)$).* Umesh N. Nehete, Vadapalli Chandrasekhar, **Vojtech Jancik**, Herbert W. Roesky, Regine Herbst-Irmer, *Organometallics* **2004**, *23*, 5372-5374.

- [14] *[LAl(μ -S₃)₂AlL]: A Homobimetallic Derivative of the Sulfur Crown S₈*. Ying Peng, Hongjun Fan, **Vojtech Jancik**, Herbert W. Roesky, Regine Herbst-Irmer, *Angew. Chem. Int. Ed.* **2004**, 43, 6190-6192.
- [15] *Preparation of [LAl(μ -S)₂MCp₂] (M = Zr, Ti) from the Structurally Characterized Lithium Complexes [$\{LAl(SH)[SLi(thf)_2]\}_2$] and [$\{LAl[(SLi)_2(thf)_3]\}_2$] · 2THF*. **Vojtech Jancik**, Herbert W. Roesky, Dante Neculai, Ana M. Neculai, Regine Herbst-Irmer, *Angew. Chem. Int. Ed.* **2004**, 43, 6192-6196.
- [16] *Synthesis and Structures of Aluminum Monohydride and Chalcogenides Bearing a Bidentate [N,O] Ligand*. Ying Peng, Haijung Hao, **Vojtech Jancik**, Herbert W. Roesky, Regine Herbst-Irmer, and Jörg Magull, *Dalton Trans.* **2004**, 3548-3551.
- [17] *Preparation of Monomeric LGa(NH₂)₂ Containing Two Terminal NH₂ Groups and of LGa(OH)₂ – in the Presence of a N-heterocyclic Carbene as HCl Acceptor [L = HC(CMeNAr)₂, Ar = 2,6-*i*Pr₂C₆H₃]*. **Vojtech Jancik**, Leslie W. Pineda, A. Claudia Stückl, Herbert W. Roesky, Regine Herbst-Irmer, *Organometallics* **2004**, submitted for publication.
- [18] *The OH Functionality of Germanium(II) Compounds for the Formation of Heterobimetallic Oxides*. Leslie W. Pineda, **Vojtech Jancik**, Herbert W. Roesky, Regine Herbst-Irmer, *Organometallics* **2004**, submitted for publication.
- [19] *N-Heterocyclic Carbene Involved in the Stepwise Hydrolysis of Aluminum Chloride Iodide LAlClI [L = HC(CMeNAr)₂, Ar = 2,6-*i*Pr₂C₆H₃]*. Hongping Zhu, Jianfang Chai, Cheng He, Herbert W. Roesky, **Vojtech Jancik**, Hans-Georg Schmidt, Mathias Noltemeyer, *Organometallics* **2004**, submitted for publication.
- [20] *The First Example of a Lanthanocene Compound Supported by an Al–O Moiety: Synthesis and Structure of Cp₂YbTHF(μ -O)AlL(Me) [L = HC(CMeNAr)₂, Ar = 2,6-*i*Pr₂C₆H₃]*. Jianfang Chai, Hongping Zhu, Cheng He, Herbert W. Roesky, **Vojtech Jancik**, Sanjay Singh, *Angew. Chem. Int. Ed.* **2004**, submitted for publication.

- [21] *A Paradigm Change in Assembling OH Functionalities on Metal Centers*. Herbert W. Roesky, Sanjay Singh, **Vojtech Jancik**, Vadapalli Chandrasekhar, *Acc. Chem. Res.* **2004**, *submitted for publication*.

Patent

Oxygen-bridged Bimetallic Complex, its Synthesis and Use as Polymerization Catalyst. Herbert W. Roesky, Guangchai Bai, **Vojtech Jancik**, Sanjay Singh. **2004**, *Pat. Appl. pending*.

Lebenslauf

Name:		Vojtech Jancik
Geboren:		20 Januar 1977 in Prostějov
Staatsangehörigkeit:		Tschechische Republik
Schulbesuch:	1983 – 1991	Masaryk-Grundschule in Drahaný, Tschechische Republik
	1991 – 1995	Gymnasium J. Wolke, Prostějov, Tschechische Republik
	31. Mai 1995	Abitur
Studium:	1995 – 2001	Masaryk Universität, Brno, Tschechische Republik Fach: Anorganische Chemie; Chemie auf Lehramt (Sek. II)
	1996 – 2001	Studentische bzw. wissenschaftliche Hilfe, Masaryk Universität, Brno, Tschechische Republik
	6. Juni 2000	Staatsexamen
Promotion:	2001 – 2004	Experimentelle Promotionsarbeit im Institut für Anorganische Chemie Göttingen unter der Leitung von Prof. Dr. Dr. h.c. mult. H. W. Roesky
	2001 – 2003	Förderung durch das Stipendium für Doktoranden durch die Stiftung Stipendien-Fonds des Verbandes der Chemischen Industrie
	2001 – 2003	Wissenschaftliche Hilfskraft bzw. Angestellter, Institut für Anorganische Chemie, Georg-August Universität Göttingen, Deutschland
	03. Nov. 2004	Tag der mündlichen Promotionsprüfung